

TABLE OF CONTENTS

Section/ Appendix	Para	Title	Page
		Acknowledgement	1
1		Introduction	2
2		Summary	3
3		Design Requirements	5
	3.1	Dynamic Ranges	5
	3.2	Accuracy	9
	3.3	Abort Considerations	10
	3.4	Handling Quality Requirements	11
4		Descent Thrust Vector Control	13
	4.1	Thrust Magnitude Control	13
	4.2	Thrust Direction Control	15
	4.2.1	Case A - Low Gain Trim Gimbal Plus RC Jets	16
	4.2.2	Case B - High Gain Gimbal Plus RC Jets	24
	4.3	Comparison Between Case A and Case B	27
5		Ascent Thrust Vector Control	31
	5.1	Thrust Magnitude Control	31
	5.2	Thrust Direction Control	31
6		Abort Considerations	38
7		Conclusions and Recommendations	39
8		Future Work	40
A		Mission Profile	41
B		RC Jet Location and Logic	46
C		Gimbal Considerations	54
D		Trim Gimbal Dynamics	68
E		RC Jet Characteristics	69
F		Preliminary Investigation of Dynamic Coupling of Propellant Sloshing with the Attitude Control System for LEM Ascent Stage	78

TABLE OF FIGURES

No.	Title	Page
3.1	LEM Configuration and Mass Properties	5a
3.2	Handling Qualities During Hover to Landing	12
4.1	Thrust Magnitude Control System	14
4.2	Simplified Block Diagram, Pitch or Yaw Axis FCS	17
4.3	RC Jet Locations	21
4.4	Landing Simulation (Single Axis)	25
4.5	Simplified Block Diagram, Pitch or Yaw Axis FCS (Preliminary)	26
4.6	LEM Rigid Structure Descent Control System Feedback Diagram	28
5.1	Simplified Block Diagram, Pitch or Yaw Axis Ascent FCS	33
5.2	LEM Control System Docking Simulator	37

TABLE OF TABLES

No.	Title	Page
3.1	Summary of Design Requirements	6
3.2	Attitude Control Torque Requirements	8
4.1	Representative Results From Analog Test of Case A and Case B Attitude Control Systems to Step Inputs	29
5.1	Pulse Modulator Characteristics	34

ACKNOWLEDGEMENT

The results and conclusions presented in this report are based to a great extent on work generated by the Dynamic Analysis and System Integration Groups.

SECTION 1. - INTRODUCTION

In accordance with the requirements of a GAEC - MSC agreement (Ref: LEM-IOM-62-47H dated 18 December 1962, subject: Technical Data Review) a preliminary study has been conducted to evaluate alternate approaches for thrust vector control of the LEM vehicle. By definition, the systems to be evaluated have been selected to be those which are utilized for modulating the magnitude and/or direction of the vehicle thrust vector throughout the mission profile. This will include all phases such as separation, injection into equi-period orbit, abort from descent coast, powered descent, abort from powered descent, flare, translation to touchdown, powered ascent, rendezvous and docking. Only the coasting phases during ascent and descent have been excluded from consideration in this study, therefore, as thrust vectoring is not accomplished during these periods.

In evaluating the alternate approaches to effecting thrust vector control, three major design constraints were adapted to serve as groundrules, and are listed below in order of highest priority.

1. Crew Safety - Only those systems with the greatest inherent reliability and crew safety will be considered.
2. Trajectories - Thrust vector control systems must be capable of effecting vehicle control over the LEM functional trajectories requirements and within the tolerances needed for satisfactory execution of all phases of the mission.
3. Handling Qualities - Astronauts shall be capable of effecting satisfactory control during all phases requiring manual inputs.

Based on the above considerations an integrated control system consisting of sixteen 100 pound reaction jets, a throttlable (1,050-10,500 pounds) descent engine gimballed for automatic trim control about the vehicle Y and Z axes, plus a fixed nonthrottlable (3,500 pounds) ascent engine is recommended at this time for effecting vehicle thrust vector control during the required mission phases.

SECTION 2. - SUMMARY

This report discusses alternate methods of thrust vector control and presents a recommended configuration. The heart of the problem lies in the means of obtaining attitude control during the descent thrusting portions of the mission. Four methods were considered:

1. Reaction control (RC) jets only
2. Gimbal control only
3. Engine gimballed for c.g. trim plus RC jets for attitude control
4. RC jets plus high gain gimbal for attitude control

The first two methods were excluded because they won't provide the required torque capability with practical designs. The last two were studied in more detail.

Method #3 was selected for recommendation in this report for the following reasons:

1. A single pair of RC jets will meet the control torque requirements for a normal mission if a slow rate trim gimbal is used for c.g. compensation.
2. The only time that high rate attitude maneuvers may be needed while thrusting is during the hover to landing phase (without considering abort). This is the time when the gimbal is least effective since thrust is close to minimum.
3. RC control torque can be doubled for possible "hard over" terrain avoidance maneuvers or abort maneuvers by employing the redundant pair of jets that is available about any one axis at a time.
4. A maximum of 6 degree gimbal deflection is considered a practical limit for space reasons. An estimated 3.5 to 4.5 degrees is needed for c.g. trim. This leaves very little for attitude control torque augmentation.
5. The high rate gimbal actuator is 20 pounds heavier than the trim gimbal and requires 45 times as much peak power (1200 watts vs. 7 watts), and roughly 18 times as much average power.
6. Although a quantitative reliability analysis has not been completed, the high rate gimbal is more complex since it needs servo loop electronics. The trim actuator is a simple open loop on-off device and is therefore more reliable.
7. The possibility of a run-away gimbal presents a much greater

crew safety hazard with the high speed gimbal (20 deg/sec) than the low speed trim gimbal (.2 deg/sec).

For these reasons the trim gimbal plus RC jets for attitude control is recommended for approval by NASA-MSC.

Additional aspects of the thrust vector autopilot that are discussed in the report include modes of operation, RC jet location, jet logic, pulse modulation schemes, handling qualities, fuel slosh problems and control dynamics. Preliminary results of recent landing and docking simulations are also discussed briefly.

Finally, future work on thrust vector control is outlined in the report, and upon approval, will be based on the recommended configuration.

SECTION 3. - DESIGN REQUIREMENTS

The design requirements for thrust vector control must be based on Navigation and Guidance requirements, integration with other subsystems including communications, environmental control and structures, human factors, and reliability. These considerations must then be weighed against the practicality of FCS implementation.

The basic design philosophy to be used in FCS design will be to use the simplest and most reliable design that will do the job. The requirements are discussed in detail here and summarized in table 3-1. The LEM vehicle characteristics are shown in figure 3-1.

3.1 Dynamic Ranges

THRUST DYNAMIC RANGE

Thrust level range for the descent main engine must be 1050 to 10,500 lbs with throttling capability between these limits. This range is based on the trajectory outlined in the mission profile given in appendix A (vehicle weight and ΔV as a function of time). Throttling over the entire range from 1050 to 10,500 lbs is required by N & G from injection to hover. During manual throttling operation from hover to landing a range of 1050 to 3000 lbs. will be used. This does not preclude the possibility of manual throttling over larger thrust ranges for contingency situations.

Ascent engine thrust can be restricted to a single level since there is no requirement for controlling thrust to weight ratio as there is during hover to landing. (Also, a second thrust level capability is available from RC jets for use during rendezvous or for ascent mid-course guidance corrections.) The main engine thrust level to be used is 3500 lbs, which corresponds to the required V and time profile given in appendix A.

THRUST IMPULSE DYNAMIC RANGE

Thrust impulse during descent will range from 2.5×10^5 lb-sec (injection) to 2.9×10^6 lb sec (flare) for powered descent, (refer to appendix A). The total thrust impulse will be approximately 3.4×10^6 lb-sec.

During ascent the range is from that needed for mid-course corrections (which are presently not known) to 10.7×10^7 lb-sec, for the main engine. For the RC jets it will range from minimum impulse of 1.2 lb-sec (minimum impulse using 2 jets) to roughly 2×10^4 lb-sec (for rendezvous).

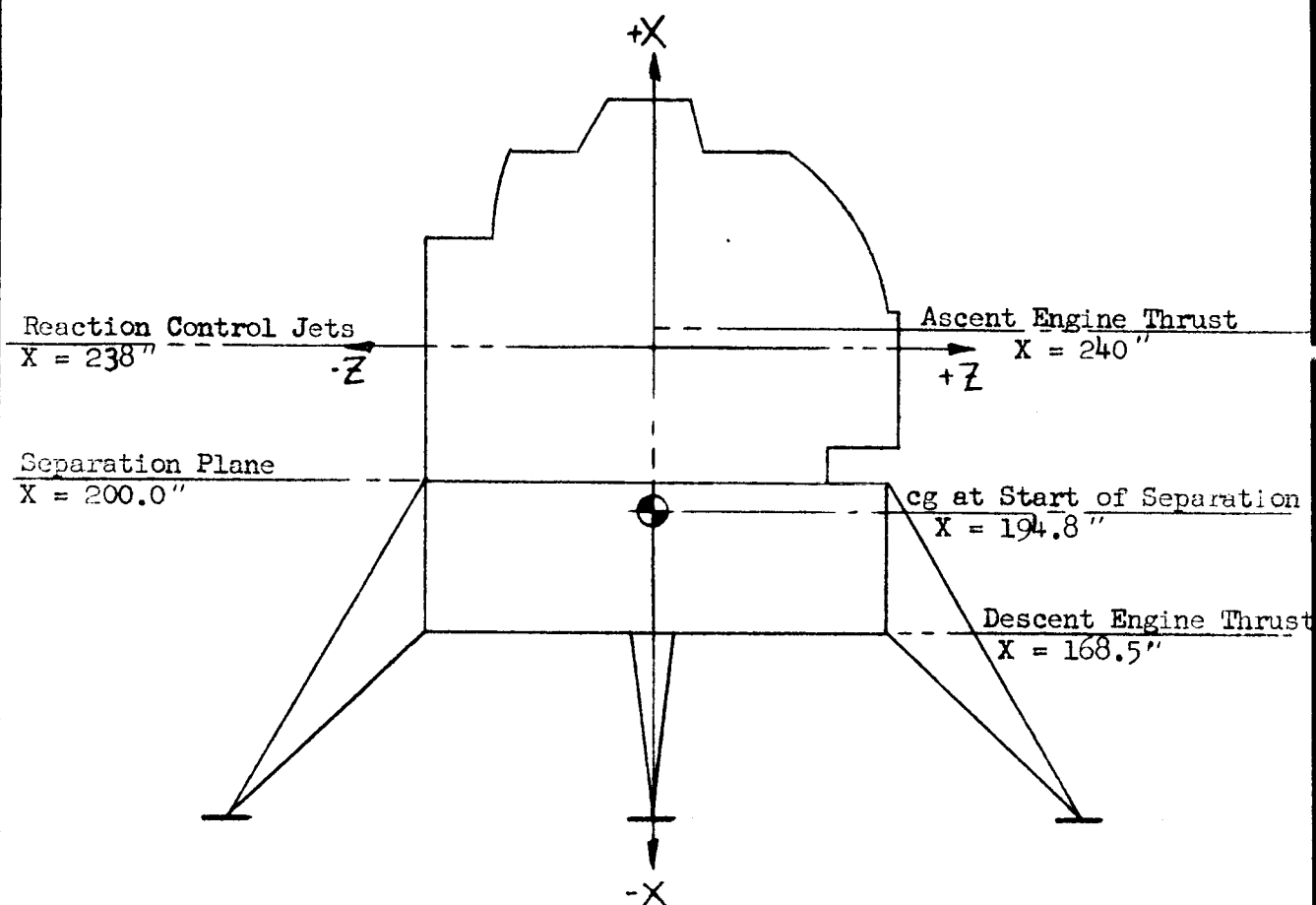
TORQUE DYNAMIC RANGE (abort Y and Z axis)

Torque dynamic range is governed by a number of factors, some of which must be traded off against each other. Maximum torque is that needed to provide compensation for c.g. offset plus maximum angular acceleration

FIGURE 3-1

LEM CONFIGURATION AND MASS PROPERTIES

(Based on Proposal Values)



MISSION PHASE		START OF SEPARATION	HOVER	LIFT-OFF
Vehicle Weight (earth pounds)		21,993.7	10,843.0	7,379.1
Position of cg along X-axis (inches)		194.8	214.8	236.7
Moments of Inertia (slug-ft ²)	Ixx	11,933	6,001	3,617
	Iyy	11,492	6,351	2,411
	Izz	11,550	6,482	2,706

TABLE 3.1

SUMMARY OF DESIGN REQUIREMENTS

MISSION PHASE	PARAMETER	DYNAMIC RANGE	ACCURACY	RESOLUTION
Descent	Thrust (T)	1050-10,500 lbs	+1% after 5 sec +10, -1% at end of duty cycle	+1% from 1050- 3000 lbs and 8400- 10,500 lbs, +5% from 3000-8400 lbs
	Thrust Impulse (Tt)	1.8×10^5 to 2.8×10^6 lb-sec.	Predictability +100 lbs-sec	-
	Torque (L)	c.g. offset: 880-2200 ft- lbs. Other: 90 ft-lbs to 2200 ft-lbs	+1.0%	-
	Torque Impulse (Lt)	With Trim Gim- bal: 6.6 to 2200 ft lbs-sec Without Trim Gimbal: 6.6 to 10^6 ft- lb-sec	Predictability +1.1 ft-lbs-sec	-
	Attitude Control Accuracy About Y&Z axes	-	+0.1 deg.std. dev., zero mean	-
Ascent	Thrust	3500 lbs	+1% after 5 sec. +10, -1% at end of duty cycle	-
	Thrust Impulse	(Not known) to 1.07×10^6	Predictability +200 ft-lb-sec	-
	Torque	c.g.offset: 120-770 ft-lbs Other: 70- 2200-ft-lbs	+1.0%	-
	Torque Impulse	6.6 to 10^5 ft-lb-sec	+1.1 ft-lb- sec	-
	Attitude Control Accuracy	-	+ 0.2 deg, std. dev, zero mean	-

plus a margin for cross coupling and other disturbances. Preliminary estimates of c.g. offset during descent indicate a maximum of 2.5" is to be expected. At maximum thrust of 10,500 lbs. the largest torque developed is 2200 ft.-lbs. This is therefore the amount needed for c.g. compensation unless a trim gimbal is used.

During ascent the c.g. offset can be as large as 2.6 inches (an average of 1.0 inches over the thrusting period is required, however, for reasons of RC fuel consumption). At a 3500 lb thrust level the required torque for compensation is 770 ft.-lbs. Column A of Table 3.2 summarizes the torque needed for c.g. compensation throughout the mission. As seen in the mission profile, no large, rapid attitude maneuvers take place during descent thrusting periods except from hover to touchdown, where the maneuvers are still rather small under normal conditions. Column B of Table 3.2 lists the attitude control torque requirements for a normal mission.

A possible need for large attitude accelerations may arise in the case of emergency terrain avoidance maneuvers. The terrain avoidance problem has not been studied to any great extent and must be approached from a more general handling qualities (HQ) viewpoint. It has been found that an attitude rate limit of 20 deg/sec during manual operation is satisfactory. In addition, response time (3 time constants) of less than 1.5 seconds is a satisfactory HQ range (HQ is discussed in more detail below). This means an angular acceleration of approximately 18 deg/sec² must be available for emergency terrain avoidance maneuvers, allowing a margin for control dynamics.

The torque required to accomplish this, using the appropriate moment of inertia, is: (hover to landing)

$$\begin{aligned} L &= I \ddot{\theta} \\ &= 6000 \text{ slug-ft}^2 \times \frac{18}{57.3} \text{ rad/sec}^2 \\ &= 1900 \text{ ft.-lbs} \end{aligned}$$

For cross-coupling and other low frequency disturbance torques including engine misalignment, 200 ft.-lbs is allowed during descent.

In summary, a maximum of 2200 ft.-lbs of torque (or a trim gimbal) is needed for c.g. offset and 2100 ft.-lb. for angular acceleration capability during hover to touchdown. Column D of Table 3.2 gives an extrapolation of the latter value to the remainder of the mission thereby giving available control torque for possible emergency abort maneuvers.

Preliminary estimates of attitude acceleration requirements during abort maneuvers indicate that the available torques given in Table 3.2 are sufficient. This is discussed further in paragraph 3.3.

TABLE 3.2 (abort Y and Z axes)

ATTITUDE CONTROL TORQUE REQUIREMENTS

MISSION PHASE	A		B	C		D	E	F
	C.G. OFFSET DISTANCE	OFFSET TORQUE	TORQUE REQ'D FOR NORMAL ATTITUDE MANEUVERS	MARGIN FOR CROSS COUPLING, ENGINE MISALIGN- MENT, ETC.	TORQUE AVAIL- ABLE FOR ABORT MANEUVERS *	MAX ACCELERATION CAPABILITY	MAX RATE RESPONSE TIME CAPABILITY (MAX RATE = 20 deg/ sec)	
Descent Orbit Injection (I ≤ 12,000)	1.0"	880ft-lbs (or Gimbal)	Negligible	200 ft-lbs	1900 ft-lbs*	9.1 deg/sec ²	2.5 sec	
Powered Descent (I ≤ 6500-12000)	2.0"	1760 ft- lbs(or Gim- bal)	Negligible	200 ft-lbs	1900 ft-lbs*	9.1 -16.8 deg/sec ²	2.5-1.5 sec	
Flare (I ≤ 6500)	2.5"	2200 ft- lbs (or Gimbal)	< 900 ft-lbs	200 ft-lbs	1900 ft-lbs*	18 deg/sec ²	1.5 sec	
Hover to Touchdown (I ≤ 6000)	2.5"	"	< 900 ft-lbs	200 ft-lbs	1900 ft-lbs (for terrain avoidance)	18 deg/sec ²	1.4 sec	
Lift Off (I ≤ 3000)	1.0"	290ft-lbs	370 ft-lbs	200 ft-lbs	1610 ft-lbs*	31 deg/sec ²	1.0 sec	
Pitch Over (I ≤ 3000)	1.0"	290ft-lbs	negligible	200 ft-lbs	1610 ft-lbs*	31 deg/sec ²	1.0 sec	
Transfer Orbit Injection (I ≤ 2500)	2.0"	580ft-lbs	negligible	200 ft-lbs	1320 ft-lbs*	31 deg/sec ²	1.0 sec	
Mid-Course Correction if used (I ≤ 2000)	2.6"	770ft-lbs	negligible	200 ft-lbs	1030 ft-lbs*	31deg/sec ²	1.0 sec	
Rendezvous (I ≤ 2000)	2.6"	120ft-lbs	undetermined	100 ft-lbs	1880 ft-lbs*	54 deg/sec ²	0.6 sec	

*Extrapolation of torque level allowed for Hover to Touchdown terrain avoidance.

NOTE: Average c.g. offset during ascent must be 1.0" to limit RC fuel consumption.

Minimum torque is totally dependent on the autopilot and torque generator response characteristics. One hundred pound ON-OFF reaction jets have been selected early in the program for the following reasons:

1. They provide a good compromise between control torque and minimum impulse needs, the minimum impulse being 0.6 lb-sec. With an 11 foot lever arm the resulting minimum angular rate that can be commanded when LEM is its lightest (1000 slug ft²) is $\dot{\theta}_{min} = 6.6$ milliradians/sec. This is an acceptable rate for limit cycle operation.
2. They are tried and proven hardware currently under development for use in the Apollo vehicles.

It should be noted that torque requirements about the Y and Z axes given above are based on vehicle inertias given the first column of table 3.2. If vehicle inertias undergo significant growth, the torque requirements must increase.

TORQUE IMPULSE DYNAMIC RANGE

For descent, the high end of the dynamic range of torque impulse (LT) is determined by the "hard over" maneuver to 20 deg/sec angular rate in 1.0 sec if a gimbal is assumed for c.g. trim. This would be a torque impulse of 2100 ft-lb-sec. If a trim gimbal is not used, the worst case torque impulse would depend on the control system dynamics.

Minimum impulse is again an RC jet design consideration. For the 100 lb jets being considered, at a lever arm of 11.0 ft, it would be 6.6 ft-lb-sec since impulse predictability becomes very poor below 0.6 lb-sec thrust impulse (refer to Appendix E).

During ascent the largest torque impulse will be that needed for c.g. offset and will also depend on control system dynamics. Minimum impulse will again be 6.6 ft-lb-sec.

3.2 Accuracy

ATTITUDE CONTROL ACCURACY

Attitude control accuracy requirements during thrusting periods have not yet been firmly established. Preliminary navigation and guidance study results and FCS implementation considerations have led to the following values. Standard deviation during descent shall be ± 0.1 deg with a mean of zero with respect to the commanded angle. Standard deviation during ascent shall be ± 0.2 deg, again with a mean of zero. These values assume an attitude sensing resolution at least an order of magnitude better, or 0.6 minutes of arc. Transient attitude error requirements have not yet been established but are not expected to greatly affect the guidance problem. These accuracies are presently being reviewed for possible relaxation.

THRUST ACCURACY

Thrust accuracy during descent need not be stringent since throttling is available for guidance corrections. It has therefore been established on the basis of present specified hardware capability, which is as follows:
 $\pm 1.0\%$ after 5 sec burning time at full thrust.
 $\pm 10\%$, $- 1.0\%$ at end of duty cycle at full thrust.

Thrust throttling resolution, however, has been established at the following values; again based on present hardware capability:

$\pm 1.0\%$ from 8400 - 10,500 lbs. thrust

$\pm 5.0\%$ from 3000 - 8400 lbs. thrust

$\pm 1.0\%$ from 1050 - 3000 lbs. thrust

Resolution is defined as the minimum change in thrust level command signal that will cause a change in thrust level.

Thrust accuracy attainable in the ascent stage is the same as the descent stage and is presently being reviewed for possible improvement.

TORQUE ACCURACY

Torque accuracy requirements can be based on minimum impulse requirements and cross coupling effects due to an unbalanced couple (causes translational motions). It turns out, however, that RC jet accuracy required for preventing cross coupling from translation accelerations to rotational motion are more stringent. Maximum tolerable error for this effect has been set at $\pm 1\%$ of nominal jet thrust level (assumed 100 lb jets). This would result in a cross coupling torque of 11 ft-lbs, or an angular acceleration of 6 milliradians/sec² as a worst case. Since the same jets are used for torque and translation, the resulting torque accuracy will also be $\pm 1.0\%$.

THRUST IMPULSE PREDICTABILITY

Thrust impulse predictability, or shut off uncertainty has been set at 100 lb-sec for the descent engine. This is based on the requirement for obtaining a vertical velocity at touchdown of less than 5 ft/sec. During ascent the impulse predictability required is 200 lb-sec and is based on the required precision for injection into a clear pericynthion orbit from lift-off.

TORQUE IMPULSE PREDICTABILITY

As explained earlier, the 100 lb RC jets have been selected for generating control torque because of availability and because they are a good compromise between maximum torque requirements and minimum impulse capability. The minimum impulse is 0.6 lb-sec (or 6.6 ft-lb-sec torque-impulse with a predictability of 0.1 lb-sec (or 1.1 ft-lb-sec).

3.3 Abort Considerations

A stringent requirement is placed upon the LEM angular rate and acceleration capability during an abort situation from powered descent to rendezvous. Assuming the abort trajectory requires an initial vertical thrust period, the LEM attitude must be changed from that which it assumes in a nominal powered descent trajectory to a vertical position. This angular change can vary between 100° and 60° depending upon the point of abort in the powered descent trajectory. A current

abort procedure indicates that the minimum acceptable rate and acceleration is $10^0/\text{sec}$ and $10^0/\text{sec}^2$ respectively.

When results from the present abort trajectory and accuracy studies are obtained, further constraints may be applied to the thrust magnitude and attitude hold accuracy requirements.

3.4 Handling Quality Requirements

Handling qualities requirements for the LEM will be developed by using data from three reference sources: 1) current aircraft handling qualities specifications; 2) related simulation programs conducted by other organizations; and 3) GAEC LEM simulation programs. The approaches being used to establish these requirements are:

1. Draw an analogy between performance requirements of the LEM for various mission phases and those of other known vehicles such as missile, airplane, helicopter.
2. Review available Handling Qualities data derived from other simulation programs (LEM, Mercury, Gemini, Apollo, etc) and use if applicable.
3. Reduce and integrate data available from the GAEC LEM docking, landing and rendezvous simulation programs.

A basic control simulator is also planned to allow evaluation of parametric variation in the control display loop.

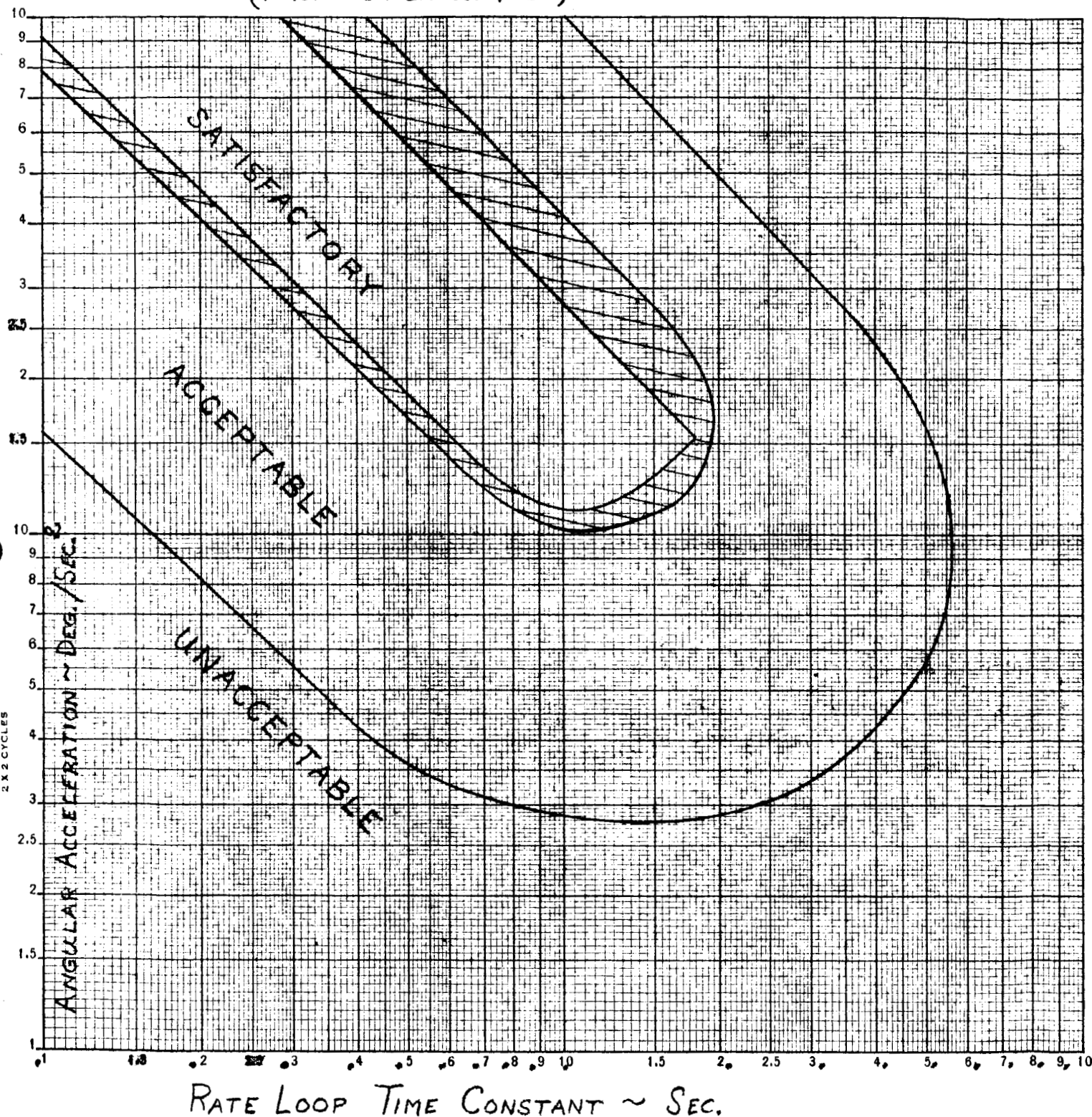
Figure 3-2 summarizes the most significant results of the simulator programs to date. It is seen that the boundary between the "satisfactory" and "acceptable" regions for the hover to landing chart was found to be less well defined than the boundary between "acceptable" and "unacceptable" regions. Hence, this boundary is shown with a fringe area of uncertainty. This curve forms the basis for the hover to landing autopilot response requirement, given in paragraph 3.1, of response time less than 1.5 sec. The lower limit on response time implied by the curve may be a misleading result of the experimental method. It is not, in any case, critical to the problem at hand.

~~CONFIDENTIAL~~

FIGURE 3-2

100-110-2
100-110-2
100-110-2

HANDLING QUALITIES DURING HOVER TO LANDING (FIRST CONSENSUS PLOT)



LED-290-2
5/14/63

~~CONFIDENTIAL~~

SECTION 4 - DESCENT THRUST VECTOR CONTROL4.1 Thrust Magnitude Control

It has already been established in the proposal ("Project Apollo - Lunar Excursion Module Proposal", GAEC, 4 September 1962) and in the study report ("Lunar Excursion Module Study, GAEC, 22 June 1962) that a single deep throttling engine will be used for descent rather than separate vernier engines. The reasons for this choice were clearly stated and need not be pursued further here. The discussion will be confined, therefore, to the throttling servo, the interface with N & G and the cockpit controller.

Figure 4-1 is a simplified diagram of the thrust magnitude control system.

Normal mode of operation is for the primary navigation and guidance system to control descent engine thrust during injection into synchronous orbit and powered descent to hover. The pilot can override at any time, and control thrust with the cockpit controller. The landing will be accomplished with the pilot manually controlling thrust. Completely automatic landing is presently being considered but its use will not be assumed for this discussion.

The main components of the descent engine throttle servo system are a pressure transducer, servo electronics, and throttle valve actuator. The transducer produces a 0 to 5 volt D.C. signal proportional to engine chamber pressure (thrust). The electronics compares this signal and actuator feedback signals to the thrust command signal and drives the throttle actuator accordingly. Stabilizing loops are provided around the torque motor. Design details of the throttle servo are being negotiated with subcontractors and are not available at this time.

Thrust commands generated by the N & G computer as the result of trajectory conditions are composed of 3200 pps pulse trains. Average pulse frequency is proportional to rate of change of thrust. This signal format is not useable by the proposed throttle servo which required as analog voltage proportional to commanded thrust level. Design of the interface equipment is under discussion between MIT and Grumman.

When the pilot elects to manually control thrust level he actuates a switch which disconnects the N & G system from the throttle servo and engages the cockpit controller. The N & G system continues to generate thrust commands which the pilot has the option of using.

Several systems are being considered to prevent step changes in thrust command when the pilot selects manual or N & G control. A servo which drives the controller to follow N & G commands is one possibility. This would prevent transients when the pilot assumes manual control, but would not prevent a step input if the N & G system were re-engaged. A de-clutching device is required to disconnect the servo when manual control is desired, and this would decrease overall system reliability.

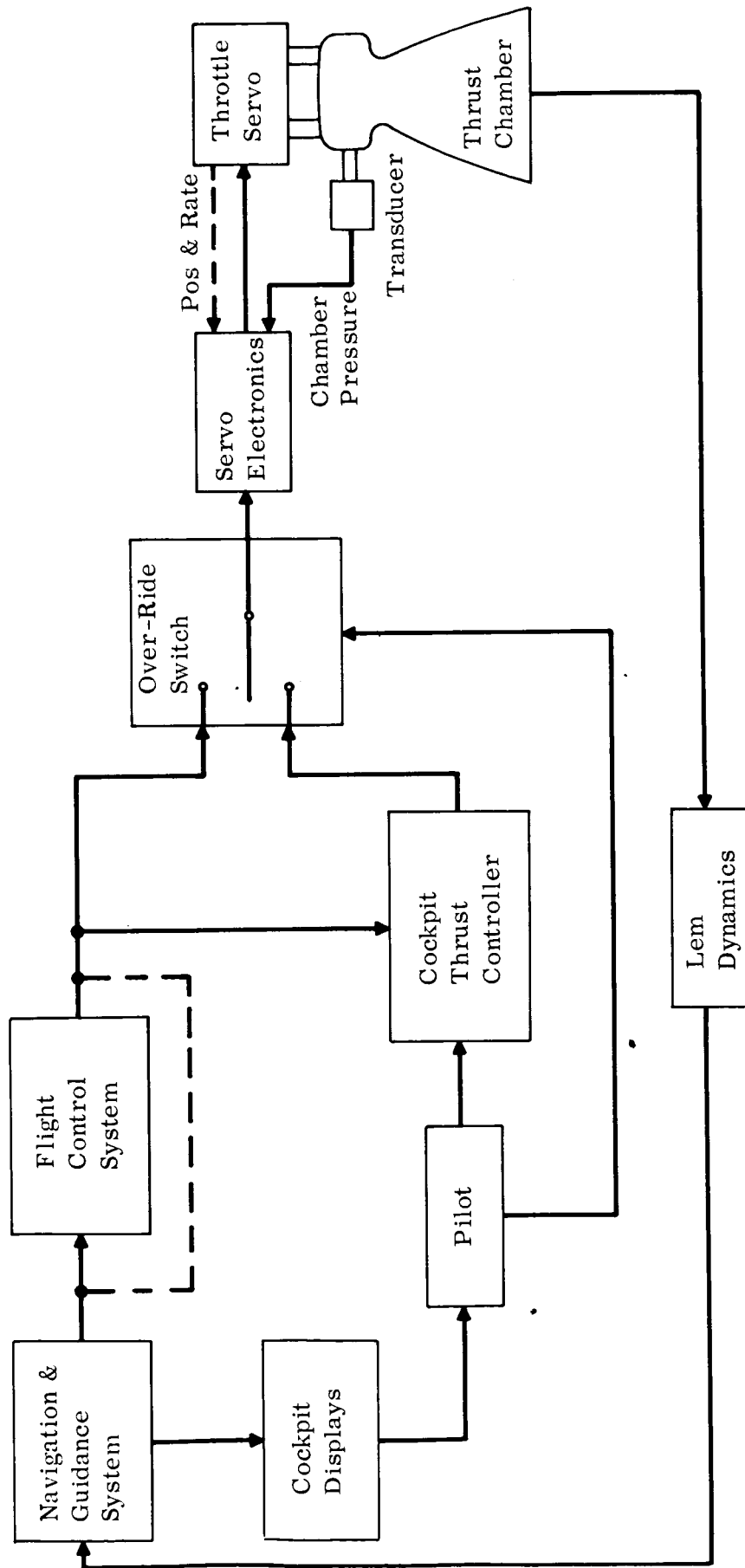


Figure 4-1. Thrust Magnitude Control System

Various shaping networks are being considered as alternatives to the above method to modify a step input, and their effects on thrust response, servo stability, system reliability, etc. are being investigated.

Present plans are to provide a dual range thrust controller mounted on the left side of the pilot station. The controller high thrust range will command continuously variable thrust between 3000 and 10500 pounds. This is the approximate throttling range used during the powered descent. Since information to be used by the pilot in determining manual thrust requirements has not been defined it may be that the high range will reduce to only a fixed level thrust position.

The low thrust range of the cockpit controller will be used during the landing portion of the powered descent. Throttling range is continuously variable between 1050 pounds and 3500 pounds. Simulation programs have shown that this range is adequate and that precise control within this range requires controller movement of at least 3 arc inches. At this time there is no requirement for manual control of thrust levels between the 2 ranges described. The controller will be provided with detents which will indicate the limits of the 2 ranges and the engine stop setting.

Three controller configurations are currently being considered for evaluation on the simulator. These can be categorized as aircraft throttle type, Apollo translational thrust controller type and helicopter collective pitch controller type. At the present time it appears desirable to provide Z and Y axis translation control while controlling descent engine thrust. This is done most conveniently by incorporating these controls, along with the X axis translation control required during docking, into a single cockpit controller. The integration of 4 distinct functions into a common controller becomes difficult when such things as pressure suit mobility and control motion/vehicle motion compatibility are considered. These man-machine interface relationships will be settled as the result of studies currently under way.

4.2 Thrust Direction Control

Four alternative methods of obtaining thrust direction control (or attitude control while thrusting) during the descent phase have been investigated, and are as follows:

1. RC jets only - the RC jets provide c.g. offset compensation as well as attitude control.
2. High gain gimbal only - gimbal is used for c.g. offset and attitude control, thereby making it a high rate and acceleration gimbal.
3. Low gain (trim) gimbal plus RC jets - the gimbal has low rate and acceleration and is used to compensate for c.g. travel. RC jets are used for attitude control.

4. High gain gimbal plus RC jets - the high gain gimbal augments the RC jets for both c.g. compensation and attitude control.

The first two alternatives were eliminated at an early stage because they will not meet the requirements established in section 3.

As shown in paragraph 4.2.1, a maximum of 2200 ft-lb. of attitude control power is available from the RC jets. This much is needed just for compensation of c.g. offset during descent so that the "RC jet only" configuration will not provide the required overall control power. Use of larger RC jets is incompatible with minimum impulse requirements. Another point that precludes the use of jets for c.g. compensation is the large amount of fuel required. Assuming an average of 1.75 inch c.g. offset (from table 3.2) a thrust level of 8800 lbs, an RC jet lever arm of 5.5 ft, an I_{sp} of 300, and a main engine burning time of 500 sec. during descent, the RC fuel weight required is:

$$RC \text{ Wt./axis} = \frac{8800 \times 1.75 \times 500}{12 \times 5.5 \times 300} = 392 \text{ lbs.}$$

This is far in excess of the added weight for a c.g. trim gimbal (≈ 80 lbs. for two axes). Adding extra jets for c.g. compensation would therefore not be a practical solution to the control torque problem.

The second alternative can be eliminated for similar reasons. In order to obtain 1100 ft-lbs. of control power (equivalent to one pair of RC jets) at minimum thrust level, the gimbal deflection angle needed is:

$$\begin{aligned} \delta &= \sin^{-1} \frac{1100 \text{ ft-lbs}}{3 \text{ ft} \times 1050 \text{ lbs}} \\ &= \sin^{-1} \frac{1100}{3150} \\ &= 20 \text{ deg.} \end{aligned}$$

Note: lever arm is approximately 3 ft. during hover when minimum thrust is used.

An additional deflection must also be added for c.g. offset. This is, of course, out of the question. An additional disadvantage of using a high gain gimbal for attitude control is the large variation in loop gain with thrust level.

Configurations #3 and #4 mentioned above are the only ones worthy of further study and are presented in detail here. They will hereafter be referred to as cases A and B.

4.2.1 Case A - Low Gain Trim Gimbal Plus RC Jets

Figure 4-2 shows a simplified block diagram of case A for a single axis (pitch or yaw). In normal operation a single pair of RC jets form a couple about each axis for attitude control. In the case of a jet failure, or for extremely high angular accelerations (emergency

Confidential

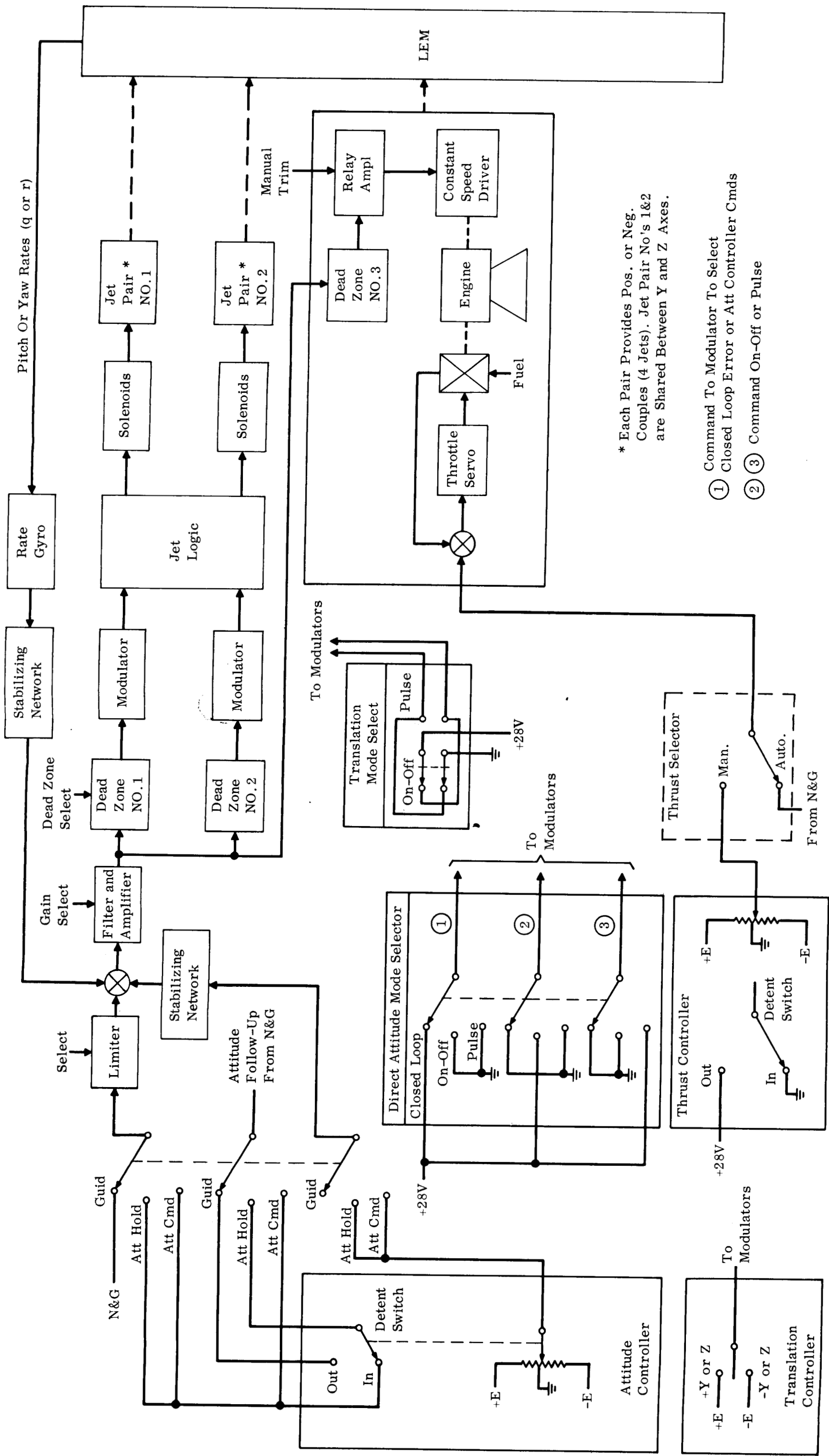


Figure 4-2. Simplified Block Diagram, Pitch or Yaw Axis FCS

hard over commands), a second pair of jets is available for control torque on a timeshare basis about the Y and Z axes, and at any time about X. This is accomplished by providing the additional dead zone #2 as shown, and appropriate jet logic. The additional modulator also provides redundancy. Very low frequency attitude disturbances, such as c.g. offset, are compensated for by the trim gimbal.

There are two possible types of trim drives; a servo drive and an open loop constant speed motor. Since the former would be considerably more complex, an effort was made to evaluate the simpler constant speed motor. The results were good and are given in detail on page 24.

The four modes of operation that the system is capable of are obtained as follows:

Guidance Mode - The guidance mode is a fully automatic mode. Attitude error signals are sent to the S & C Subsystem from the Navigation and Guidance Subsystem or from the Backup Guidance Section. The attitude error signal is passed through the limiter and combined with the rate gyro damping signal as shown in figure 4-2. The resultant signal then controls the firing of the reaction jets through the logic and pulse generating circuits. This same signal (attitude error and rate) operates the gimbal drive motor for automatic trim when the descent engine is firing. The guidance mode provides fully automatic attitude control capabilities during all phases of the mission except hover, landing and docking (manual rendezvous is also being considered).

Attitude Hold Mode - In the Attitude Hold Mode, the pilot commands an angular rate proportional to displacement of the attitude controller. When the controller is in its neutral position, the vehicle will hold attitude.

As shown in figure 4-2, when the controller is out of detent, the attitude loop is opened and the attitude synch. is in follow up. The output of the attitude controller is compared to the rate gyro, thereby providing a proportional rate command. When the controller is returned to detent, the rate command goes to zero and the attitude loop is closed.

This mode is the primary attitude control mode during the docking phase of the mission. It would also be used anytime the pilot wished to reorient the vehicle during coasting flight.

Attitude Command Mode - This mode is a tentative one for possible use during landing. In this mode the pilot commands attitude from local vertical proportional to his attitude controller displacement. That is, when the pilot "tilts" the control stick, the vehicle tilts; when he lets go of the stick, the vehicle erects. This mode can be used to translate during the hover and landing phase and is mechanized in the pilot pitch and roll axes only (pilot yaw remains in the Attitude Hold Mode). Note that control axes are

referred to in the pilot-oriented (not body-axis) sense. A procedure for translating while hovering would be:

1. Pilot yaws vehicle about the X-axis to line it up in the direction he wants to translate. (Yaw and pitch in Attitude Hold Mode)
2. Pilot pitches forward about the Y-axis - linear acceleration proportional to pitch angle which in turn is proportional to pilot input. Roll and yaw on attitude hold.
3. Pilot centers control stick - vehicle erects and maintains constant linear velocity. All three axes in attitude hold. Establish rate of sink via throttle control.
4. Pilot pitches in opposite direction to reduce translational velocity, throttle to control rate of sink. RC jets may be used for vernier control near ground.

Direct Attitude Mode - This mode would be used only in the case of malfunction of the closed loop autopilot. It provides the pilot only with open loop type acceleration control and is therefore selectable on an individual axis basis. The need for two types of direct control is indicated; a minimum pulse control to provide the precision necessary for docking, and an on-off type full thrust control for rapid maneuvering (or unmaneuvering).

As indicated in figure 4-2, the on-off type of control is called "direct" and the minimum pulse control is called "pulse". Several types of "pulse" control are under consideration a "one-shot" type whereby one minimum impulse is commanded each time the attitude controller detent switch is operated; a "repeated pulse" type which commands repeated minimum impulses at a low frequency as long as the stick is out of detent; and a "proportional" type which utilizes the pot in the controller to command proportional pulse width (still at a low frequency).

Jet Logic

Although the actual logic design has not been firmed as yet, a set of logic ground rules has been established as a design guide. They are as follows:

1. The reaction control system will be assumed to be comprised of 16 jets only.
2. The control logic shall be capable of commanding translation along X, Y and Z simultaneously.
3. The control logic shall be capable of commanding angular motions about X, Y and Z simultaneously.
4. Capability should exist to use either 2 or 4 jets for translation along X, as required.
5. Four jets shall be available for torque about Y and Z during normal (no malfunctions) operation.
6. In the event of a single vertical or horizontal jet failing open, the failed jet and the adjacent vertical or horizontal jet, respectively, in the same quad, will be isolated.

7. In the event of a single vertical or horizontal jet failing closed, the failed jet and the adjacent vertical or horizontal jet, respectively, in the same quad, may or may not be isolated. Control logic shall be capable of handling either alternative.

These ground rules are subject to minor modification if logic complexity warrants it. Figure 4-3 shows a view of the RC jet layout with respect to the body axes. The reasons for selecting this layout are given in appendix B, the main reason being the redundancy obtainable about each axis.

Thrust Controller

The thrust controller is a left-hand control device which contains a position potentiometer in one axis only and a pair of detent switches in each of three axes. The potentiometer is used for proportional manual throttle control, as described earlier, and the detent switches are used to fire the reaction jets for translation control.

Attitude Controller

The attitude controller contains a position potentiometer and a pair of detent switches in each axis. The potentiometer provides proportional rate commands in the Attitude Hold Mode or proportional attitude commands in the Attitude Command Mode in the pitch and roll axes. The detent switches synchronize the attitude followup function in the Attitude Hold Mode or command jet firings in the direct Attitude Mode.

Trim Gimbal

The trim gimbal is driven by a constant speed motor, such as a synchronous type. It acts like a very low gain (or very long time constant) integrator which responds to low frequency c.g. motion. Dead zone no. 3 in figure 4-2 provides a threshold below which the drive motor is not actuated. Two parallel drive units are felt to be necessary for redundancy. Details of the trim gimbal dynamics are given in Appendix C. The following trim gimbal characteristics are applicable:

Maximum gimbal displacement	= + 6.0 deg.
Maximum Gimbal rate	= 0.2 deg/sec.
Gimbal resolution (dead zone), based on 5% RC jet usage for c.g. compensation	= +1.5 milliradians (.86 deg.)
Gear train ratio	= 12×10^4 (assumes motor speed of 4000 RPM)
Power required	= 6.8 watts AV., 27 watts peak
Maximum overshoot	= 6.2×10^{-5} radian (.0035 deg.)
Drive mechanism weight including elec- tronics	= 22 lbs. (for 2 units)
Gimbal ring weight	= 40 lbs.

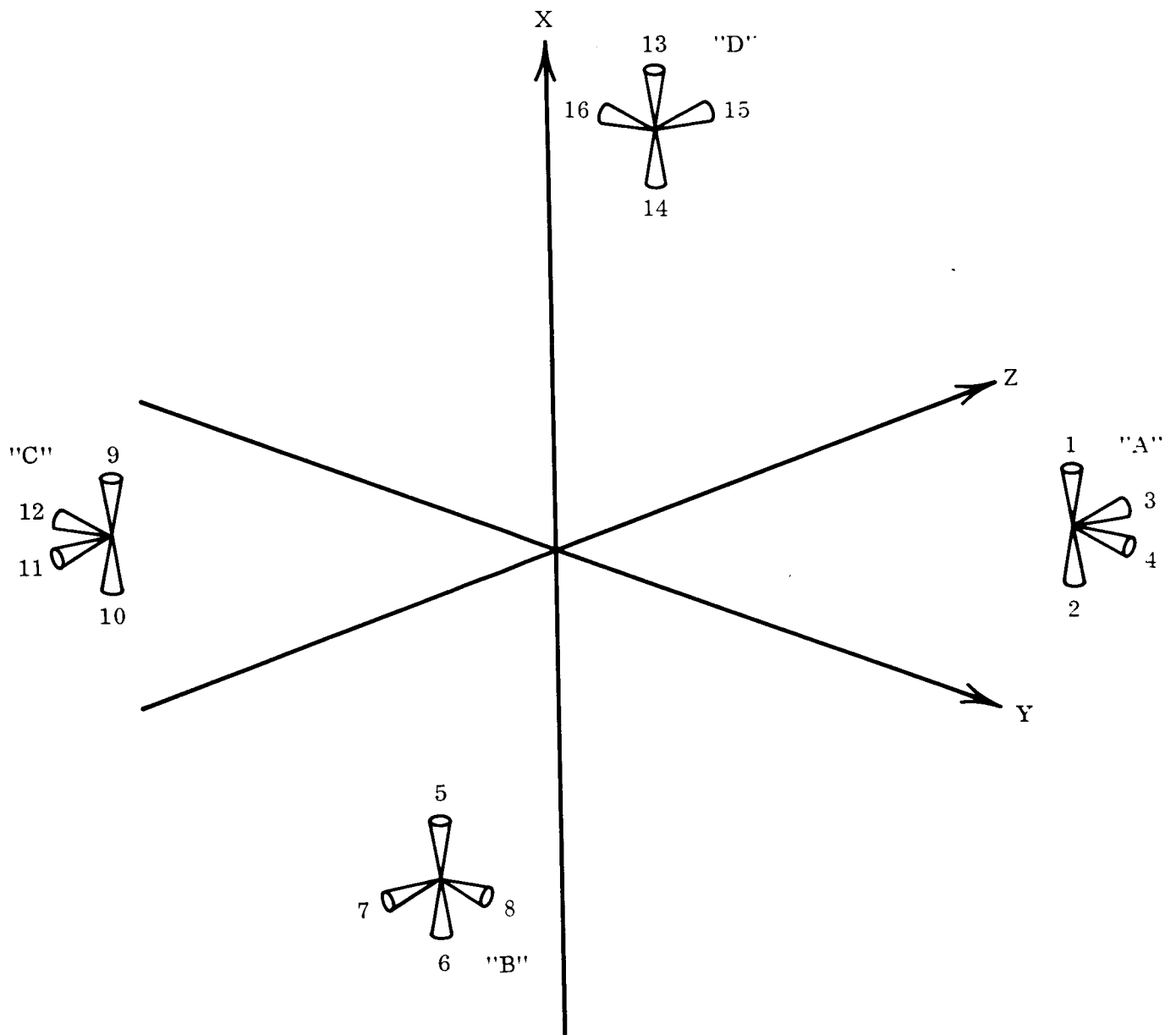


Figure 4-3. RC Jet Locations

Appendix D provides a describing function stability analysis of the trim gimbal plus RC jet system. The important conclusions reached in the analysis are:

1. Satisfactory stability can be achieved with a simple constant speed gimbal drive mechanism.
2. An acceptable range of equivalent motor time constants is 0.05 sec. to 0.3 seconds. Although larger equivalent time constants provide more relative stability, gimbal response times would be degraded.
3. A gimbal rate ($\dot{\delta}$) of 0.2 deg/sec appears to be satisfactory and is recommended.
4. Use of this trim scheme makes the use of on-off control undesirable. Pulse modulation should be used with this type of trim control.
5. The trim servo can be operated with the trim relay threshold above or below the modulator deadzone. For the former case, the attitude error can be maintained at a small steady state off-set for a constant moment unbalance. Since the RCS is operating at moment unbalances below 5% of rated control torque, some RCS propellant will be consumed. Considering the latter case a zero average attitude error can be achieved for a constant moment unbalance. A negligible amount of RCS propellant will be consumed for this case. However, a much higher trim servo duty cycle will result.
6. When gimbal rate is at steady state value of 0.2 deg/sec gimbal angle overshoot should be less than .02 degree when the gimbal motor voltage is removed.
7. Assuming 500 ft-lb. initial c.g. unbalance moment, thrust vector alignment at the start of powered descent must be within 1.15 deg (3 σ) of the line passing through the true c.g. The gimbal will then align within 6 seconds.

Modulator

The modulator shown in figure 4-2 is required to convert error signals to ON-OFF pulses for actuating the RC jets.

During normal attitude modes of operation (Guidance, Attitude Hold, and Attitude Command), the reaction jets are controlled by an error signal composed of a command signal from either the guidance system or the pilot's attitude controller and feedback signals from the positional and rate sensors. Because the reaction jets are bistable devices and multi-functional with regard to vehicle control, it is necessary to process the error signal before it can be applied to the jets. This is the purpose of the pulse modulator and jet select logic circuits. This section will discuss the several pulse modulation techniques currently being studied at GAEC and presents some results obtained to date.

ON-OFF Modulation

The on-off modulator provides a constant amplitude whenever the input error signal is non-zero. This signal is sent through the jet select logic to generate vehicle torques such that the error

signal is driven toward zero. The system has several advantages such as 1) supplying maximum available control torque which minimizes system response time and 2) it is inherently a simple and reliable configuration. The main disadvantage is in its limit cycle performance. A comparison of the modulation techniques shows that the ON-OFF modulator gives the largest duty cycles and largest minimum rate change and therefore the poorest limit cycle performance. The system performance is also very sensitive to gain changes.

ON-OFF (Induced Rate Feedback)

This system uses the same modulation technique as discussed above, except the input error signal contains an additional component proportional to the integral of the applied jet torque. Proper adjustment of the relative magnitude of this component makes it possible to achieve improved limit cycle operation. Thus this system maintains the torque capability and simplicity of the on-off system and provides in addition lower duty cycles and minimum rate changes. A disadvantage of this technique is that the average positional error increases when an external torque (such as main engine thrust misalignment torque) is applied to the vehicle. A study is presently being conducted to determine if the normal and induced rate on-off systems can be used selectively throughout the LEM mission phases so as to achieve high performance and reliability.

Pulse Ratio Modulator

The pulse ratio modulator provides a constant amplitude, variable width, variable frequency pulse train output with a duty cycle proportional to the input error signal. The output is applied through the jet select logic such that the subsequent vehicle reaction jet torque nulls the input error signal. Since the vehicle essentially integrates the applied reaction jet torques, i.e., it averages the torque pulses, and since the modulator duty cycle is proportional to the average applied torque, the pulse ratio modulator will closely approximate a linear gain. This gain is adjusted such that the system positional errors during thrusting periods are less than the maximum allowable values. A possible disadvantage of the pulse ratio modulator is that for a linear gain, with a minimum pulse width of 6 msec, the modulator will operate at a maximum frequency of 40 pps when a duty cycle of .5 is needed. The frequency may be too high for the reaction jet system capability.

Pulse Width Modulator

The performance and operation of the pulse width modulator is similar to the pulse ratio modulator discussed above. In this system the pulse amplitude and frequency is fixed, while the pulse width is varied proportional to the error input signal. Studies on this system have started and show promise of being as good as PR modulation performance-wise with a simpler design.

The dynamic performance of the modulators is most critical during the ascent phase and will therefore be discussed in more detail in section 5.

Lunar Landing Simulation

Figure 4-4 shows a block diagram of a single axis of the lunar landing simulation presently set up at GAEC. The simulator is capable of a full six degrees of freedom with combined display and base motion. Only the Attitude Hold Mode has been flown to date but others are presently being programmed.

One significant result that has been obtained is that a single pair of RC jets about each axis plus a trim gimbal have provided satisfactory control effectiveness. More detailed results must await data reduction and will be included in a subsequent report. A description of the simulation itself is given in GAEC report No. LED-570-1 "Detailed Presimulation Report for Phase A Lunar Hover and Landing Simulation:", 4 March 1963.

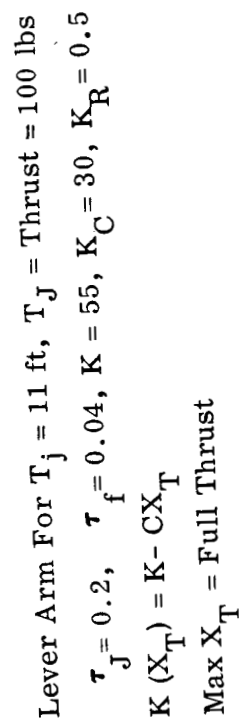
4.2.2 Case B - High Gain Gimbal Plus RC Jets

Figure 4-5 shows a block diagram of this configuration. Modes of operation, jet location, jet logic and modulation schemes for the RC jets are basically the same as for case A. The gimbal drive requirements, however, are much more stringent. Details of the gimbal drive are discussed in Appendix C. The important characteristics are the following:

Max displacement	= 12 deg
Max rate	= 0.5 rad/sec (28.6 deg/sec)
Acceleration	= 10 rad/sec ² (573 deg/sec ²)
Accuracy	= 0.02 deg
Gear train ratio	
Power required	= 1232 W peak = 123 W average (assuming duty cycle - 10%)
Drive mechanism wt.	= 42 lbs.
Gimbal ring weight	= 40 lbs.

The gimbal rate was based on a requirement for at least 0.3 rad/sec for control system stability. This was determined in a computer study which will be described in section 4.3. The margin over 0.3 rad/sec must be limited since peak power increases to enormous values as gimbal rate increases. (see Appendix C)

The maximum deflection angle was determined by nominally setting vehicle acceleration at 10 deg/sec² with hover to touchdown inertias. This is the minimum value for which the gimbal is at all worth considering (roughly 1/2 the capability of a pair of RC jets). Reducing the deflection angle to 6 degrees, as in the case of the trim gimbal, makes the control gimbal practically useless during hover to touchdown.

Pitch & Yaw Axis Only
ED = Emergency Direct

4.3 Comparison Between Case A and Case B

A comparison is made here between the two systems in question by discussing analog computer responses, gimbal requirements, reliability, and crew safety.

Analog Computer Study

Figure 4-6 shows a diagram of the computer simulation used to compare the two systems. The study was confined to four in-plane degrees of freedom; x and y vehicle translation, absolute vehicle rotation (ψ), and relative engine gimbal angle (δ). System response to attitude commands were studied without adding c.g. offset. The trim gimbal is therefore not included in the RC jet control system (Case A). Stability with the trim gimbal present is treated separately in Appendix D. For the gimbal plus RC jet control system (Case B) the effect of c.g. offset is to impose a bias on the system.

It has been assumed that the gimbal engine actuator has the characteristics of a simple electric motor. A torque is applied to the gimbal engine that, at zero engine rotation velocity ($\dot{\delta} = 0$) is proportional to the engine error angle ($\delta_e - \delta$). The maximum available torque is equivalent to the maximum stalled motor torque of the electric actuator. The "steady state" rotation velocity of the unrestrained gimbal engine is proportional to the "steady state" gimbal engine error angle. The maximum engine velocity ($\dot{\delta}_{\max}$) is equivalent to the maximum velocity of the electric actuator.

The following results were obtained from the study:

1. In the Case B system the RCS loop predominates when large errors are present. When error approaches that value inherent in the On-Off RCS limit cycle, the gimbal control loop predominates and causes the steady state error to approach zero. The RCS loop is, however, a simple On-Off system in this simulation so that limit cycle performance is not optimum.
2. Stability considerations lead to the conclusion that it is unnecessary to have high torque gimbal actuator characteristics. A moderate torque actuator, providing a $\dot{\delta}_{\max}$ of 3 rad/sec², with a lead-lag feedback network is adequate. The power required to deliver the needed torque for a 3 rad/sec² acceleration is discussed in Appendix C.
3. Table 4-1 lists some response times under various conditions for the two systems. (In addition, as a matter of interest, some runs were made using gimbal control only. The results for these runs were very poor.)

It is seen that when main engine thrust (F) is at its maximum, the Case B system demonstrates considerable improvement in response time. At one third maximum thrust, however, which is the upper end of the hover-to-touchdown thrust range, there is little or no difference between Case A time response and Case B time response.

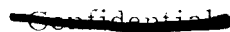


Figure 4-6. Lem Rigid Structure Descent Control System Feedback Diagram

Table 4-1

Representative Results From Analog Tests of Case A and Case B Attitude Control Systems to Step Inputs										
θ_c (Degrees)										
	1	2	4	8	16	θ Steady State	Test #			
Time (seconds) for $\theta = \theta_c + .5$	Case A (RCS only)	.60	.75	1.0	4.0	7.0	1			
	Case B (RCS & gimbal) F_{max}	.56	.80	1.1	2.7	6.0	2			
	Gimbal control only F_{max}	.60	2.0	7.2	30	∇	3			
	Case A	.40	.65	.84	1.2	3.2	4			
	Case B $1/3 F_{max}$.28	.46	1.0	1.8	3.2	5			
	Case B F_{max}	.26	.46	.92	1.8	2.6	6			
	Gimbal control only $1/3 F_{max}$.52	3.6	11.5	20	∇	7			
	Gimbal control only F_{max}	.30	.66	2.2	10	20	8			
	Case B $G=3, K=1$ F_{max}	.24	.40	1.8	6.0	*	9			
	Case B $G=1, K=1$ F_{max}	.28	.53	.80	1.8	3.4	10			
	Case B $G=1, K=1/3$ F_{max}	.40	.54	1.2	∇	∇	11			

∇ Divergent Oscillations

* Not Tested

Note: F = Main Engine Thrust, θ_c = Attitude Command

Gimbal Requirements

A comparison of gimbal characteristics for the Case A and Case B systems is as follows:

<u>Parameter</u>	<u>Case A</u>	<u>Case B</u>
Max deflection angle	6.0 deg	12.0 deg
Max rate	0.2 deg/sec	28.6 deg/sec
Max acceleration	.035 deg/sec ²	10 rad/sec
Peak Power	27 w	1232
Av Power	6.8 w	123 w
Gimbal Ring Weight	40 lb	40 lbs.
Gimbal Drive Weight		
(including redundant drive units and electronics)	22 lb.	42 lbs.

It is seen that the control gimbal of Case B has three significant disadvantages; (1) a large deflection angle is needed when c.g. compensation and attitude control needs are summed, (2) extremely large peak power is needed when large vehicle rates are commanded, and (3) weight is roughly 20 pounds greater for the control gimbal drive mechanism.

Reliability and Crew Safety

Although reliability has not been investigated quantitatively for the two systems in question, it is obvious that the Case A system is more reliable from a complexity viewpoint, all other things being equal. In order to verify this point, a reliability analysis will be performed.

A point that must be considered related to crew safety is risk involved in using a high speed gimbal versus a very low speed trim gimbal. In the latter case there is time to take corrective action in the event of a run-away gimbal. With the high speed gimbal the time available for corrective action will be extremely small at best.

SECTION 5. ASCENT THRUST VECTOR CONTROL5.1 Thrust Magnitude Control

As explained in Section 3 a constant main engine thrust level of 3500 lbs is used during the ascent phase. Reaction control jets are also available for translation along the main engine axis (x-axis) yielding either 200 or 400 lbs of thrust, the latter being on an emergency or redundant basis. The following thrust levels are therefore available during ascent.

RC level = 200 lbs
RC level = 400 lbs
Main engine minus RC = 3300 lbs
Main engine minus RC = 3100 lbs
Main engine only = 3500 lbs
Main engine plus RC = 3500 lbs
Main engine plus RC = 3900 lbs

Selection of these levels will be done by direct switching. The main engine is turned on and off automatically by either the primary or back-up guidance systems. Manual override of the main engine will also be provided for emergency situations.

During normal manual operation in docking and in rendezvous the RC jets are used.

Appendix F summarizes the preliminary ascent engine specifications. An important problem area that remains to be resolved is the thrust level accuracy that is attainable. The accuracy presently specified is +10, -1% at the end of the duty cycle. This would preclude possible open loop velocity change commands from guidance, which may be required in the back up guidance system. Since the back-up guidance system has not yet been established this problem can not be properly pursued until a later date. A possible solution would be to tighten thrust level predictability requirements rather than reducing thrust variation.

5.2 Thrust Direction Control

Present plans are for thrust direction control (attitude control) during ascent to be obtained solely by means of RC jets. This includes normal maneuvers plus compensation for c.g. shift, etc. The use of a gimballed engine was investigated briefly but was excluded for the following reasons:

1. Size of the gimbal would be prohibitive in the ascent stage.
2. The same RC jets that are used in descent are used during ascent. The control torque available is therefore more than ample since vehicle inertias are much lower. The torque and torque impulse requirements given in Section 3 are well within the capability of the RC jets alone. The possibility also exists of using the RC jets as an unbalanced couple for c.g. compensation. This would probably complicate the jet logic, however.

3. It is felt that a reasonable balance can be made between fuel management techniques for limiting c.g. travel, and RC fuel required for c.g. offset compensation, so that overall weight with and without a trim gimbal is not greatly different.

The last item is presently undergoing careful scrutiny in a general weight distribution study.

The ascent thrust vector control system will therefore be basically the same as that pictured in Figure 4-1 in Section 4 with the trim gimbal loop deleted. For clarity the diagram is redrawn in Figure 5-1. The same modes of operation are available as in the descent configuration, and the remaining portions of the system retain the same characteristics with the exception of forward loop gain. At least one gain change will be required over the final descent gain.

CONTROL DYNAMICS

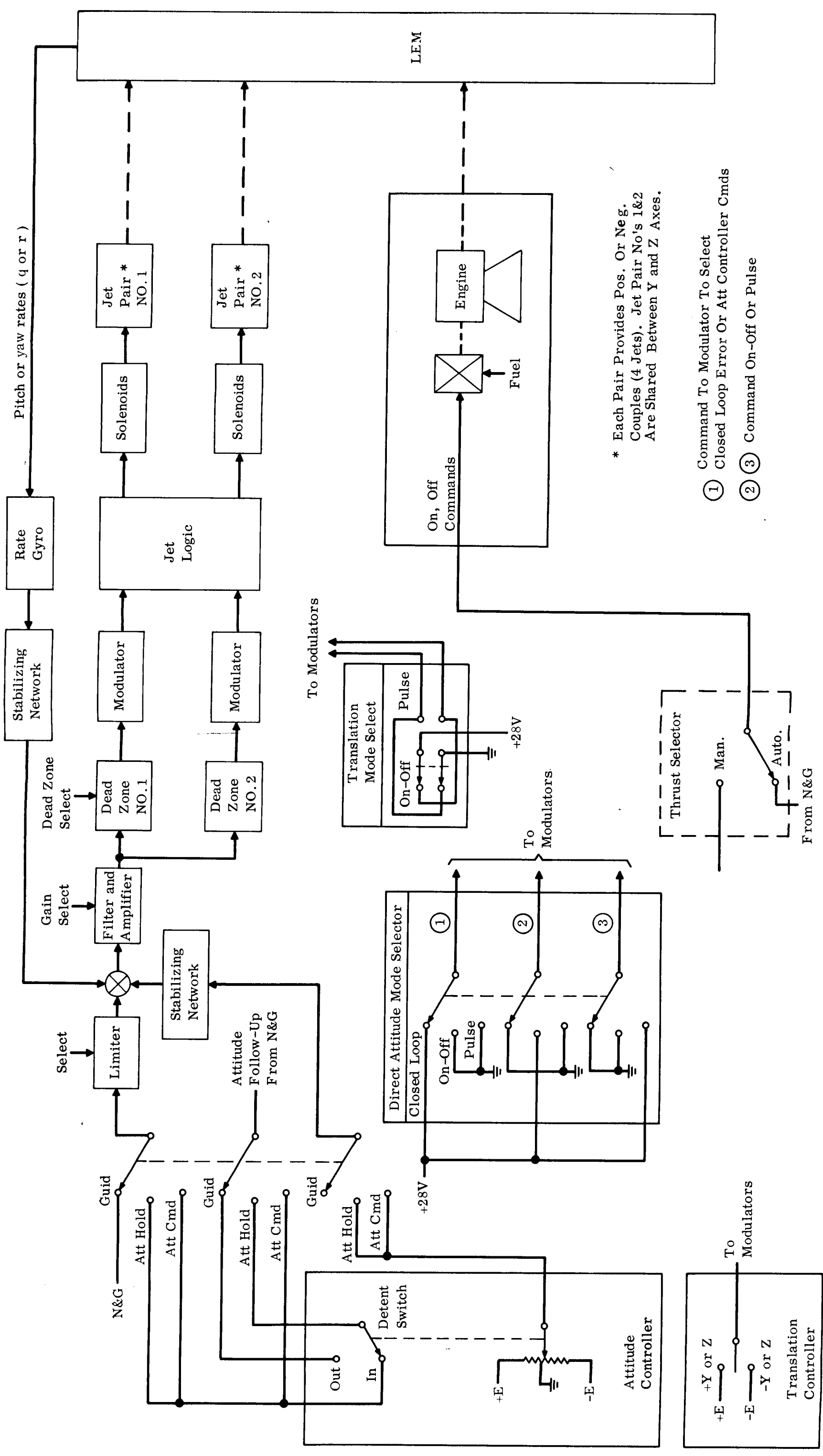
There are five basic considerations that will determine the selection of any reaction jet control system for the LEM vehicle. They are:

1. Duty Cycle (D) - ratio of the jet on time and limit cycle period.
2. Residual Rate ($\Delta \dot{\theta}$) - rate at which vehicle drifts during limit cycle operation.
3. Maximum Angle of Excursion (θ_M) - maximum value of attitude excursion about some nominal during limit cycle operation.
4. Capability to control large moment unbalances, and resulting jet pulse frequency.
5. Transient Response.

Also of interest is the range of rate gain (K_R) which is interrelated with the first four items above.

A computer study was made of the ascent autopilot to determine steady state limit cycle response and response to a steady state disturbance torque of 250 ft-lbs. The latter case is approximately the disturbance that results from a one inch c.g. offset during ascent engine thrusting periods. The four pulse modulator techniques described in Section 4 were compared with these conditions imposed. Details of the study are given in Appendix D. The important conclusions that were reached are the following:

1. Both the PR modulator and the PW modulator can meet the limit cycle residual rate requirements during rendezvous and docking that $\Delta \dot{\theta} < 0.5$ deg/sec and provide low values of D and θ_M (see Table 5-1).



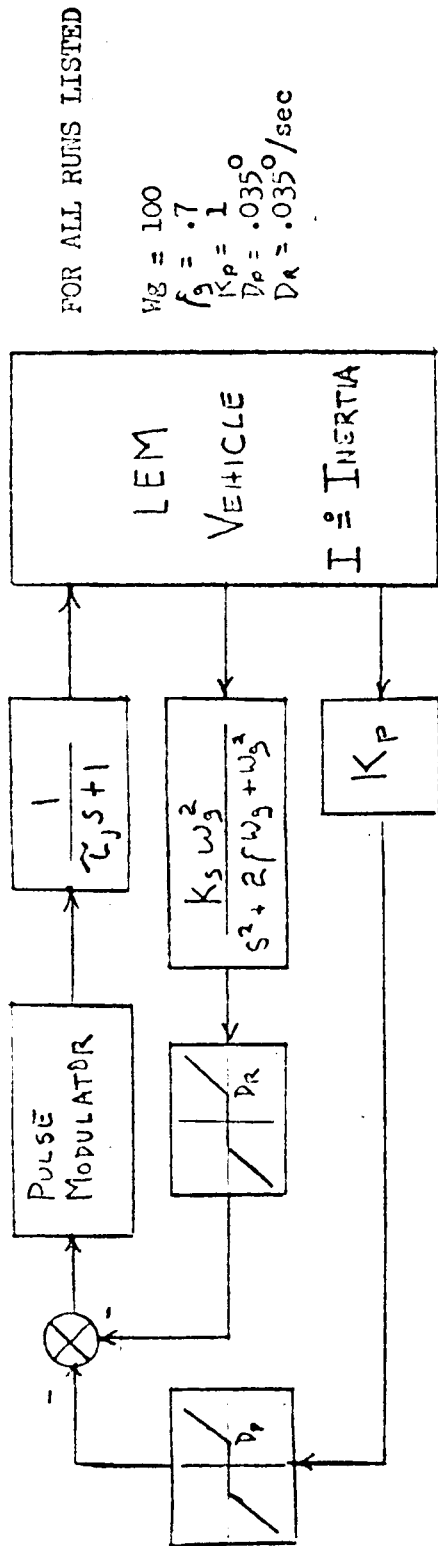
* Each Pair Provides Pos. Or Neg. Couples (4 Jets). Jet Pair No's 1&2 Are Shared Between Y and Z Axes.

① Command To Modulator To Select
 Closed Loop Error Or Att Controller Cmds
 ② ③ Command On-Off Or Pulse

Figure 5-1. Simplified Block Diagram, Pitch or Yaw Axis Ascent FCS

PULSE MODULATOR CHARACTERISTICS

TABLE 5-1



RESULTS

PARAMETERS

MODULATOR CHARACTERISTICS	Ω	t_r	τ_y	K_g	I	MINIMUM RATE CHANGE $\Delta\dot{\theta}$ (DEG/SEC)	MAX. POSITION ERROR θ_m (DEG)	DUTY CYCLE γ	PERIOD T (SEC)	REMARKS
ON-OFF 	.5	1%	7ms	.25	1050	1.3	.263	.170	1.0	Small changes in K_g causes large changes in $\theta_m, \gamma, \Delta\dot{\theta}$
	.5	1%	7ms	.4	2200	.575	.282	.065	1.7	
	.1	1%	7ms	.05	1700	1.32	.095	.470	.375	
INDUCED RATE	.1	1%	7ms	.05	1700	.286	.032	.020	2.7	Induced feedback loop shows a wide tolerance to gain changes.
PULSE RATIO	.01	-	0	.15	1050	.303	.029	.018	.7	$\Delta\dot{\theta}$ is independent of K_g over a wide range.
	.01	-	0	.2	2200	.173	.026	.010	1.1	

2. The PR modulator appears to offer slightly better limit cycle performance throughout the mission. Both require two gain changes during flight (additional analysis required on PWM to confirm this estimate).
3. Both modulators exhibit good large angle transient response characteristics.
4. Both modulators effectively control large moment unbalances. The attitude oscillations during limit cycle about Θ_{AV} will be smaller using PRM than PWM. However, because of a significant decrease in RC jet specific impulse at shorter pulse widths, use of a pulse width modulator will reduce RCS propellant consumption during powered ascent by approximately 50 lbs (for a constant 250 lb-ft moment unbalance).
5. Use of Pulse Width modulation is tentatively recommended for LEM flight control system, with PRM as the alternate choice.
6. Analytical studies are in process to confirm that a PW modulator frequency change need not be made during flight.

In addition to the above study, a preliminary study of the fuel slosh problem during ascent has been made. The results of this study are given in appendix F and are briefly summarized as follows:

1. Fuel slosh coupling with FCS dynamics is significant but stable.
2. Baffles are more effective than bladders in the ascent stage fuel tanks for reducing slosh effects.
3. The time response of the system to a step command is that of a well damped rigid body mode with a lightly damped, small amplitude slosh mode superimposed on it.

CONTROL ACCURACY

Control accuracy during ascent has been tentatively established at ± 0.2 degree during ascent. The reason for relaxing from ± 0.1 deg is that if 0.1 deg is used the control loop may require more complex compensation networks in the presence of large steady state disturbances due to c.g. shift. It is questionable however, whether this error can be allowed from a guidance viewpoint. If further investigation deems it necessary the requirement may have to be tightened to ± 0.1 deg.

Another consideration here is that the actual thrust direction may be misaligned by as much as 0.5 deg relative to the engine reference line, or x-axis of the vehicle. It is considered a guidance function to sense undesired cross axis accelerations due to this misalignment and provide corrective attitude commands to compensate for it.

DOCKING SIMULATION

A docking simulation was performed at NAA, Columbus using the system representation shown in Figure 5-2. The simulator provided a full 6 degrees of freedom by means of a visual display. The cockpit was fixed based. The simulation and its results will be described in detail in a forthcoming report. Some of the early results are as follows:

1. A desirable system rate response time is 0.2 seconds.
2. Direct on-off attitude control is very undesirable for manual control whereas direct minimum impulse is satisfactory.
3. Direct on-off translation control is satisfactory for manual docking.
4. Docking maneuvers were performed satisfactorily with RC jet failures and with open rate and position feed back loops (i.e., both open together). The pilot could not compensate for an open rate loop only for any extended time period.
5. Docking can be performed by using only visual cues.
6. A trapeze docking device is preferred by pilots in malfunction situations.

Further data reduction is needed to determine such items as the relation between translational and rotational motion.

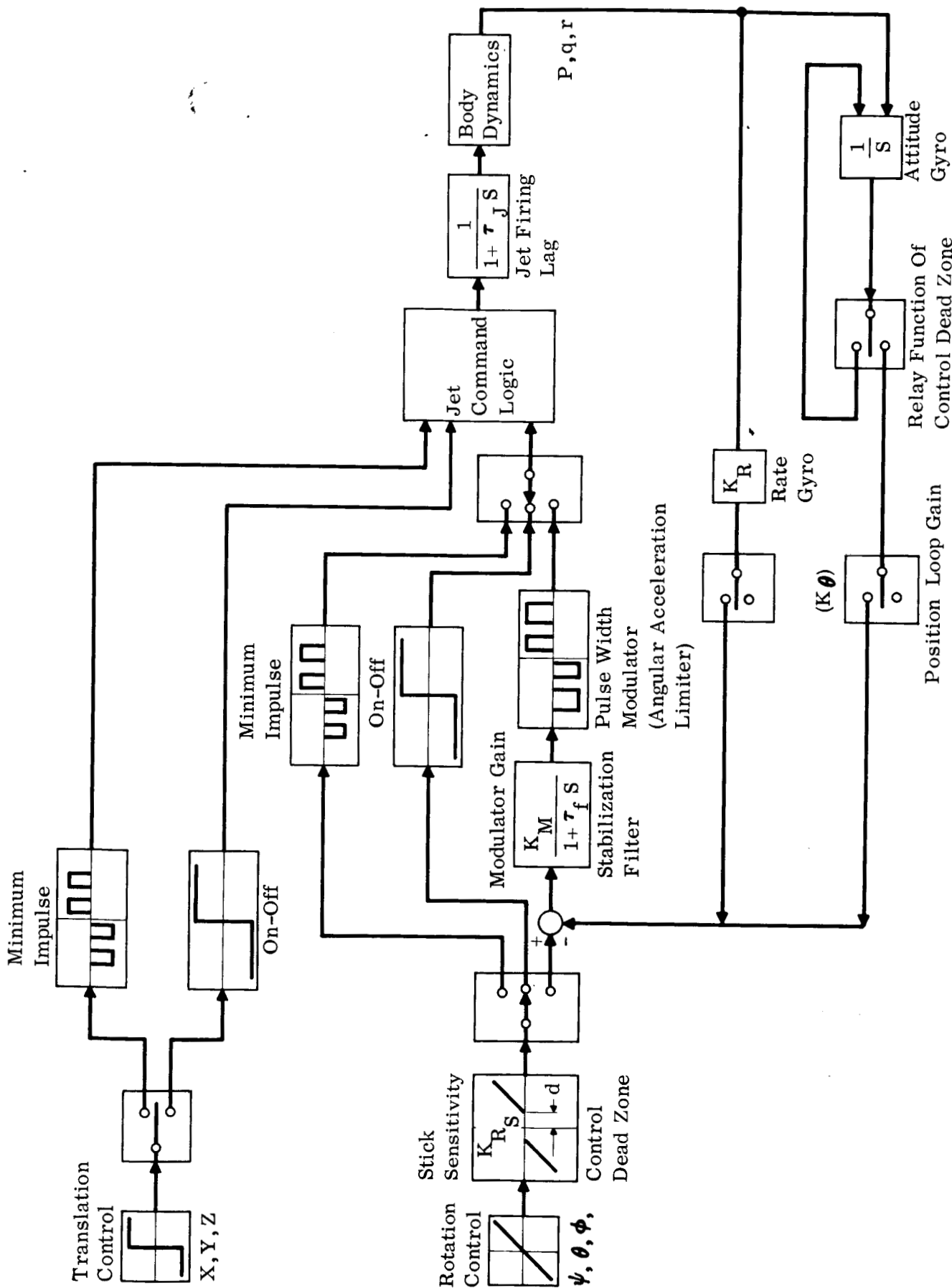


Figure 5-2. Lem Control System Docking Simulator

SECTION 6. ABORT CONSIDERATIONS

This section will not be available until a subsequent version of the thrust vector report is released. A brief statement on abort restraints to the FCS is given in Section 3.

SECTION 7. CONCLUSIONS AND RECOMMENDATIONS

The primary conclusion that is reached in this report is that Reaction Control jets working in conjunction with a very slow rate trim gimbal will meet the thrust vector control requirements during the descent phase of the mission. The important reasons that support this conclusion are the following:

1. A single pair of RC jets will meet the control torque requirements for a normal mission if a slow rate trim gimbal is used for c.g. trim.
2. The only time that large attitude maneuvers are needed while thrusting is during hover to landing. This is the time when the gimbal is least effective since thrust is close to minimum, or conversely very large gimbal angles would be needed to make the gimbal effective.
3. A maximum of 6 degrees deflection is considered practical. An estimated 3.5 to 4.5 degrees is needed for c.g. trim. This leaves very little for attitude control torque augmentation.
4. RC control torque can be doubled for possible "hard over" terrain avoidance maneuvers or abort maneuvers by employing the redundant pair of jets that is available about any one axis at a time.
5. The high rate gimbal actuator is 20 pounds heavier than the trim gimbal and requires 45 times as much peak power (1200 watts vs. 7 watts), and roughly 18 times as much average power.
6. Although a quantitative reliability analysis has not been completed, the high rate gimbal is more complex since it needs servo loop electronics. The trim actuator is a simple on-off device and is therefore more reliable.
7. The possibility of a run away gimbal presents a much greater crew safety hazard with the high speed gimbal (20 deg/sec) than the low speed trim gimbal (.2 deg/sec).

For these reasons the system designated as case A in Section 4 is recommended for the LEM vehicle.

It was also concluded that hover to touchdown maneuvers and abort maneuvers are the primary factors that determine the maximum torque required for thrust direction control.

During ascent the preliminary conclusion is that the RC jets can provide the thrust direction control requirements, provided a gain change is made.

~~CONFIDENTIAL~~

REPORT LEM-290-2
DATE 5/14/63

SECTION 8. FUTURE WORK

The following areas will be investigated and will be discussed in the next thrust vector control report:

1. Optimization of control dynamics.
2. Detailed designs of RC jet logic, throttle serve, gimbal drive unit and RCS modulator.
3. Interface with N & G as well as other subsystems.
4. Requirements for automatic landing.
5. Descent slosh dynamics.
6. Main engine flexure modes.
7. Abort aspects of thrust vector controls.
8. Detailed results of simulation programs.
9. Control and display aspects of thrust vector control.
10. Recheck Flight Control design for a 28,000 lb. vehicle and its corresponding inertias.

In addition, it is hoped that many of the areas that are preliminary in this report will be firmed.

APPENDIX AMISSION PROFILE

Tables A-1 and A-2 provide the detailed FCS requirements and sequence of events in terms of a nominal mission profile. It is emphasized that this profile is very preliminary and subject to change. The purpose of presenting it is to offer a typical operational profile for the FCS. The present nominal mission includes an 80 n.mi circular orbit, in which the CSM remains from separation until docking. The mission profile pictured in the table, starts at $t = 0$ at separation. Except for the flare and hover phases, a constant thrust of 8800 lbs. was assumed for the nominal descent trajectories.

Descent: The LEM separates 100 ft. from the CSM within 78 sec. The vehicle is given an initial Δv of 1.3 fps in the negative x direction and is then allowed to coast for an additional 94 ft. A Δv of 1.3 fps is then applied in the positive x-direction. At the termination of this phase the LEM is 100 ft. displaced from the CSM and is traveling at a zero relative velocity in an 80 n.mi circular orbit. In order to align the thrust axis (x axis) to the local vertical, a 90° negative pitch command is given. Both separation and pitch is achieved within 2 min. The astronauts are now allotted 8 min for necessary checkout procedures before injecting into synchronous orbit. Pulsing the reaction jets will be necessary to maintain the x axis along the local vertical. Separation was achieved with two reaction jets (100 lb. of thrust per jet) as was the pitch maneuver.

Various preliminary computer studies were conducted for several synchronous orbits using circular orbital altitudes and pericynthian altitudes as parameters. For a CSM orbital altitude of 50,000 ft the Δv required for injection into synchronous orbit is 375 fps.

The burning time for injection is approximately 0.466 minutes. During this time the orientation of the thrust axis is changed by 4° to attain the proper thrust direction.

At the present time there is a trade-off study of synchronous orbit vs. fully powered descent. The biggest draw-back for fully powered descent seems to be the low circular orbital altitudes that will be necessary in order not to exceed the Δv requirement. A nominal altitude for this condition turns out to be approximately 40 n.mi. This will place an additional requirement on the CSM plus it will add a tighter launch window requirement. The main disadvantages of the synchronous orbit approach is a longer flight time and an unfavorable LEM lead angle (assuming injection on down-side of synchronous orbit and initiation of powered descent at pericynthian). The nominal missions listed in Table #A-1 uses the synchronous orbit type of descent. The nominal mission presently considered does not include one complete coast in synchronous orbit. However, in view of the fact that the mission profile is still open to changes, the attitude constraints during one complete coast in synchronous orbit was also considered. Injection into synch. orbit occurs at point (1) (refer to synchronous orbit diagram in table #A-1), at point (2) the vehicle requires an

approximate pitch of 95° to align the z axis with the local vertical and the thrust axis opposite the flight path. Before point (3) is reached there will be five land mark sitings of a duration of 5 minutes per siting. Minimum limit cycling is required during sitings. Pulsing of the RC jets will be required to maintain the z axis along the local vertical. At point (3), the situation arises which requires a maneuver to protect the LEM windows (Z_L) from facing either the sun or lunar reflections. The following is the necessary sequence of events to satisfy the sun constraint and at the same time avoid gimbal lock. First roll by 90° . While LEM is traveling from point (3) to point (4) it will rotate through 180° w/r to inertial space but remains in the same attitude w/r to the lunar local vertical. This can be achieved by a single coupled pulse, about Z_L that will provide 180° rotation in approximately 60 minutes. From point (4) to point (5) the vehicle will maintain its positions w/r to inertial space for sighting on two stars for updating the IMU. During this observation time (10 min.) minimum limit cycling will be required. During this period LEM will pass through a lunar central angle of approximately 31° . After the IMU has been updated, LEM must be reoriented to observe two landmarks, for updating the synchronous orbit. Again to avoid gimbal lock it is necessary to first roll and then pitch -90° and $+31^{\circ}$ respectively. From the start of synchronous orbit updating to initiation of powered descent @peri, the vehicle's attitude w/r to the local vertical can be maintained by a single coupled pulse about Y. Before initiation of powered descent an additional 4.5° negative pitch is required. At point (6) LEM is at pericynthian in its proper orientation to initiate powered descent.

The phase lead of LEM w/r to the CSM (at pericynthian) makes this point unfavorable for starting powered descent. There are a few studies which are presently being conducted to eliminate this phase problem. Two of the trade-offs presently under consideration are initiating powered descent before pericynthian and injection into synchronous orbit on the up side rather than the down side.

For the first 320 sec of powered descent the thrust is kept constant and the altitude drops from 50,000 ft. down to approximately 2,000 ft. In the next 36 sec a flare maneuver is performed in which the thrust variations is approximately 5:1. The LEM now starts its hover phase from an altitude of 1000 ft. Essentially LEM will be belly down all the way to hover. Hover to touchdown should be completed in approximately 120 sec. During this time it might be required to roll as much as 180° , for proper radar coverage prior to lift-off.

Ascent: Table #A-2 provides similar information for ascent as did the previous table for descent. For the first 17.4 sec the thrust vector is vertical. A roll of $+90^{\circ}$ might be required for full radar coverage. Presently there are studies being made to increase the radar coverage and in turn eliminate the roll maneuvers necessary to satisfy the present

radar restraint. IEM is then pitched at a constant rate of 1.02 deg/sec for 85.6 sec. The attitude w/r to the local horizontal is then maintained for the remaining burning period (approximately 253 sec). Hohmann transfer is achieved immediately after burnout (356 sec from launch). If a 50,000 ft parking orbit is desired, burnout will occur between 350-356 sec from launch.

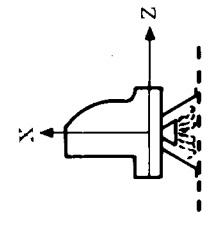
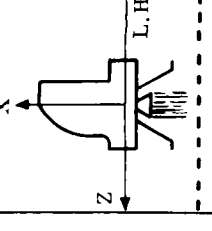
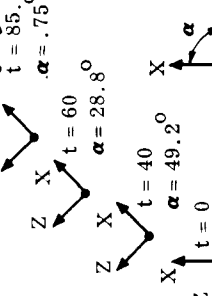
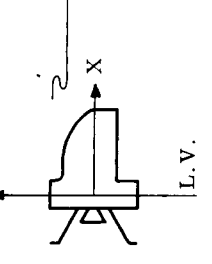
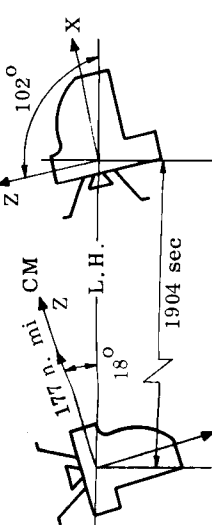
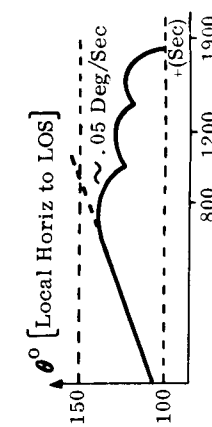
During the entire transfer it is desired to have the LOS aligned with the z axis at all times. Minimum limit cycles will be required. At the start of Hohmann, a rate command of 5 deg/sec will achieve the necessary attitude after 13.6 sec. The remainder of the transfer orbit will require a few coupled pulses in order to maintain the z axis alignment with the LOS.

Trade-off studies are being made to determine an optimum range to start rendezvous. The ranges under consideration are 40, 30 and 20 n.mi. It seems that 20 n.mi is optimum from a radar standpoint. Rendezvous, as presently planned, will be accomplished through the use of reaction jets only. The jets will be used to reduce the relative range and closing velocity to less than 500 ft. and 3 fps, respectively. The IEM z and x axes are subject to a number of attitude constraints during this mission phase:

1. z axis constraints:
 - a. continuous alignment with LOS to CM.
 - b. inertially fixed w/r to stars to facilitate a manual-visual rendezvous.
2. x axis must be normal to the LOS angular rate vector in order to null this rate by using only x axis reaction jets.

At this time not much can be said for docking for much of the constraints will be determined from simulation data. However, one major constraint that is presently being considered is to require a minimum impulse as low as 0.2 lb-sec/per jet.

Mission Profile * - Lift-Off to Docking

						<p>* (1) LEM wt @ L.O. = 7379 lb (2) Main Engine Thrust = 3K lb (3) Isp = 310 (M.E.) (4) Isp = 300 (RC jets) (5) 80 n. mi (circ. orbit)</p>
<p>Mission Phase (Time)</p>	<p>Lift Off at 90° t = 17.4 sec</p>	<p>Pitch Over @ a rate of 1.02 deg/sec, until pitch att w/r L.H. = 75° Δt = 85.6 sec</p>	<p>Maintain Attitude w/r to Local Horizontal Δt = 253 sec</p>	<p>Coast in Hohmann (2230 sec) Coast in Hohmann. Pulse jets to keep LOS aligned with Z axis Δt = 13.6 sec</p>	<p>Rendezvous from 20 mi out. .2 millirad/sec radar resolution; 0% thrust variation Δt = 1600 sec</p>	<p>NOTES (1) The req'd min. impulse is not a definite constraint at the present. Inputs from simulator results will be the determining factor. (2) Hohmann transfer is achieved immediately after burnout (356 sec from launch). If a 50,000 ft parking orbit is desired, burnout will occur between 350-356 sec from launch. (3) Start rendezvous at a 20 n. mi range for radar optimization. (4) The ΔV requirements for rendezvous are rough cut numbers from preliminary studies. Additional studies are now in progress (5) Attitude rates and accelerations are nominal values which will do the job.</p>
<p>Parameters</p> <p>Deg Δφ Δθ Δψ</p> <p>Deg/sec p q r</p> <p>Deg²/sec ṗ ḡ ṙ</p>	<p>+90° - - 5.16 - - 5.94 - -</p>	<p>89.25 - 1.02 - - 0.238 -</p>	<p>Pulse jets to maintain Attitude w/r to L.H.</p>	<p>+67.15° - - 4.94 - - 7.26 - Neglect</p>	<p>See figure above ~ 0.05 Undetermined</p>	<p>Docking from 500 ft</p>
<p>RC - ΔV -fps RC-Fuel Consumed (earth lbs)</p>	<p>- 5.74</p>	<p>- 26</p>	<p>- 76.5</p>	<p>- - 0.103</p>	<p>110 (in X direct-400 lb thrust); 35 (Z direct-200 lb) ~65 lbs</p>	<p>Awaiting Simulation Data</p>
<p>Main Engine ΔV fps Fuel Consumed b. M.E. -lbs</p>	<p>198 168.5</p>	<p>1220 830</p>	<p>4760 2445</p>	<p>- - -</p>	<p>- -</p>	<p>- -</p>
<p>Req'd Min. Impulse/ per jet Req'd Att Error Req'd Att Rate Error</p>	<p>0.6 lb-sec 0.1°</p>	<p>0.6 lb-sec 0.1°</p>	<p>0.6 lb-sec 0.1°</p>	<p>0.6 lb-sec 0.1°</p>	<p>0.6 lb-sec 0.1°</p>	<p>- -</p>
<p>Slug-ft² Station -CGx (inches from CGv thrust axis)</p>	<p>3617-3525 2411-2380 2706-2630 236.7 sta = const assume 1 inch offset throughout Ascent</p>	<p>3525-3200 2380-2280 2630-2250</p>	<p>3200-2130 2280-1950 2250-1050</p>	<p>2130 1950 1050</p>	<p>2100 1930 1000</p>	<p>- -</p>
<p>Range from CM X btwn LOS & Z axis Pitch Att w/r L.H. (α)</p>	<p>98 n. mi @ L.O. 124° @ L.O. 90°</p>	<p>123 n. mi. @ End of Phase 50.75° @ End of Phase 90°-0.75°</p>	<p>177.4 n. mi @ End of Phase 71.8° @ End of Phase 75°</p>	<p>177.4 n. mi 71.8° to 0° -67.15°</p>	<p>20 n. mi - 500 ft 0° +12° - +10°</p>	<p>- -</p>

APPENDIX B - RC JET LOCATION AND LOGICREACTION JET LOCATION

The reaction jet arrangement shown in Fig. B-1 made up of sixteen 100 lb. thrusters has been selected because it offers complete redundancy, is least vulnerable to damage, and has good control response for all modes of operation.

The arrangement presented in the LEM proposal (Fig. 1) positioned the sixteen (16) thrusters in four groups (or quads) of four each oriented along the principal axes. However, since the forward docking hatch also lies on a principal area, and because of the proximity of the LEM windows, the four thrusters in this area cannot be designed as a single unit and must be separated. Problems associated with this arrangement are:

- 1) Complex line runs around pressure cabin in area of windows. Possible thrust degradation of the one remote thruster.
- 2) Thrusters under docking hatch extremely vulnerable to possible damage during docking operation.
- 3) Rocket exhaust near window area.
- 4) Nozzles extend below ascent stage separation plane.

The revised configuration (Fig. B-1) rotates the thruster groups 45° about the roll axis but keeps their orientation along the principal axes. This configuration removes the thrusters from the area of the windows and the forward docking hatch and permits the design of four identical quads. These units can all be located well above the separation plane and will also permit removal of the length of the forward docking hatch that was provided for nozzle clearance. Also, further studies as to the feasibility of a modular type system will now be possible.

Propellant Requirements and System Performance

A comparison of propellant requirements between present and revised thruster locations has been made on a common set of ground rules. The general ground rules are listed in Table B-1. A summary of propellant requirements is tabulated in Table B-2. A comparison is given in Table B-3 for the various types of operations, e.g. limit cycle, maneuvers, etc. As can be seen, an additional 17% of propellant are required for the new orientation. This represents about a 5% penalty.

In comparing system performance, certain advantages are obvious with the revised location of thrusters. Minimum impulse bit control (limit cycle) is improved because of the shorter moment arms. In spite of the shorter moment arms, higher control torques about each of the axes are also available if desired, by firing two pairs rather than one in any given direction. For a one quad failure mode of operation, complete rotational control is still attainable with the revised configuration, since couples are still available. Translational performance for either configuration is identical. In Table B-4 are listed the advantages and disadvantages of the 45° mounting of jets.

~~CONFIDENTIAL~~

PAGE 47

FIGURE B-1 - REACTION JET THRUSTER ARRANGEMENT

ROTATION	THRUSTERS USED	TRANSLATION	THRUSTERS USED
Pitch Up About Y-Y	2, 5 or 9, 14 2, 5 + 9, 14	+ Along Z-Z - Along Z-Z	7, 11 3, 15
Pitch Down About Y-Y	1, 6 or 10, 13 1, 6 + 10, 13		
Yaw Right About Z-Z	1, 14 or 5, 10 1, 14 + 5, 10	+ Along Y-Y - Along Y-Y	12, 16 4, 8
Yaw Left About Z-Z	2, 13 or 6, 9 2, 13 + 6, 9		
Roll CW About X-X	8, 16 or 3, 11 8, 16 + 3, 11	+ Along X-X	2, 10 or 6, 14 2, 10 + 6, 14
Roll CCW About X-X	7, 15 or 4, 12 7, 15 + 4, 12	- Along X-X	1, 9 or 5, 13 1, 9 + 5, 13

~~CONFIDENTIAL~~REPORT LED-290-2
DATE 5-14-63

TABLE B-1 - GENERAL GROUND RULES FORPROPELLANT REQUIREMENT COMPARISON *

1. Minimum impulse bit = .6 lb. sec. (each jet).
2. Maneuvers performed by accelerating for half time and decelerating for half time.
3. $I_{sp} = 300$ sec. (continuous) or 260 sec. (pulsing).
4. 3500 in-lb. moment unbalance continuous about pitch and yaw for complete powered ascent phase.
5. 30 sec. translation prior to touchdown.
6. $V = 330$ ft/sec. from rendezvous to docking (translation).
7. Steady-state thrust equal to 100# (each jet).
8. All moment arms equal to 6.67 ft. for orthogonal mounting. Pitch and yaw moment arms equal to 5.5 ft. and roll moment arms equal to 5.0 ft. for 45° mounting.
9. All operations performed assumed pairs of jets operating.
10. Limit cycle times were computed neglecting control system parameters (longest limit cycle periods attainable).

* Specific ground rules are tabulated under remarks on summary sheet.

~~CONFIDENTIAL~~

TABLE B-2 - SUMMARY OF REACTION CONTROL PROPELLANT REQUIREMENTS *

MISSION PHASE	TIME OF MISSION PHASE	PROPELLANT REQUIRED ORTHOGONAL MOUNTING	PROPELLANT REQUIRED 45° MOUNTING	REMARKS
Checkout	-----	6.00	8.00	Each jet assumed on for 1.5 sec.
Separation	1.3 min.	5.83	5.83	V = 2,56 ft/sec; W = 22,000# (earth)
Pitch 90°	-----	4.84	5.32	Accelerate 45°; Decelerate 45°; I = 11,200 slug-ft. ²
Descent Coast	29.5	.19	.15	25 min. limit cycle; 5° deadzone 4.5 min. limit cycle; 250 deadzone; I = 11,200 slug-ft. ²
Coast One Orbit	123 min.	.21	.17	123 min. limit cycle; 5° deadzone; I = 11,200 slug-ft. ²
Powered Descent	5.5 min.	.87	.70	5.5 min. limit cycle; 1° deadzone; I = 6,000 slug-ft. ²
Roll 180°	-----	4.92	5.68	Accelerate 90°; Decelerate 90°; I = 5,800 slug-ft. ²
Hover to Touchdown and Translation	2.0 min.	22.50	23.00	30 sec. translation corrected for unbalance moment.
Roll 180° at Liftoff	-----	.28	.22	1.7 min. limit cycle; .1° deadzone; I = 5800 slug ft. ²
Powered Ascent	5.0 min.	93.50	113.40	Accelerate 90°; Decelerate 90°; I = 3300 slug-ft. ² 3500 in-lb moment unbalance continuous about pitch and yaw for 5 min.

~~CONFIDENTIAL~~

TABLE B-2 - SUMMARY OF REACTION CONTROL PROPELLANT REQUIREMENTS * (Continued)

MISSION PHASE	TIME OF MISSION PHASE	PROPELLANT REQUIRED ORTHOGONAL MOUNTING	PROPELLANT REQUIRED 45° MOUNTING	REMARKS
Pitch 90°	-----	2.31	2.54	Accelerate 45°; Decelerate 45°; I = 2500 slug-ft. ²
Ascent Coast	60.0 min.	3.96	3.11	50 min. limit cycle, 5° deadzone; 10 min. limit cycle; 25° dead- zone; I = 1700 slug-ft. ² about X and Y; I = 760 slug-ft. ² about Z
Rendezvous and Docking	25.0 min.	146.40	142.18	V = 330 ft/sec; W = 3700# (earth); correction for moment unbalance; 25 min. limit cycle; 1° dead- zone; I = 1700 slug-ft. ² about X and Y; I = 760 slug-ft. ² about Z
		TOTAL = 297.53	TOTAL = 314.60	

* All operations performed assumed pairs of jets operating. An Isp = 260 sec. was assumed during limit cycles and an Isp = 300 sec. was assumed during all other phases. A minimum impulse bit from each jet of .60 lb-sec. was assumed. Steady-state thrust equal to 100# for each jet was assumed. All moment arms were set at 6.67 ft. for orthogonal mounting. Pitch and yaw moment arms were set at 5.5 ft. and roll moment arms at 5.0 ft. for 45° mounting. Limit cycle times were computed neglecting control system parameters.

TABLE B-3 - PROPELLANT COMPARISON

Operation	Orthogonal Mounting	45° Mounting
Idmit Cycling	25.33	19.93
Maneuvers	15.79	17.84
Translations	152.33	152.33
Moment Unbalances	96.08	116.50
Miscellaneous	8.00	8.00
TOTAL	297.53	314.60
Or Approximately	298.00	315.00

TABLE B-4 - 45° MOUNTING OF REACTION CONTROL JETS

Advantages*	Disadvantages*
1. Eliminates split quad in front. a. Removes thrusters from window area and ascent separation plane. b. Removes exhaust plume-pilot visibility interaction. c. Permits feasibility of individual modules.	1. Requires a small increase in propellant (about 5%). 2. 20% less torquing ability.
2. Improves minimum impulse bit control (shorter moment arms).	
3. During powered ascent can provide torquing corrections for as much as a 7.54" C.G. shift as compared to 4.57" for orthogonal mounting.	
4. During powered ascent can provide torquing corrections, during a one quad failure mode, for as much as a 3.77" C.G. shift as compared to 2.29" for orthogonal mounting.	
5. Allows complete rotational control during a one quad failure mode.	

* Compared to orthogonal mounting.

Z-AXIS THRUSTERS

Since no firm requirement has been established for additional Z-Axis thrusters, they are not presently planned.

The idea of adding two (2) additional thrusters along the Z-axis evolved from the desirability of maintaining continual Z axis LOS with the CSM during rendezvous. If a Z-axis thruster failed, switching to the additional pair would allow maintaining the spacecraft orientation, without a propellant penalty, while the closing maneuver was being performed. However, a Z-axis thruster is not the only type of failure that can occur. A bladder failure in one of the RCS propellant tanks for example would require implementing at least a portion of the closing velocity along the X-axis to insure covering the tank discharge port and thereby not lose the use of this propellant. The final closing velocity maneuver, say from one (1) nautical mile away can then be performed along the Z-axis since sufficient propellant can be insured from the dual tank at this point.

If these thrusters are required, they can be implemented at a later date since they will be identical to those now being considered.

APPENDIX C - GIMBAL CONSIDERATIONSTRIM GIMBAL

Since the c.g. of the vehicle is not fixed, a trimming of the descent engine thrust vector so that it always travels through the c.g. must be implemented. This can be accomplished by rotating the engine which is mounted in a two-axis gimbal at a rate that will compensate for c.g. travel and positioning the gimbal such that the steady-state loading on the Reaction Control Subsystem due to c.g. shift is no more than 5% of total torquing capability.

Since the rate of such a system is so low, an open loop control system can be used. The system (See Fig. C-1A) consists of a phase sensitive relay amplifier that drives an induction motor. The motor driving through a gear train that includes a lead screw will position the gimbal to an accuracy equal to the threshold of the relay amplifier. Manual trim will be available.

CONTROL SYSTEM

A simplified block diagram is shown in Fig. C-1 and the following equations define the system response. The summary of torques is,

$$L_c + L_d = J_g \ddot{\delta}$$

where L_c = control torque

L_d = disturbance torques

J_g = gimbal and engine inertia

δ = gimbal angle

From the block diagram,

$$T_c = \frac{\delta_0 N \delta_e}{(s+1)}$$

$$s = \frac{\delta_0 N \delta_e + T_d (\tau_m s + 1)}{J_g s^2 (\tau_m s + 1)}$$

It must be remembered that this system operates in parallel with the RCS control loop. The response of the integrated system is discussed in Section 4. A preliminary stability analysis is discussed in Appendix D.

GIMBAL DISPLACEMENT

The trim gimbal travel limits have been set to $\pm 6^\circ$ based on predicted c.g. shift. Although the actual c.g. history is expected to be such that no more than $\pm 4^\circ$ of gimbal angle will be required, a margin of 50% was added to preclude any future difficulties. If later studies show that less angle is required the gimbal stop limits can be changed. Although the gimbal control system will meet design reliability, it would be desirable to limit gimbal angle such that a runaway can be overpowered by R.C.S.

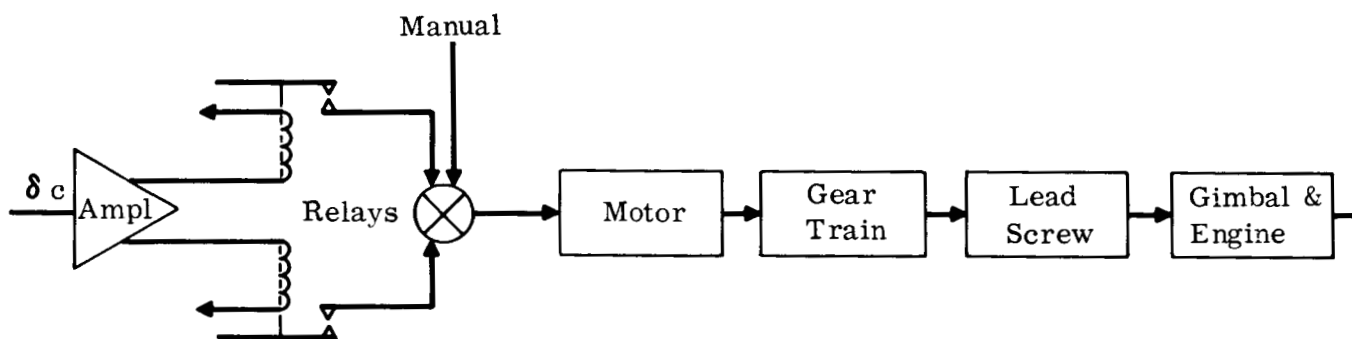


Figure C-1A. Trim Gimbal Control Block Diagram

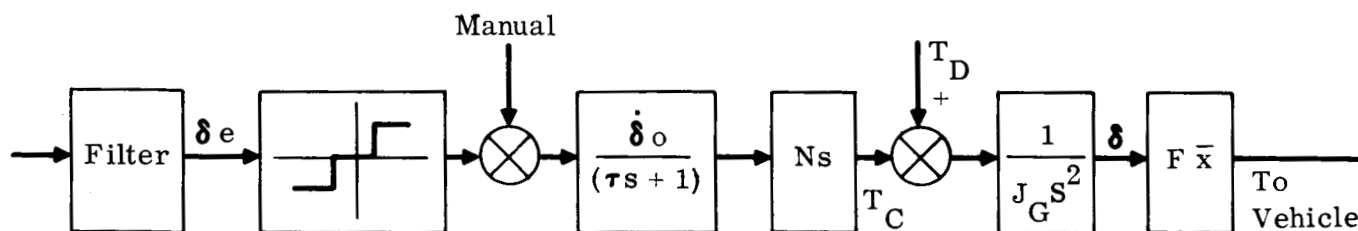


Figure C-1B. Trim Gimbal Control

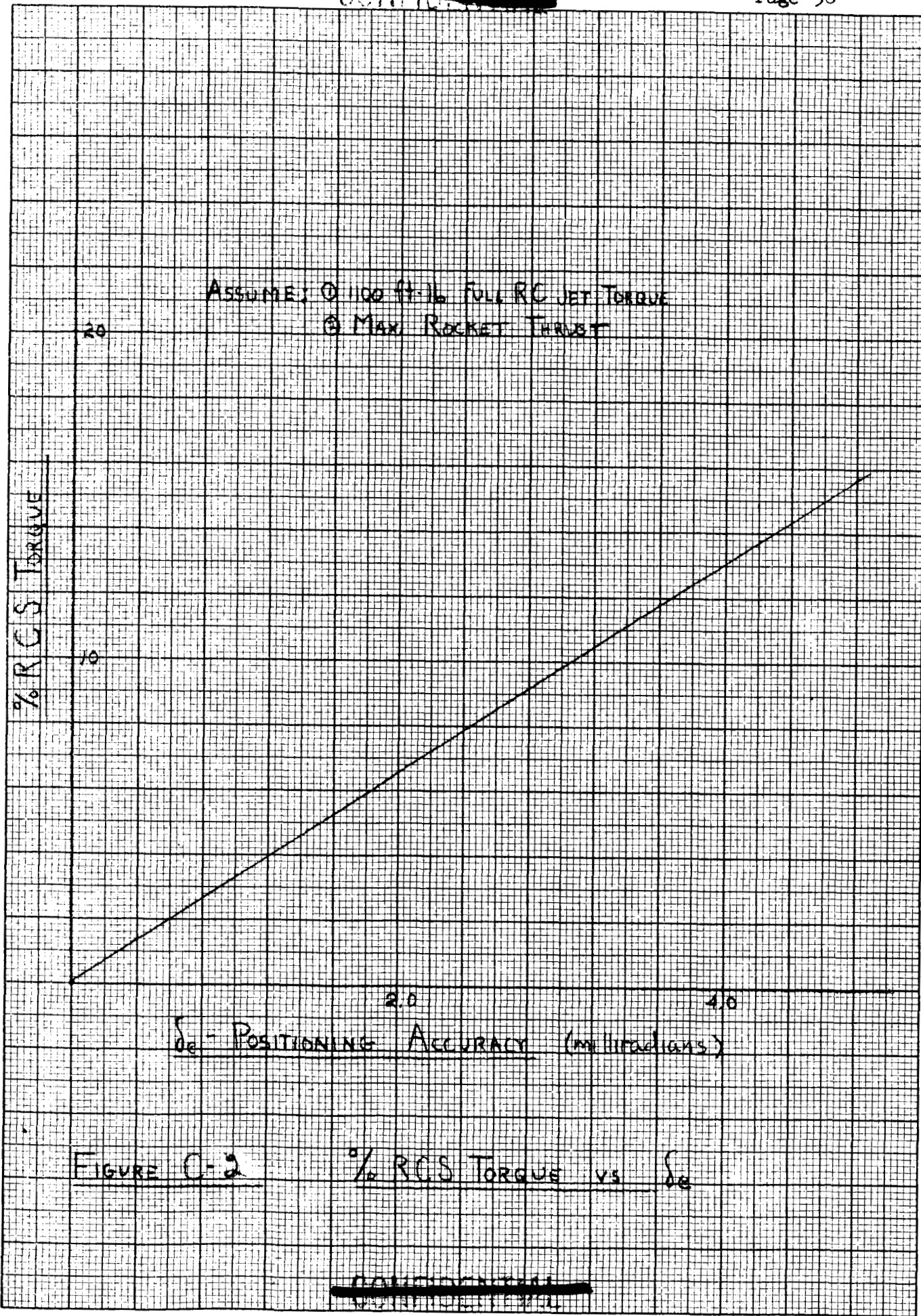


FIGURE C-2

% RCS TORQUE vs δ_e

K&E
KENNEL & EGGERS CO.
10 X 10 TO THE 1/2 INCH
VTBYNEM ②
MADE IN U.S.A.
329L-11

GIMBAL RATE

Preliminary studies of probable c.g. histories indicate that a gimbal rate of $0.2^\circ/\text{sec.}$ is more than adequate. Although the studies show that $0.1^\circ/\text{sec.}$ is required, the uncertainty of c.g. motion which is largely due to fuel flow dictate a $0.2^\circ/\text{sec.}$ rate. The higher rate will allow for a lighter motor duty cycle making for greater reliability. This rate is also compatible with the required accuracy.

TRIM GIMBAL RESOLUTION

The trim gimbal positioning resolution has been determined on the basis of limited sharing of RCS power for c.g. mission. In order to limit bias to less than 5% of total Reaction jet power, the positioning resolution must be ± 1.5 milliradians as shown in Fig. C-2. The preliminary stability analysis shown that the system can be stable with a dead band as low as $.04^\circ$. Although studies will take into account non-linearities and random disturbances, no positioning problems are anticipated.

APPLIED LOADS

The model shown in Fig. C-3 is used to establish the torque requirement for the gimbal drive.

δ = gimbal angular displacement

F = rocket thrust = 1050 - 10,500#

J_R = (engine inertia) = 70 Slug-ft.²

K_S = Fuel line restraining constant = $250 \frac{\text{ft-lb}}{\text{rad.}}$

f = Coulomb friction (bearings) = 8 ft-lb.

f = Thrust misalignment = $100 \frac{\text{ft-lb}}{(\text{max})}$

The torque summation is:

$$L = L_C + L_F + L_S + L_T = J_R \ddot{\delta}$$

$$L_C = J_R \ddot{\delta} \pm 250 \pm 100 + 8$$

The maximum value of restraining torque is:

$$L = 250 \left(\frac{6}{57.3} \right) = 26.4 \text{ ft-lb.}$$

The power required for the systems is given by:

$$P_{in} = \frac{1}{n} \left[(L_F + L_S + L_T) \dot{\delta} + J_R \ddot{\delta} \right]$$

If overall efficiency is 10%;

$$P = 10 (100 + 8 + 26.4)(.0035) + 70 (.035)(.0035) = 6.8 \text{ watts}$$

Although the steady state axial loading is approximately 134 pounds, the peak loading can be 3 times this much due to dynamic loading and column flexure. The column flexure loading is the result of increased friction at the close tolerance lead screw threads and the dynamic loading is the force applied due to changes in the kinetic energy of the engine (thrust level fluctuation). For the above stated reasons the peak power is estimated to be approximately 27 watts.

OVERSHOOT

The overshoot can be approximated by assuming braking capabilities.

Kinetic energy of motor and gear train.

$$J = J_m + n^2 J_G = 7.5 \times 10^{-6} \text{ Slug-ft.}^2$$

$$(K.E.)_m = \frac{1}{2} J \omega^2 = \frac{1}{2} (7.5 \times 10^{-6}) \left[(4000) \frac{2}{60} \right]^2 = .655 \text{ ft-lb-rad.}$$

Kinetic Energy of gimbal and engine

$$(K.E.)_e = \frac{1}{2} (70)(.0035)^2 = 4.4 \times 10^{-4} \text{ ft-lb-rad. (neglect)}$$

Assume 25% braking power

$$L_e \delta = (.25) K.E.$$

$$\delta = \frac{W_m}{N}, L_m W_m = (K.E.)_m$$

$$= \frac{KE}{NL}, \text{ assuming 25\% efficiency in screw}$$

$$= \frac{(.655)}{(12 \times 10^4)} \frac{(.25)}{(2.23 \times 10^{-2})}$$

$$\delta = 6.2 \times 10^{-5} \text{ rad. (overshoot)}$$

Mechanization

Although a detailed design analysis is required in order to determine the actuator configuration some general remarks can be made about mechanization at this time (see Fig. C-4). The weight of each actuator is estimated to be 9#. The control electronics which is redundant for each actuator should weigh about 4 pounds per axis.

Motor redundancy can be achieved by driving through a planetary gear train. Further, if back lash is a problem, the brakes can have a minimum energy setting so that the gear train is always preloaded. In this case 4 motors will be required per actuator. Two reversing motors can accomplish the same general effect except that certain types of motor failures will lead to back lash in the train. The lead screw can be irreversible @ the expense of power. On the other hand, a ball screw would require a higher energy brake. With a low power system such as this, an acme thread will probably be used. Some of the mechanical parameters are estimated. If the motor $\frac{1}{2}$ speed is assumed to be 4000 rpm, the gear ratio (N) is $.12 \times 10^4 \text{ rad/rad}$.

Indicators

Since it appears desirable to have a gimbal angle indication in the crew compartment, a position indicator can be driven by the actuator gearing to yield a signal to the instrument.

Manual Input

Manual trim inputs will be implemented for initial setting and manual override.

C-2 Attitude Control Gimbal

Because of the response and accuracy requirements of an attitude control gimbal, the control must be a feedback system with a constant speed motor driving the gimbal thru a clutch. The clutch is required since the system time constant must be short ($\tau=0.3$). If an attitude gimbal is to be used, it will work in conjunction with the R.C. Sub-system. Its input would be in parallel with the RCS input and be configured as shown in Figure C-4.

Control Loop

The control loop block diagram is essentially that shown in Figure C-4.

The gimbal displacement is

$$\begin{aligned}\delta &= \frac{L_c + L_D}{J_G S^2} = \frac{\left(\frac{K_c N}{\tau_m S + 1}\right) \left(\frac{1}{J_G S^2}\right) \delta_c + \frac{1}{J_G S^2} (L_D)}{1 + \left(\frac{K_c N}{\tau_m S + 1}\right) \left(\frac{1}{J_G S^2}\right) (K + K_2 S)} \\ &= \frac{K_c N \delta_c + (\tau_m S + 1) L_D}{J_G S^2 (\tau_m S + 1) + K_c N (K + K_2 S)} \\ &= \frac{1}{J_G \tau_m} \left[K_c N \delta_c + (\tau_m S + 1) L_D \right] \\ &= \frac{1}{S^3 + \frac{1}{\tau_m} S^2 + \frac{K_c N K}{J_G \tau_m} S + \frac{K_c N K}{J_G \tau_m}}\end{aligned}$$

The analysis for this system is discussed in Appendix D. The analysis indicates that the gimbal rate must be greater than 0.3 rad/sec.

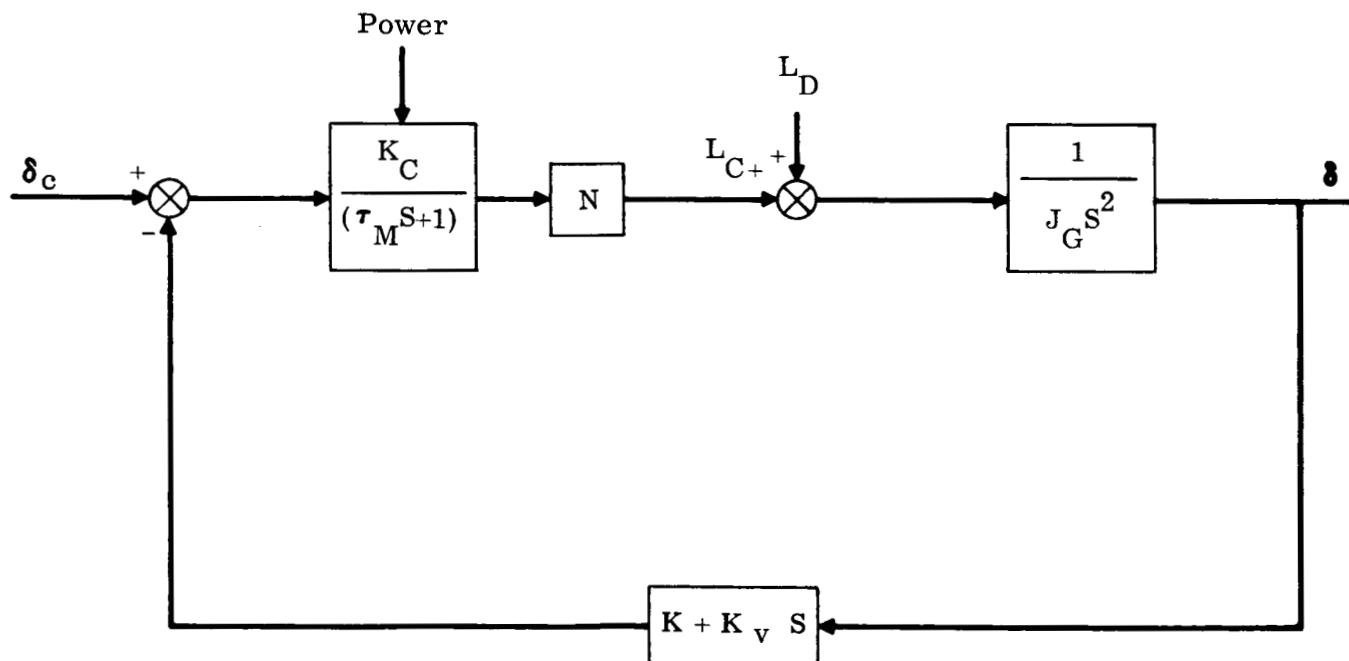
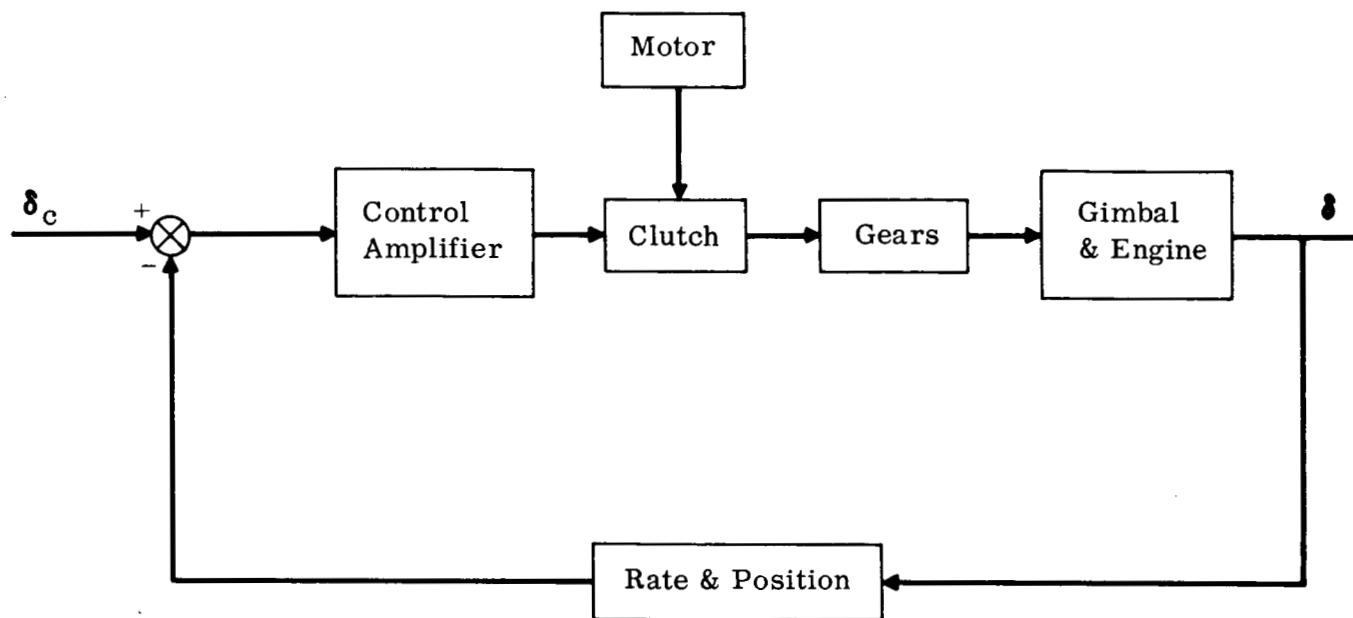


Figure C-4. Attitude Gimbal Control System

Applied Loads

The applied loads are approximately the same as for the trim gimbal so far as the disturbances are concerned. The difference are in the restraining torque and the inertial torque.

The torque equation is:

$$L_c + L_g + L_f + L_P = J_R$$

The symbols are defined in the trim gimbal section.

$$L_g = 250 \left(\frac{8}{37.3} \right) = 35.0 \text{ ft.-lb.}$$

$$L_f = 8 \text{ ft.-lb.}$$

$$L_P = 100 \text{ ft.-lb.}$$

Power Requirements

The power required for a gimbal with $\dot{\delta} = 0.5 \text{ rad/sec.}$ and $\ddot{\delta} = 5.0 \text{ rad/sec.}^2$ is,

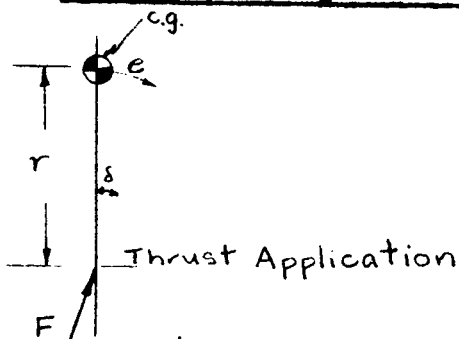
$$P_{in} = \frac{1}{\eta} [(108 + 35) (0.5) + 70 (5) (0.5)]$$

if $\eta = 20\%$ (use ball screw actuator)

$$P_{in} = 5 (71.5 + 175) = 1,232 \text{ watts}$$

Gimbal Rate Analysis

Derivation of expression for gimbal rate



For the vehicle

$$\int L(t) dt = \int J_v \ddot{\theta} dt$$

$$\text{The torque } L(t) = \int F r \dot{\delta}(t) dt$$

Where $\dot{\delta}(t)$ is the gimbal rate. If we assume a gimbal velocity profile as shown in Figure C-5,

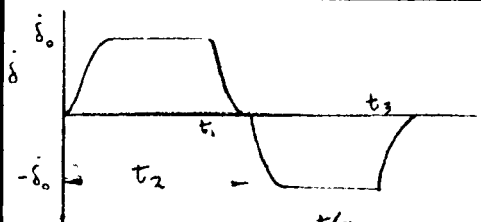


Fig. C-5 Gimbal Rate Profile

$$\dot{\delta} = \dot{\delta}_0 \left[(1 - e^{-t/\tau}) u(t) - (1 - e^{-\frac{(t-t_1)}{\tau}}) u(t-t_1) - (1 - e^{-\frac{(t-t_2)}{\tau}}) u(t-t_2) + (1 - e^{-\frac{(t-t_3)}{\tau}}) u(t-t_3) \right]$$

If we assume $\tau_{t_1} = \tau_{t_2} = \tau$

$$\dot{\delta} = \dot{\delta}_0 \left[(1 - e^{-t/\tau}) u(t) - (1 - e^{-(t-t_1)/\tau}) u(t-t_1) + \dots \right]$$

where τ is the actuator time constant

The torque for half a cycle (from $0 \leq t \leq t_2$) is

$$L(t) \Big|_0^{t_2} = Fr \dot{\delta}_0 \left[\int_0^{t_2} (1 - e^{-t/\tau}) dt - \int_{t_1}^{t_2} (1 - e^{-\frac{(t-t_1)}{\tau}}) dt \right]$$

$$L(t) \Big|_0^{t_2} = Fr \dot{\delta}_0 \left[(t + \tau e^{-t/\tau}) \Big|_0^{t_2} - (t + \tau e^{-\frac{(t-t_1)}{\tau}}) \Big|_{t_1}^{t_2} \right]$$

The impulse for the same period is

$$I \Big|_{t_2} = J_v \dot{\theta} = Fr \dot{\delta}_0 \left[\int_0^{t_2} (t + \tau e^{-t/\tau}) dt - \int_{t_1}^{t_2} (t + \tau e^{-\frac{(t-t_1)}{\tau}}) dt \right]$$

$$J_v \dot{\theta} = Fr \dot{\delta}_0 \left\{ \left(\frac{t^2}{2} - \tau^2 e^{-t/\tau} \right) \Big|_0^{t_2} - \left(\frac{t^2}{2} - \tau^2 e^{-\frac{(t-t_1)}{\tau}} \right) \Big|_{t_1}^{t_2} \right\}$$

$$J_v \dot{\theta} = Fr \dot{\delta}_0 \left\{ \frac{t_2^2}{2} - \tau^2 e^{-t_2/\tau} + \tau^2 - \frac{t_1^2}{2} + \tau^2 e^{-\frac{(t_2-t_1)}{\tau}} + \frac{t_1^2}{2} - \tau^2 \right\}$$

$$J_v \dot{\theta} = Fr \dot{\delta}_0 \left(\frac{t_2^2}{2} - \tau^2 e^{-t_2/\tau} + \tau^2 e^{-\frac{(t_2-t_1)}{\tau}} \right)$$

Solving for $\dot{\delta}_0$

$$\dot{\delta}_0 = \frac{J_v \dot{\theta}}{Fr \left[\frac{t_2^2}{2} + \tau^2 e^{-t_2/\tau} (e^{t_1/\tau} - 1) \right]}$$

Where

$\dot{\delta}_0$ = gimbal angle rate (maximum)

F = main engine thrust

J_v = inertia of the vehicle

$\dot{\theta}$ = $\frac{1}{2}$ the desired vehicle final rate for a given gimbal excursion and return to null.

t_2 = half time for total maneuver.

$t_1 = t_2 - 3$

r = d.g. travel along the x-axis of the vehicle

In we assume that higher order terms are small, the equation becomes:

$$\dot{\theta} = \frac{2J_v \dot{\theta}_D}{F_A t_1^2} ; \theta = \frac{\dot{\theta}_D}{2}$$

Where $\dot{\theta}_D$ is the desired vehicle rate. The equation is plotted in Figure C-6. A mean operating maximum of $\dot{\theta}_D = 0.5$ rad/sec has been chosen for this design.

Gimbal Displacement

Gimbal displacement as a fraction of vehicle acceleration and descent engine thrust is shown in Figure C-7. For the gimbal control to be at all worthwhile it should be capable of providing vehicle acceleration of at least 10 deg/sec² with a hover to landing vehicle inertia of 6000 slug-ft². This means a gimbal displacement of about 1.5 degrees at full thrust. However, during hover to landing operations the thrust level will be more like 2000 lbs., in which case gimbal deflection must be 8 degrees. To this approximately 4 degrees must be added for c.g. compensation making the total deflection 12 degrees.

Gimbal Accuracy

The steady state positioning accuracy of this gimbal must be an order of magnitude better than 0.1 degrees which is the nominal vectoring accuracy for thrust. The accuracy has been selected on the basis of steady-state bias on the reaction control power time sharing to be 2 miliradians.

Mechanization

In order to achieve the low time constant, the actuator must have a constantly running motor with a controlled clutch output. Since an attitude gimbal requires high positioning accuracy, very little backlash is a requirement. The use of two clutch drives, one for each direction, will eliminate this problem (see figure C-8). A double nut on the lead screw, be it ball-screw or acme thread, should bring the backlash to acceptable limits. The actuator will consist of 2 motor-generators (generator used for rate F.B.), a position feedback transducer, 4 clutches, a lead screw and all the associated gearing. This unit would be similar to the unit used on the service module gimbal drive. In the event of failure, the alternate drive system must be energized. The actuator assembly is estimated to weigh 18 pounds and the associated electronics are estimated to weigh 8 pounds per actuator. Gimbal angle will be displayed in the cockpit.

~~CONFIDENTIAL~~

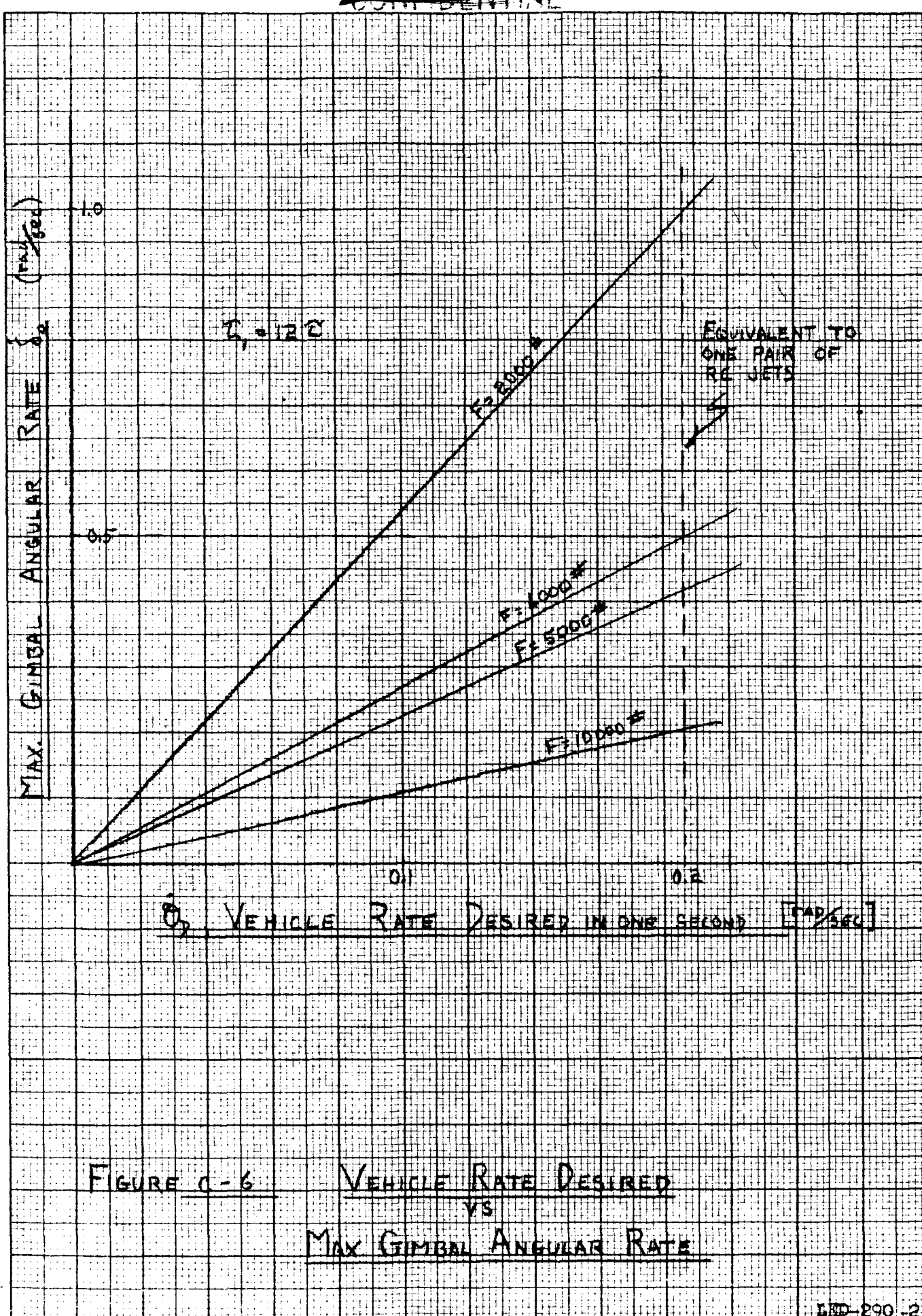


FIGURE C-6 VEHICLE RATE DESIRED
VS
MAX GIMBAL ANGULAR RATE

~~CONFIDENTIAL~~

KE
10 X 10 TO THE 1/2 INCH
KEUFFEL & ESSER CO.
ALBANY, N.Y.

359T-11
MADE IN U.S.A.

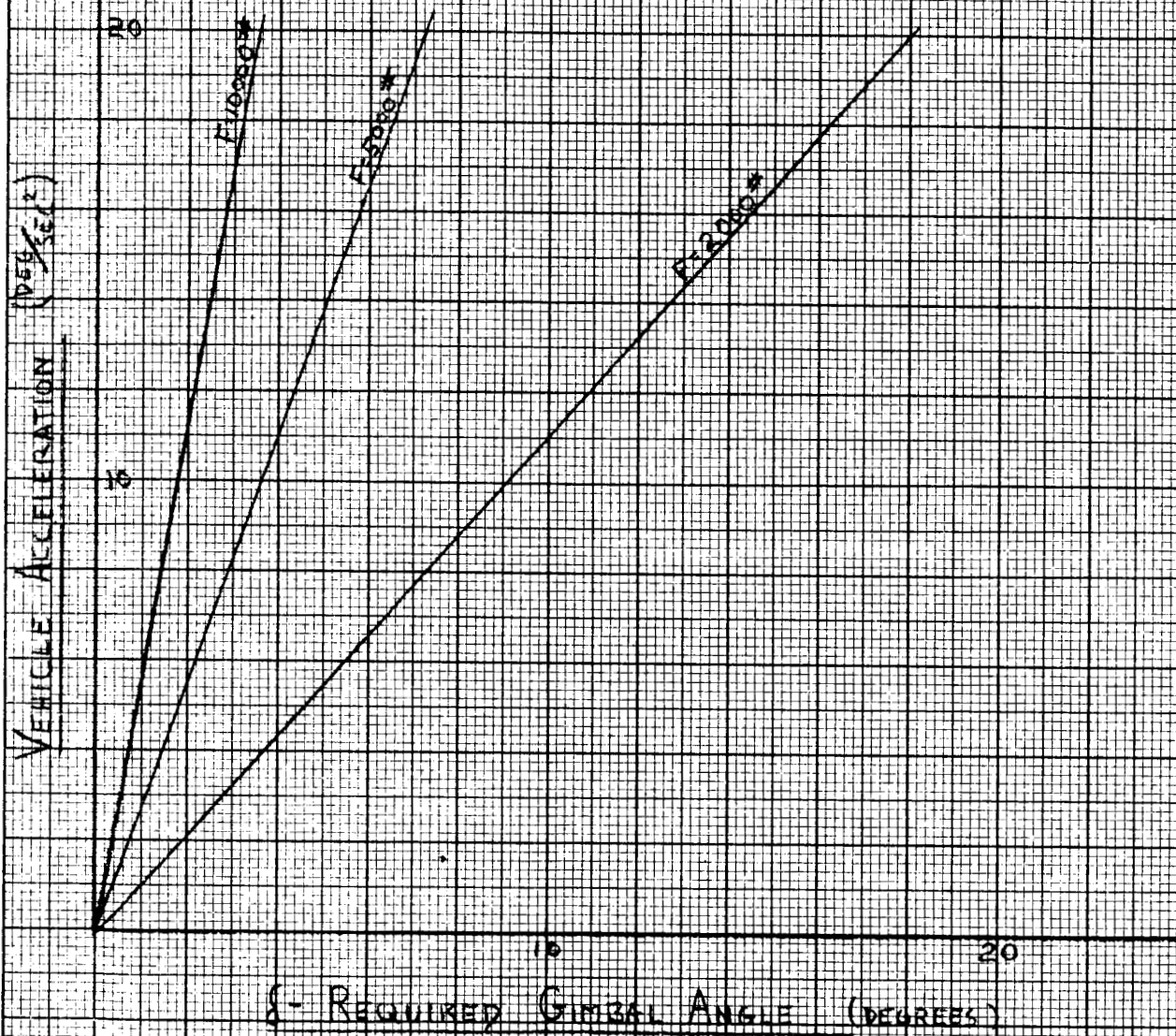


FIGURE C-7 VEHICLE ACCELERATION VS GIMBAL ANGLE

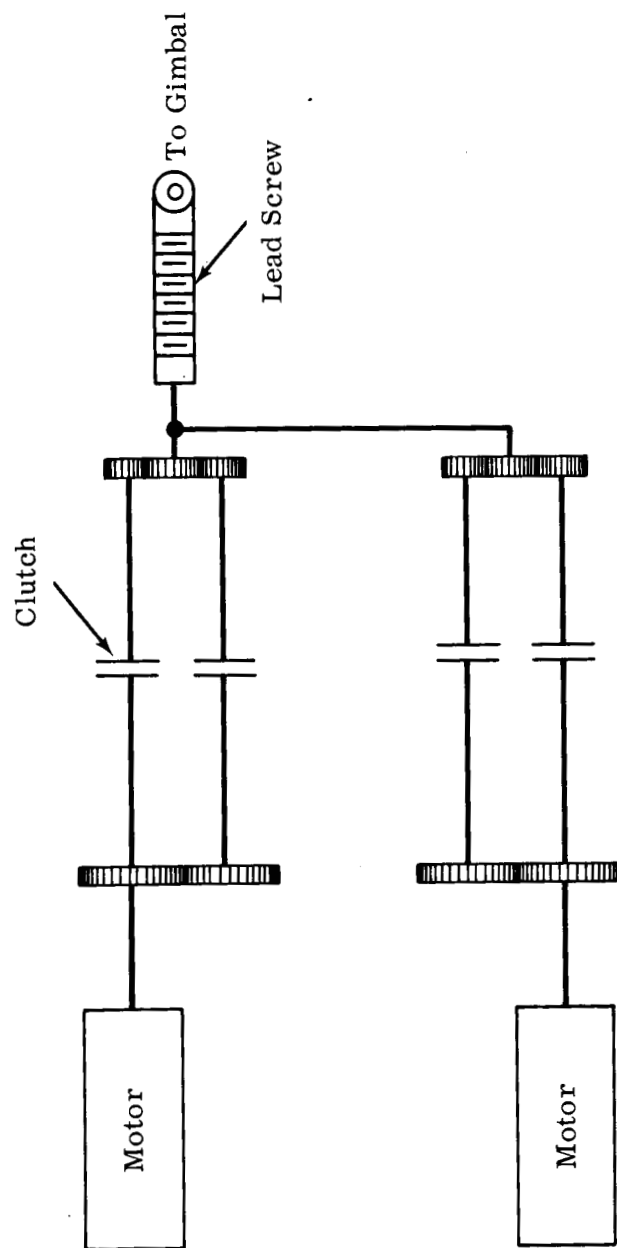


Figure C-8. Actuator Arrangement

~~CONFIDENTIAL~~

PAGE 68

APPENDIX D

Trim Gimbal Dynamics

This appendix will be submitted separately as an addendum in order to prevent delay to the report.

~~CONFIDENTIAL~~

REPORT LED-290-2
DATE 5/14/63

GRUMMAN AIRCRAFT ENGINEERING CORPORATION

APPENDIX E - RC JET CHARACTERISTICS

The following curves summarize the performance data currently available and of interest to various personnel for the Marquardt radiation cooled 100 lb. thruster.

Fig. 1 Vacuum Steady State Specific Impulse vs. Mixture Ratio

Fig. 2 Vacuum Specific Impulse vs. Electrical Pulse Width

Fig. 3 Vacuum Total Impulse vs. Electrical Pulse Width

Table I presents electrical characteristics and performance data for the injector mounted two coil solenoid propellant control valves.

In addition to the above information there are attached, copies of four figures illustrating thruster performance taken from the Marquardt "Apollo Reaction Control Rocket Engine Status Report" dated 22 February 1963. These figures augment or are the basis for information contained in Figures 1, 2 and 3. As additional information is received from Marquardt, it will be transmitted in the form of addendums to this memo. Any additional information required at this time should be requested from the authors.

TABLE I

Electrical characteristics of the two coil solenoid propellant valve used with Marquardt 100 lb. thruster.

AUTOMATIC COIL

1. Resistance	14.1 OHMS
2. Inductance	29 Millihenrys (closed), 25 (open)
3. Current at which Poppet starts to move	1.00 amps at 30 volts d.c. 0.96 amps at 24 volts d.c.
4. Number of turns	590
5. Coeff. of coupling	0.81 @ 100 cps

EMERGENCY COIL

1. Resistance	64.4 OHMS
2. Inductance	225 Millihenrys (closed)
3. Current at which Poppet starts to move	0.31 amps (calculated)
4. Number of turns	1820
5. Coeff. of coupling	0.92 @ 100 cps

WEIGHT 0.86 lb.

STROKE 0.021 in.

AUTOMATIC COIL CURRENT 2.0 amps max. @ 28v

EMERGENCY COIL CURRENT 0.5 amps max. @ 32v

NOMINAL RESPONSE

Full opening from signal	0.010 sec.
Full closing from signal	0.005 sec.

VACUUM SPARKING IMPULSES - SEC.

280

240

200

160

120

80

40

0

0

20

40

60

80

100

ELECTRICAL PULSE WIDTH - SEC.

○ 1ST PULSE IN SERIES

□ LOW POINT

△ HIGH POINT

DATA FROM INDEPENDENT
 PLOT OF 2/7/63 FOR
 PULSING TESTS RUN ON
 ENGINE ASSEMBLY TEST STAND
 PROPELLANTS - H₂/O₂

SOLENOID VOLTAGE - 24-30 VOLTS D.C.

SOLENOID VALVE - TWO COIL

POINTS CORRECTED TO
 ALTITUDE FROM SEA
 LEVEL TEST DATA

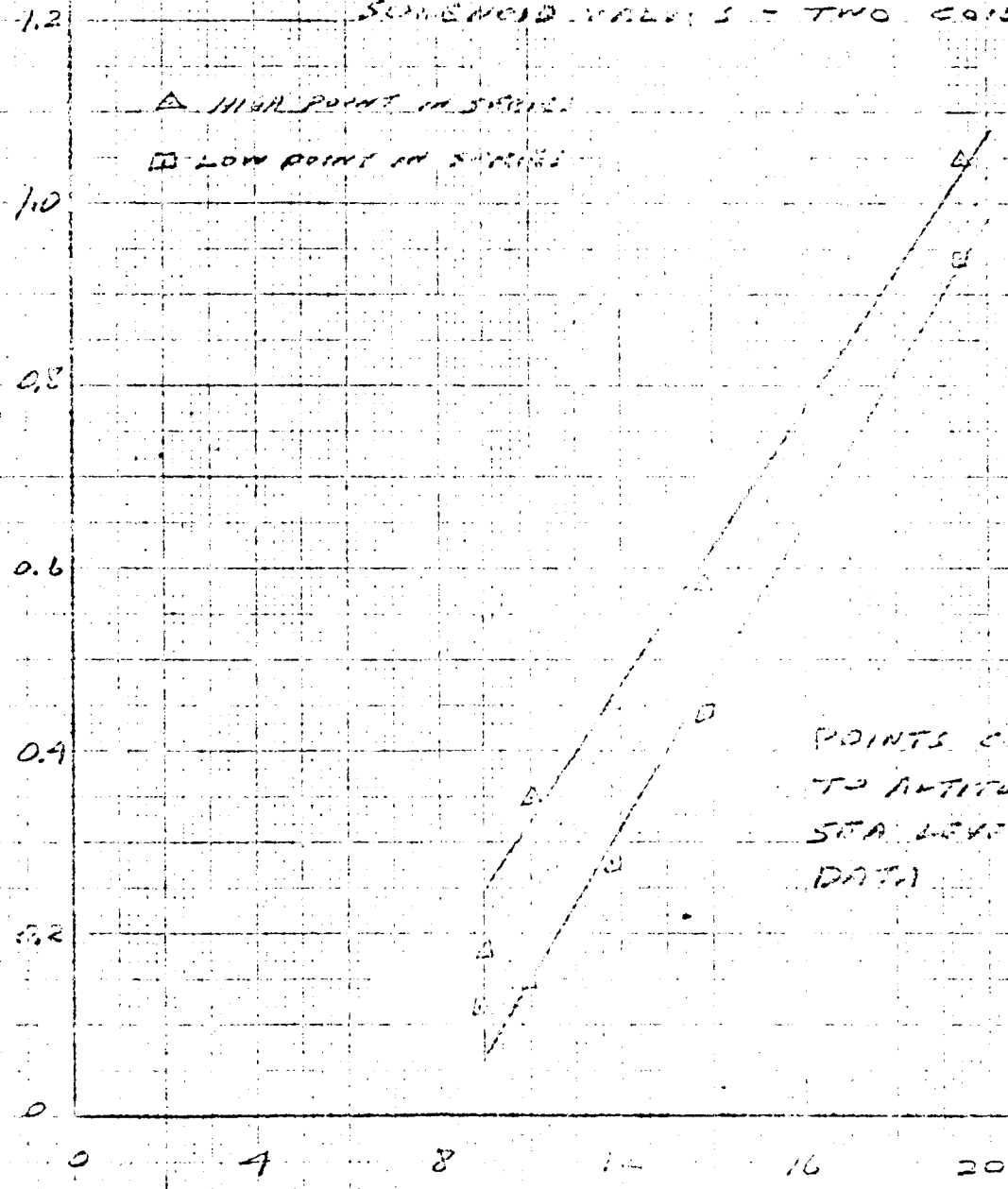
FIG. 2

~~CONFIDENTIAL~~
~~CONFIDENTIAL~~

VACUUM TOTAL IMPULSE - LB/SEC

DATA FROM HANQUARDT
PLOT OF 2/14/63 FOR
PULSING TESTS RUN ON
ENGINE ASSEMBLY T7305, S/N 21
RUN DATE 1/17/63
PROPELLANTS - N2O4/HF
SOLENOID VOLTAGE - 20 VOLTS DC.
SOLENOID VALVES - TWO COIL

△ HIGH POINT IN SPIKE
□ LOW POINT IN SPIKE



POINTS CORRECTED
TO ALTITUDE FROM
SEA LEVEL DATA

ELECTRICAL PULSE COUNT - 17

FIG. 3

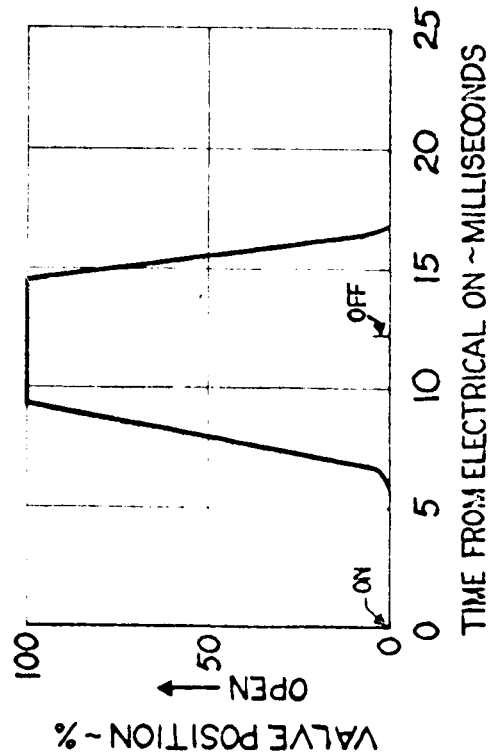
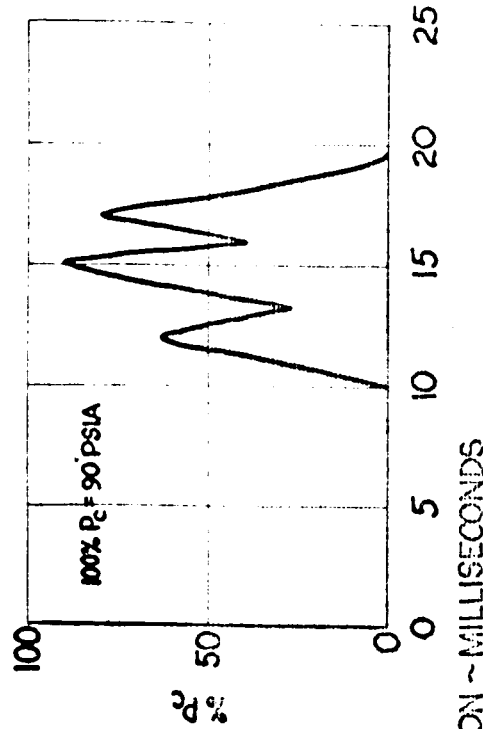
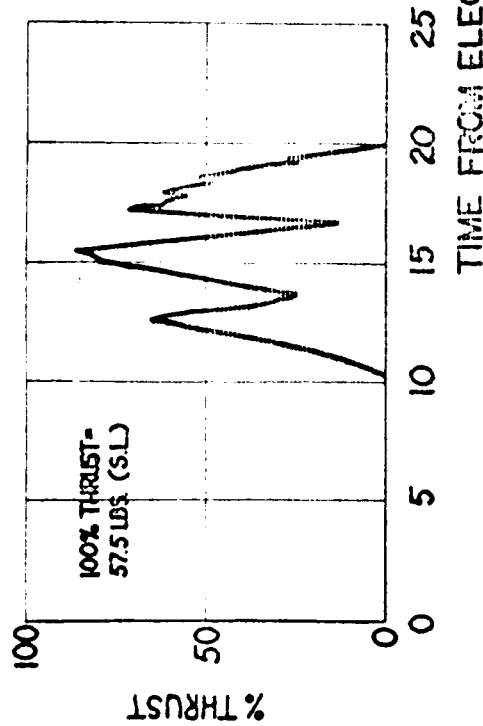
Fig 3

~~CONFIDENTIAL~~
~~CONFIDENTIAL~~

AVERAGE PULSE AT 11.8 MS ELECTRICAL PULSE WIDTH AT 28 VOLTS D.C.

ENGINE ASSEMBLY - T7305, S/N 001, 2 COIL SOLENOID VALVE

DRIBBLE VOLUME: FUEL 56% OF A 10MS PULSE FLOW
OXIDIZER 100% OF A 10MS PULSE FLOW

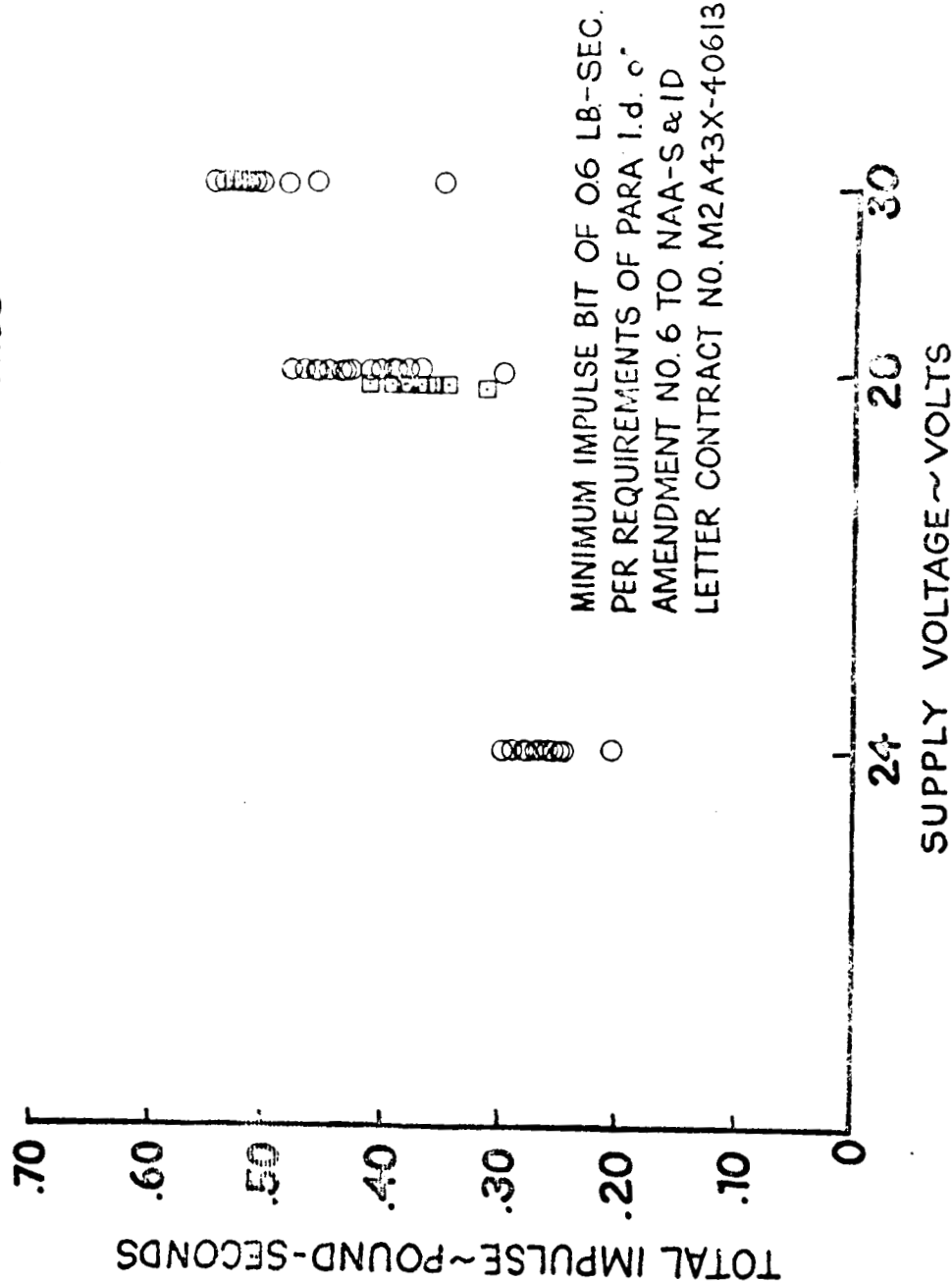


COMPARISON OF THRUST, CHAMBER
PRESSURE AND VALVE OPEN POSITION
CHARACTERISTICS AS A FUNCTION OF
ELECTRICAL ON TIME.

TOTAL IMPULSE vs. SUPPLY VOLTAGE

2-COIL VALVES

ENGINE ASSY. T7305 5/N 001
 FUEL DRIBBLE VOLUME - 56%
 FUEL-MMH
 OXIDIZER - 100% OXIDIZER - N₂O₄
 B-PULSES RUN WITH RAMAPO FLOWMETERS REMOVED
 ELECTRICAL PULSE WIDTH 118 MILLISECONDS



~~CONFIDENTIAL~~

END-2000-2
 4/14/83

TOTAL IMPULSE VS ELECTRICAL PULSE WIDTH

2 COIL VALVE -

ENGINE ASSEMBLY ~ T2305, S/N 001

FUEL ~ MMH

OXIDIZER ~ N2O4

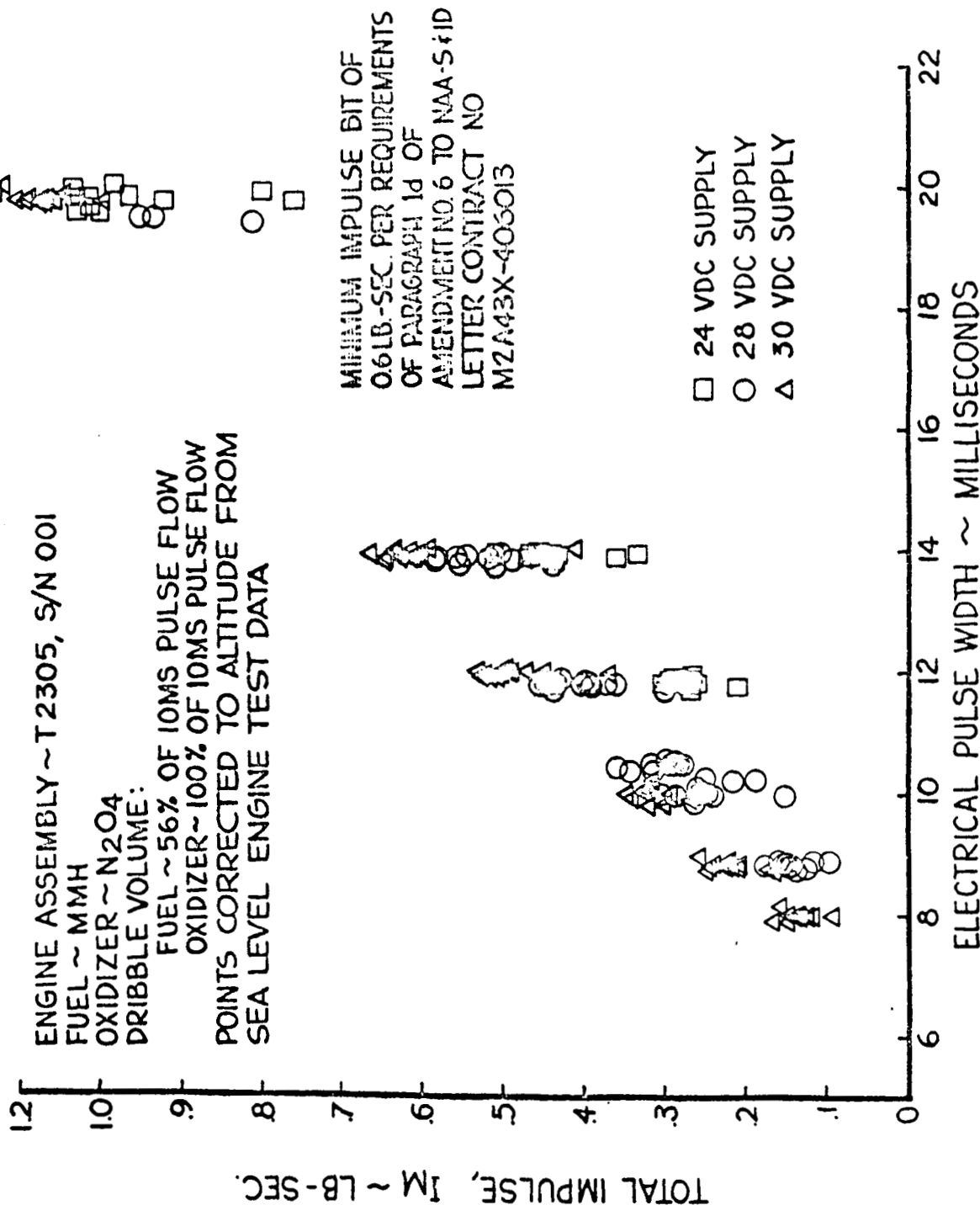
DRIBBLE VOLUME:

FUEL ~ 56% OF 10MS PULSE FLOW

OXIDIZER ~ 100% OF 10MS PULSE FLOW

POINTS CORRECTED TO ALTITUDE FROM

SEA LEVEL ENGINE TEST DATA



APPENDIX F

PRELIMINARY INVESTIGATION OF DYNAMIC COUPLING OF PROPELLANT SLOSHING WITH THE ATTITUDE CONTROL SYSTEM FOR LEM ASCENT STAGE

- Reference: 1. "Sloshing of Liquids in Circular Canals and Spherical Tanks", B. Budiansky; Journal of the Aerospace Sciences, Vol. 27, No. 3, March 1960.
2. "Approximate Transfer Functions for Flexible-Booster-and Autopilot Analysis", WADD Report TR-61-93; D. R. Lukens, A. F. Schmitt, G. T. Broucek; April 1961.

Introduction

A preliminary analysis has been conducted to estimate the dynamic stability of the coupled propellant sloshing-attitude control system oscillatory modes for the ascent stage. Existence of marginal or unstable propellant sloshing modes will impose significant design requirements upon the propulsion tankage and flight control subsystems. Use of bladders in the main propulsion tanks excludes the use of anti-slosh baffles and therefore may require the addition of sensors and complex filters in the stabilization and control subsystem to obtain improved vehicle stability.

Fluid Damping

A key parameter in stabilizing the coupled sloshing modes is damping of the fluid caused by the internal configuration of the propellant tank. The damping provided by a smooth-wall spherical tank of LEM diameters to the propellant used is negligible ($\xi/\xi_c = 0.0025$)*.

In order to estimate the damping produced by a bladder, a review of available test data on bladders in spherical tanks has been conducted. A considerable quantity of test data has been accumulated by the NASA Lewis Research Center for the damping in spherical tanks with various fluids (water, water-glycerin mixtures, mercury, TBE manometer fluid) with and without diaphragms. The majority of this data has not been published at this date, but detailed review of the results and experimental methods with Lewis personnel indicates valid data. Specifically, damping tests were conducted on spherical tanks of 32-inch diameter with diaphragms of three different thickness of butyl rubber and with T.B.E. fluid; on a 20.5 inch diameter sphere with diaphragms and bags of three thicknesses (butyl rubber) with T.B.E. fluid; on a 9.5-inch diameter sphere with diaphragms and bags of three thicknesses using both T.B.E. and mercury as fluids.

* Oblate spheroids of same size exhibit approximately the same damping ratio.

Additional damping tests on these three smooth-walled spheres (no diaphragms or bags) for various viscous fluids were conducted.

The damping ratio for a 47-inch diameter sphere with an 0.01 inch diaphragm was extrapolated from the diaphragm test data available using TBE fluid. The effect of the viscosity difference between TBE and LEM propellants on damping was then estimated by means of the test data for smooth-walled spheres with various fluid viscosities. The fundamental trend was checked through comparison of damping with diaphragms for the 9.5 inch sphere between TBE fluid and mercury. The damping ratio thus calculated was 1% of critical for fluid depth in the approximate range from 0.8 dia. to 0.2 dia. The effect of bladder material differences could not be obtained from the test data. Because of the uncertainties in the data and extrapolation method, the error in calculated damping ratio is estimated at $\pm 30\%$ of nominal value.

Use of certain types of baffles can produce a very great increase in fluid damping per unit baffle surface area, and therefore are quite efficient in terms of structural weight because of the small forces involved. Preliminary review of published and unpublished data on baffle damping in spherical tanks and oblate spheroids indicate that the circular ring baffle parallel to the fluid surface is very efficient for fluid depths in the region $0.2 < h/2R < 0.8$. At shallow depths where relatively large fluid damping may be desired to prevent outlet unporting, two small partial ring baffles in perpendicular vertical plane, which form a small cruciform, is effective. A typical anti-slosh baffle design might consist of two circular ring baffles located at $h/2R = 0.5$ and 0.3 with a ring width of 0.06 dia*, plus a cruciform of width 0.06 dia. and arc length $\pi D/4$. Detailed design is dependent upon vehicle slosh stability analysis.

Sloshing Stability Analysis

A preliminary analysis of the stability of the coupled attitude control-propellant sloshing modes has been completed. This analysis was conducted for one point in time during the ascent thrusting trajectory, and considerable simplification was made in the equations in order to obtain an assessment of the basic stability character in minimum time.

The time point examined was 223 seconds after lunar lift-off for the proposal configuration. This time is approximately two-thirds with less than maximum $h/2R = 0.5$ in a constant acceleration field, a fluid depth somewhat less than this will give maximum slosh force per unit surface angle because the thrust acceleration is increasing as the tank drains. The particular time chosen is not necessarily the point of maximum control coupling, but is estimated to be approximately the worst condition.

The analysis was restricted to consideration of rigid body planar motion with a rotational and translational degree of freedom. The first natural sloshing mode for each tank was included, and higher modes neglected.

The sloshing mode of each tank was coupled to the vehicle equation of motion in a simplified manner, which retained the major coupling modes.

The dynamics of fluid motion in a spherical tank in response to lateral tank acceleration can be rigorously represented by equations analogous to a spring-mass plus a fixed mass within the tank, as demonstrated in References 1 and 2. Such treatment facilitates the stability analysis and was employed. For the pitch (Y axis rotation) and yaw (Z axis rotation) stability analysis, the location of the lateral slosh force was assumed to act at the center of the sphere. A linear representation of the pulse modulated behavior of the reaction control system was used, and control by reaction jets was assumed.

Stability Results

A root locus of the linearized attitude control system for pitch or yaw rigid body without sloshing is shown in Figure 1. An operating gain ($K = 12.95$) was chosen to prevent the steady-state attitude error from exceeding 0.1 degree in the presence of a 3000 inch-pound moment from the main engine thrust offset. Selection of the rate gain to provide a damping ratio of 0.7 for the rigid body, provides a frequency of 6 rad./sec.

The root-locus plots for pitch or yaw including sloshing are given in Figures 2A, B and C. Location of the rigid body mode has not changed significantly; but sloshing has introduced four dipoles along the imaginary axis with a stable locus between each pole-zero pair.. At the operating gain, the coupled frequencies are approximately 4.84 rad./sec. and 4.36 rad./sec. The dipole at high frequency has such a minute pole-zero spread that its residue, and hence coupling with the control system, is negligible. The lower frequency dipole has a considerably greater residue and is more significant.

Examination of the roll axis (rotation about X axis) stability (Figure 3A, B, and C) shows that the slosh coupling in one mode is much greater than for the pitch axis, but all modes are stable. The time response of the system to a step attitude command will thus consist of a well damped rigid body mode with a very lightly damped small amplitude slosh mode superimposed on it.

Propellant Tank Unporting Consideration (Proposal Configuration)

A. Descent Stage

When the fluid depth is low, slosh mass is small enough to preclude control instability, but the existence of large amplitude fluid motion may cause exit port uncovering. Therefore, the maximum overshoots to be expected using bladders or baffles should be calculated.

*This produces an approximate damping ratio = 0.05 for $h/2R = 0.5$ and large surface amplitudes

~~CONFIDENTIAL~~

REPORT LED-290-2
DATE 5/14/63

GRUMMAN AIRCRAFT ENGINEERING CORPORATION

A roll maneuver during hover calling for a rate of 10 deg/sec will require a reaction jet on-time of 1.05 second; smaller roll rates will require proportionately less on-time. These angular acceleration periods may therefore easily persist for one-fourth of the slosh mode period, since the sloshing frequencies run from $\omega = 6.1$ rad/sec at full throttle to $= 1.88$ rad/sec at minimum throttle. The angle of the total acceleration vector with respect to vehicle centerline at the tank center is:

$$\theta = \tan^{-1} \frac{1}{T/M} \ddot{\phi} \quad \text{where } \ddot{\phi} \text{ body angular acceleration about X axis}$$

T/M = acceleration from main engine thrust

$$\theta_1 = 8.45 \text{ deg. at hover thrust}$$

$$\theta_2 = 13.4 \text{ deg. at minimum thrust}$$

If duration of $\ddot{\phi}$ is $1/4$ of slosh period and the damping ratio provided by a bladder is $\zeta = 0.2$ the fluid dynamic overshoot will be 92% of input. Thus peak angle $\theta_2 = 25.7$ deg. Use of a baffle near the bottom instead of the bladder could greatly reduce the peak overshoot and thus permit emptying the tank to a lower level.

B. Ascent Stage

A check on the ascent stage near burnout reveals that the overshoots are much less, unless the roll limit cycle frequency equals the slosh mode frequency. A roll thruster firing gives $\theta = 4.45$ deg. The high roll acceleration results in short firing times compared to the slosh frequencies $\omega_s = 4.8$ rad/sec, $\omega_{tm} = 4.65$ rad/sec. However, with $\zeta \leq 0.05$, the maximum expected from a bladder at large amplitude and roll limit cycle frequency of 4.8 rad/sec. (corresponding to a dead-band of approximately 0.50 deg.) the peak overshoot angle would be $\theta = 44$ deg. Therefore, it might be necessary to insure that the limit cycle frequency does not coincide with slosh frequencies. The currently estimated roll limit cycle frequency is approximately 2.7 rad/sec.

Discussion

Results of the ascent stage (proposal configuration) stability analysis show significant but stable coupling of propellant sloshing with the control system. Slosh coupling with the roll axis control loop is quite pronounced. Note that at the roll operating gains the length of the vector to the root from the pole on the upper dipole (Figure 3C) is approximately 0.7. The introduction of 1% of critical damping into the tanks by a bladder would not shift the open loop pole far enough into the left half-plane to make this mode gain stabilized; so that it would still require phase stabilization. However, anti-slosh baffles could easily gain stabilize this mode.

Although the preliminary analysis shows stability, approximations have been made in the equations and the vehicle mass data is quite approximate, so that phase stability for all sloshing modes throughout the ascent trajectory cannot be guaranteed.* If detailed analysis shows instability or marginal stability, and bladders are installed in the tanks, it appears that phase stabilization must be achieved by use of high order filters and/or the use of lateral acceleration feedback or tank differential pressure feedback.

Conclusion

Results of the ascent stage preliminary stability analysis show significant but stable coupling of propellant sloshing with the attitude control system. The fluid damping provided by bladders in the propulsion tanks does not appear to be adequate to insure against marginal sloshing stability which may arise from future vehicle and control changes, data refinement, or analysis refinement. The ability to use anti-slosh baffles would permit great flexibility in achieving the desired slosh stability without resorting to complicated filter and extra sensors in the control system; thus represents a much more reliable method of slosh control. The existence of marginal slosh stability may be objectionable to the pilot, even though acceptable for the automatic control system.

Significant propellant slosh amplitudes may be generated by maneuvers during descent stage hover which would lead to outlet unporting, and the damping provided by a bladder is insufficient to reduce these amplitudes. To avoid large slosh amplitude near burn-out of the ascent stage (using main engine) it may be necessary to restrict the roll limit cycle frequency from coinciding with the slosh frequency if the tank contains a bladder. Fuel slosh tests are presently part of the test LEM test plan (reference LPL-600-1, Test Plan for LEM, 15 May 1963).

*Effect of guidance steering loop on short stability has not been considered here.

~~CONFIDENTIAL~~

DEVELOPMENT OF EQUATIONS

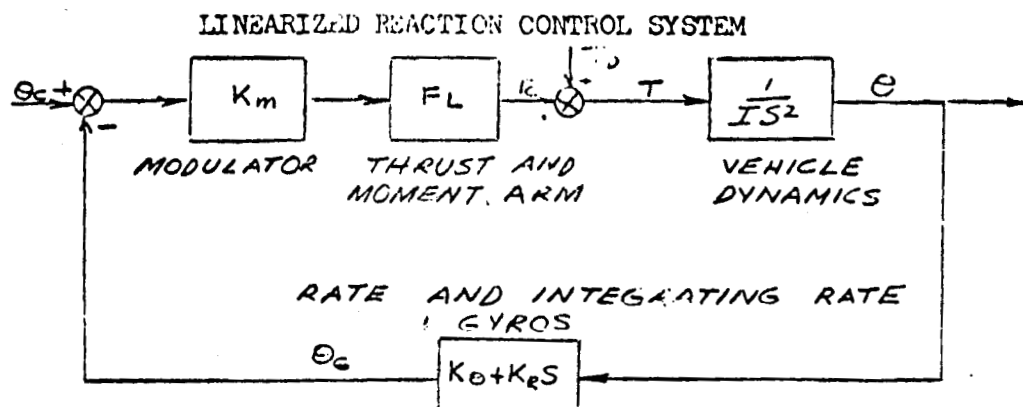


Fig 1A

I. Closed Loop Transfer Functions:

Command

$$(1) \frac{\theta}{\theta_c} = \frac{1}{K_\theta} \cdot \frac{K_\theta K_m FL/I}{s^2 + \frac{K_m FL K_R}{I} s + \frac{K_m FL K_\theta}{I}}$$

Torque Disturbance:

$$(2) \frac{\theta}{T_D} = \frac{1/I}{s^2 + \frac{K_m FL K_R}{I} s + \frac{K_m FL K_\theta}{I}}$$

Criterion

1. Steady state offset due to constant torque disturbance.
2. Transient response;

The largest moment unbalance is expected to occur during powered ascent. A C.G. shift of 1 inch along the Y or Z axis with a thrust of 3000 lbs. along the X axis would result in a moment unbalance of 3000 in-lbs. The required steady state guidance accuracy during powered ascent is assumed to be 0.1 degree. Utilization of the final value theorem on Eq. (2) determines the required loop gain. For a constant moment unbalance,

$$(3) T_D(s) = \frac{T_D}{s}$$

Therefore,

$$(4) \theta(s) = \frac{T_D}{s} \cdot \frac{1/I}{s^2 + (K_m FL K_R/I)s + K_m FL K_\theta/I}$$

Using the final value theorem,

$$(5) \theta(s)_{ss} = \lim_{s \rightarrow 0} \frac{s \cdot T_D}{s} \cdot \frac{1/I}{s^2 + (K_m FL K_R/I)s + K_m FL K_\theta/I} = \frac{T_D}{K_m FL K_\theta}$$

~~CONFIDENTIAL~~

LED-200-2
5/14/53

The reaction control system parameters during powered ascent are:

$$\begin{aligned} F &= 200 \text{ lbs.} \\ L &= 5.5 \text{ ft.} \\ I &= 2000 \text{ slug-ft}^2 \end{aligned}$$

Substituting into Eq. (5),

$$(6) \quad K_m K_\theta = 130 \text{ 1/rad.}$$

The linearized reaction control system shown in Fig. 1A is second order. The natural frequency is given by:

$$(7) \quad \omega_n = \sqrt{K_\theta K_m F L / I} = 8.45 \text{ rad./sec.}$$

The damping ratio is:

$$(8) \quad \zeta = \frac{K_m F L K_R}{2 \omega_n I}$$

$$\text{For a damping ratio of } \zeta = 0.7 \\ K_m K_R = 21.5 \text{ 1/rad, sec}$$

A root locus of the linearized reaction control system is shown in Fig. 1.

II. Sloshing:

The effect of fuel sloshing on reaction control system stability for planar motion during powered ascent is being considered. One condition of powered ascent is being investigated, namely 233 seconds after lift-off. Significant parameters with respect to the pitch axis are as follows:

$$\begin{aligned} \text{Gross Weight} &= 5100 \text{ lbs} \\ I_{yy} &= 1900 \text{ slug-ft}^2 \\ \text{C.G. Station} &= 163.2 \text{ in.} \\ \text{Thrust/weight} &= 0.6 \end{aligned}$$

The fuel and oxidizer tank parameters are as follows:

Ascent Fuel Tanks:

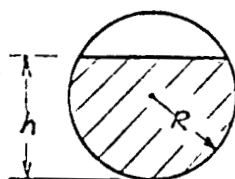
$$\begin{aligned} \text{No. of tanks} &= 2 \\ \text{Weight fuel/tank} &= 227.17 \text{ lbs.} \\ \text{X-station location} &= 136 \text{ in.} \\ \text{Tank radius} &= 17.5 \text{ in.} \\ \text{Fuel density} &= 55.66 \text{ lbs./ft}^3 \\ \text{Uncoupled natural frequency} &= 4.42 \text{ rad./sec.} \end{aligned}$$

Ascent Oxidizer Tanks:

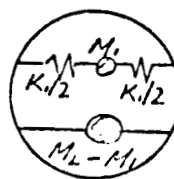
$$\begin{aligned} \text{No. of tanks} &= 2 \\ \text{Weight ox./tank} &= 454.33 \text{ lbs.} \\ \text{X - station location} &= 176 \text{ in.} \\ \text{Tank radius} &= 18.5 \text{ in.} \\ \text{Oxidizer density} &= 88.47 \text{ lbs./ft}^3 \\ \text{Uncoupled Natural Frequency} &= 4.34 \text{ rad./sec.} \end{aligned}$$

~~CONFIDENTIAL~~

A mass-spring analogy is used to represent a sloshing fluid in a spherical tank (Fig. A2).



TANK



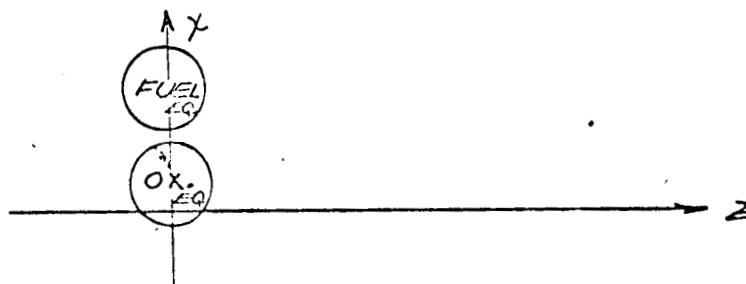
MATHEMATICAL MODEL

Fig. A2

Where

- h is the height of the fluid (ft.)
- R is the tank radius (ft.)
- M_1 is the equivalent sloshing mass (slugs)
- K_1 is the equivalent spring constant
- M_L is the total fluid mass

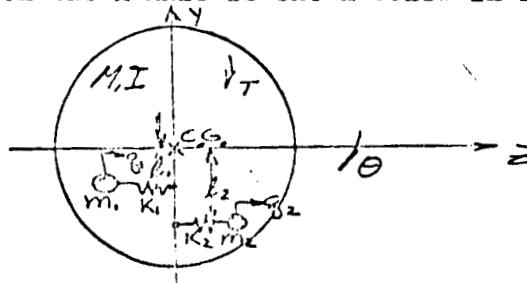
Each pair of ascent fuel tanks and oxidizer tanks are symmetrical with respect to the X-Axis (fig. A3)



CONFIGURATION OF ASCENT FUEL AND OXIDIZER TANKS WITH RESPECT TO THE PITCH AXIS

Fig A3

Equivalent tanks corresponding to the two fuel and oxidizer tanks were placed on the X-Axis (fig. A3). The equivalent tank has twice the mass and spring constant of a single tank. The mechanical analog of the tanks on the X-Axis is shown below in fig. A4.



MECHANICAL ANALOG OF ASCENT TANKS WITH RESPECT TO THE PITCH AXIS

Fig 4A

~~CONFIDENTIAL~~

The degrees of freedom being considered are:

1. One rigid and two slosh degrees of translation.
2. One rigid degree of rotation.

The equations of motion for the vehicle and ascent tanks are given below:

$$\begin{aligned}
 (9) \quad M\ddot{z} + K_1(z - g_1 - l_1\theta) + K_2(z - g_2 - l_2\theta) &= 0 \\
 (10) \quad I\ddot{\theta} + K_1l_1(l_1\theta - z + g_1) + K_2l_2(l_2\theta - z + g_2) &= T \\
 (11) \quad m_1\ddot{g}_1 + K_1(g_1 + l_1\theta - z) &= 0 \\
 (12) \quad m_2\ddot{g}_2 + K_2(g_2 + l_2\theta - z) &= 0
 \end{aligned}$$

The reaction control system equations for pitch are as follows:

$$\begin{aligned}
 (13) \quad \theta_e &= \theta_c - \theta_G \\
 (14) \quad T_c &= K_m FL \theta_e \\
 (15) \quad T &= T_c + T_D \\
 (16) \quad \theta_G &= K_\theta \theta + K_R \dot{\theta}
 \end{aligned}$$

Assume the input functions are zero (i.e. $\theta_c = T_D = 0$). Combining equations and using laplace notation,

$$\begin{aligned}
 (17) \quad (Ms^2 + K_1 + K_2)z - (l_1K_1 + l_2K_2)\theta - K_1g_1 - K_2g_2 + 0\theta_e &= 0 \\
 (18) \quad -(l_1K_1 + l_2K_2)z + (Is^2 + K_1l_1^2 + K_2l_2^2)\theta + K_1l_1g_1 + K_2l_2g_2 - K_mFL\theta_e &= 0 \\
 (19) \quad -K_1z + K_1l_1\theta + (m_1s^2 + K_1)g_1 + 0g_2 + 0\theta_e &= 0 \\
 (20) \quad -K_2z + K_2l_2\theta + 0g_1 + (m_2s^2 + K_2)g_2 + 0\theta_e &= 0 \\
 (21) \quad 0z + (K_\theta + K_RS)\theta + 0g_1 + 0g_2 + \theta_e &= 0
 \end{aligned}$$

In matrix form, equations (17) - (21) can be written as,

$$(22) \quad \begin{pmatrix} (Ms^2 + K_1 + K_2) & -(l_1K_1 + l_2K_2) & -K_1 & -K_2 & 0 \\ -(l_1K_1 + l_2K_2) & (Is^2 + K_1l_1^2 + K_2l_2^2) & K_1l_1 & K_2l_2 & -K_mFL \\ -K_1 & K_1l_1 & (m_1s^2 + K_1) & 0 & 0 \\ -K_2 & K_2l_2 & 0 & (m_2s^2 + K_2) & 0 \\ 0 & (K_\theta + K_RS) & 0 & 0 & 1 \end{pmatrix} \begin{pmatrix} z \\ \theta \\ g_1 \\ g_2 \\ \theta_e \end{pmatrix} = \begin{pmatrix} 0 \\ 0 \\ 0 \\ 0 \\ 0 \end{pmatrix}$$

Using the characteristic matrix, a digital routine was used to generate a root locus. The following parameters were used in the characteristic matrix for ascent pitch.

- | | |
|------------------------------|-------------------------------------|
| $l_1 = -2.265 \text{ Ft.}$ | $m_1 = 10.12 \text{ slugs}$ |
| $l_2 = 1.064 \text{ ft.}$ | $m_2 = 19.7 \text{ slugs}$ |
| $K_1 = 197$ | $K_\theta = 1 \text{ volt/rad}$ |
| $K_2 = 370$ | $K_R = 0.165 \text{ volts/rad/sec}$ |
| $I = 1831 \text{ slug-ft}^2$ | $K_m = 130 \text{ volts/rad}$ |
| $M = 128.7 \text{ slugs}$ | |

The root locus is shown in Figure 2A. The tank dipoles are shown blown-up in Figure 2B and 2C. From the root locus in Figures 2A, 2B, and 2C, the natural frequency and damping ratio of the reaction control system and ascent tanks are determined (see Table 1).

Table 1

System	ω_n - rad/sec Natural Freq.	ζ Damping Ratio
Rigid Body Mode	8.95	0.74
Fuel Tank	4.84	0.0006
Oxidizer Tank	4.37	0.0032

NATURAL FREQUENCIES AND DAMPING RATIOS OF REACTION CONTROL SYSTEM (PITCH) AND ASCENT TANKS WITH SLOSHING

A similar analysis was done for the roll axis during powered ascent. The configuration of the fuel and oxidizer tanks are shown in Figure A5.

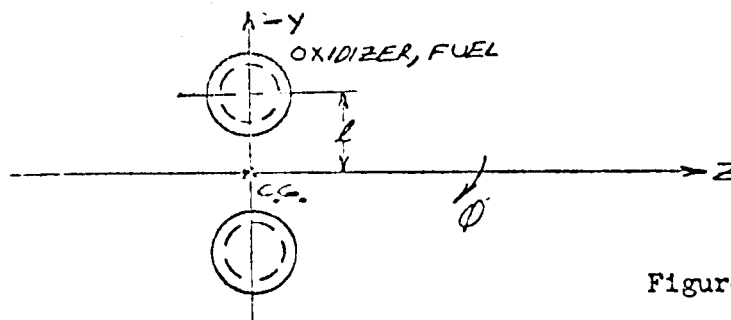


Figure A5

CONFIGURATION OF ASCENT FUEL AND OXIDIZER TANKS WITH RESPECT TO THE ROLL AXIS

~~CONFIDENTIAL~~

The two oxidizer and two fuel tanks were each lumped into one equivalent tank. Below in Figure A6 is shown the mechanical analog of the ascent tank with respect to roll.

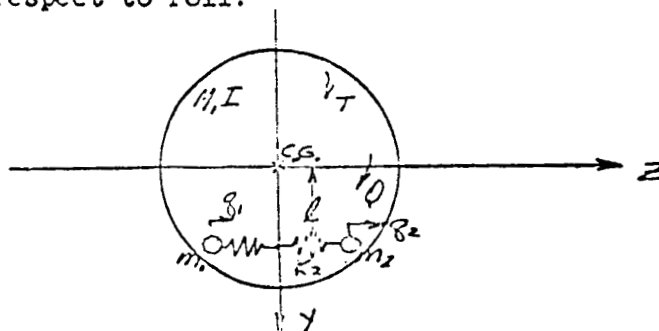


Figure A6

MECHANICAL ANALOG OF ASCENT TANKS
WITH RESPECT TO THE ROLL AXIS

A torque applied about the x-axis will cause a net sloshing force of zero in the z or y direction. This is apparent since the tanks are symmetrical with respect to the c.g. (See Figure A5). The overall reaction control system equations for the roll axis are given below in Laplace notation.

$$(23) \quad [IS^2 + l^2(K_1 + K_2)]\theta + K_1 l q_1 + K_2 l q_2 - K_m FL \theta_e = 0$$

$$(24) \quad K_1 l \theta + (m_1 S^2 + K_1) q_1 + 0 q_2 + 0 \theta_e = 0$$

$$(25) \quad K_2 l \theta + 0 q_1 + (m_2 S^2 + K_2) q_2 + 0 \theta_e = 0$$

$$(26) \quad (K_\theta + K_R S)\theta + 0 q_1 + 0 q_2 + \theta_e = 0$$

In matrix form, equations (23) - (26) can be written as,

$$(27) \quad \begin{pmatrix} [IS^2 + l^2(K_1 + K_2)] & K_1 l & K_2 l & -K_m FL \\ K_1 l & (m_1 S^2 + K_1) & 0 & 0 \\ K_2 l & 0 & (m_2 S^2 + K_2) & 0 \\ (K_\theta + K_R S) & 0 & 0 & 1 \end{pmatrix} \begin{pmatrix} \theta \\ q_1 \\ q_2 \\ \theta_e \end{pmatrix} = \begin{pmatrix} 0 \\ 0 \\ 0 \\ 0 \end{pmatrix}$$

Again using the characteristic matrix shown above, a digital routine was used to generate a root locus. All parameters remained the same except the following:

$$I = 1850 \text{ slug-ft.}^2$$

$$l = 4.125 \text{ ft.}$$

~~CONFIDENTIAL~~

~~CONFIDENTIAL~~

The root locus for the ascent roll case is shown in Figure 3A. The tank dipoles are shown blown-up in Figure 3B and 3C. Table 2 indicates the natural frequency and damping ratio for the reaction control system and the ascent tanks.

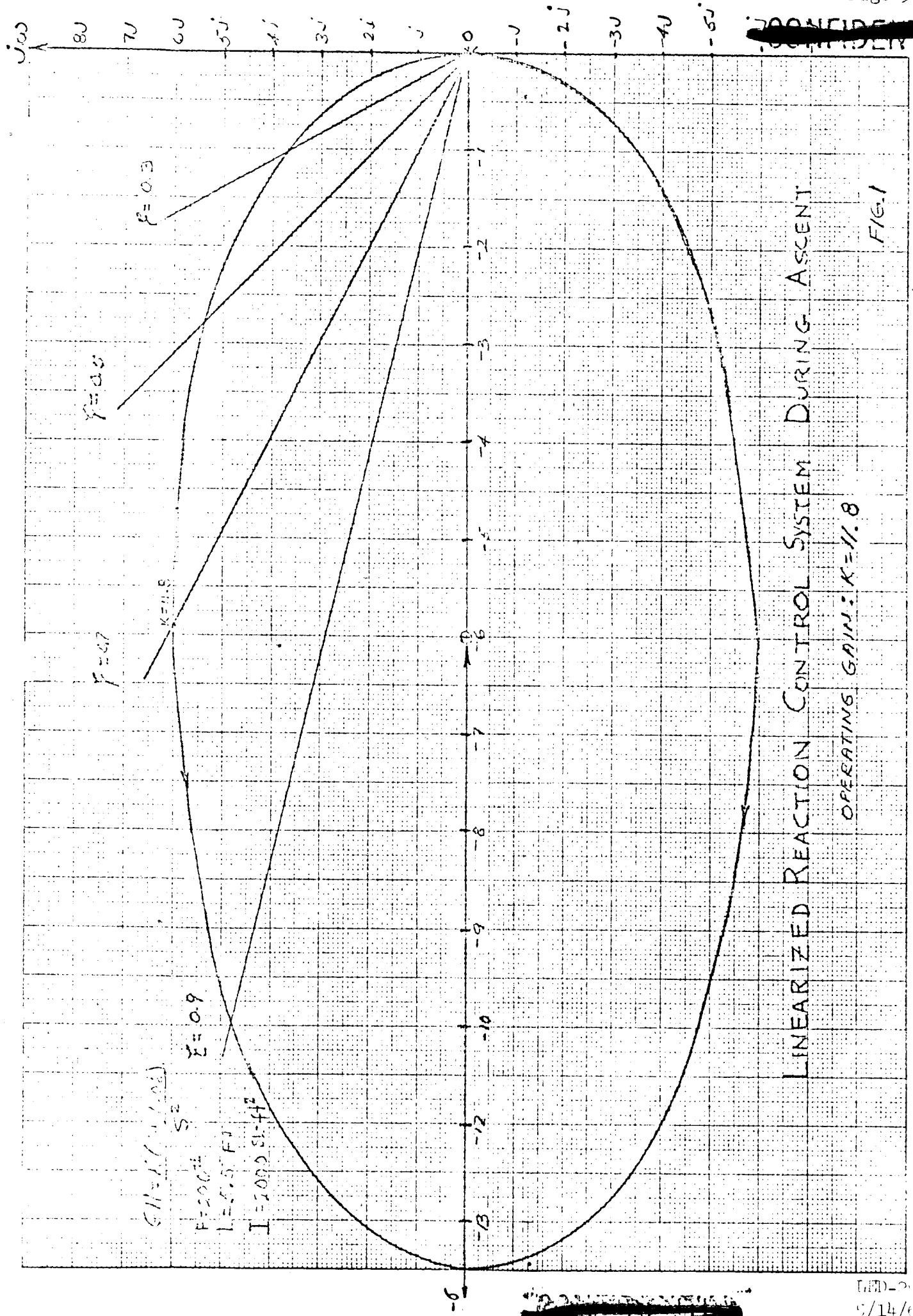
Table 2

System	ω_n - rad/sec Natural Freq.	γ Damping Ratio
Rigid Body Mode	9.2	0.7
Fuel Tank	4.393	0.0011
Oxidizer Tank	4.255	0.0202

NATURAL FREQUENCIES AND DAMPING RATIOS OF REACTION CONTROL
SYSTEM (ROLL) AND ASCENT TANKS WITH SLOSHING

~~CONFIDENTIAL~~

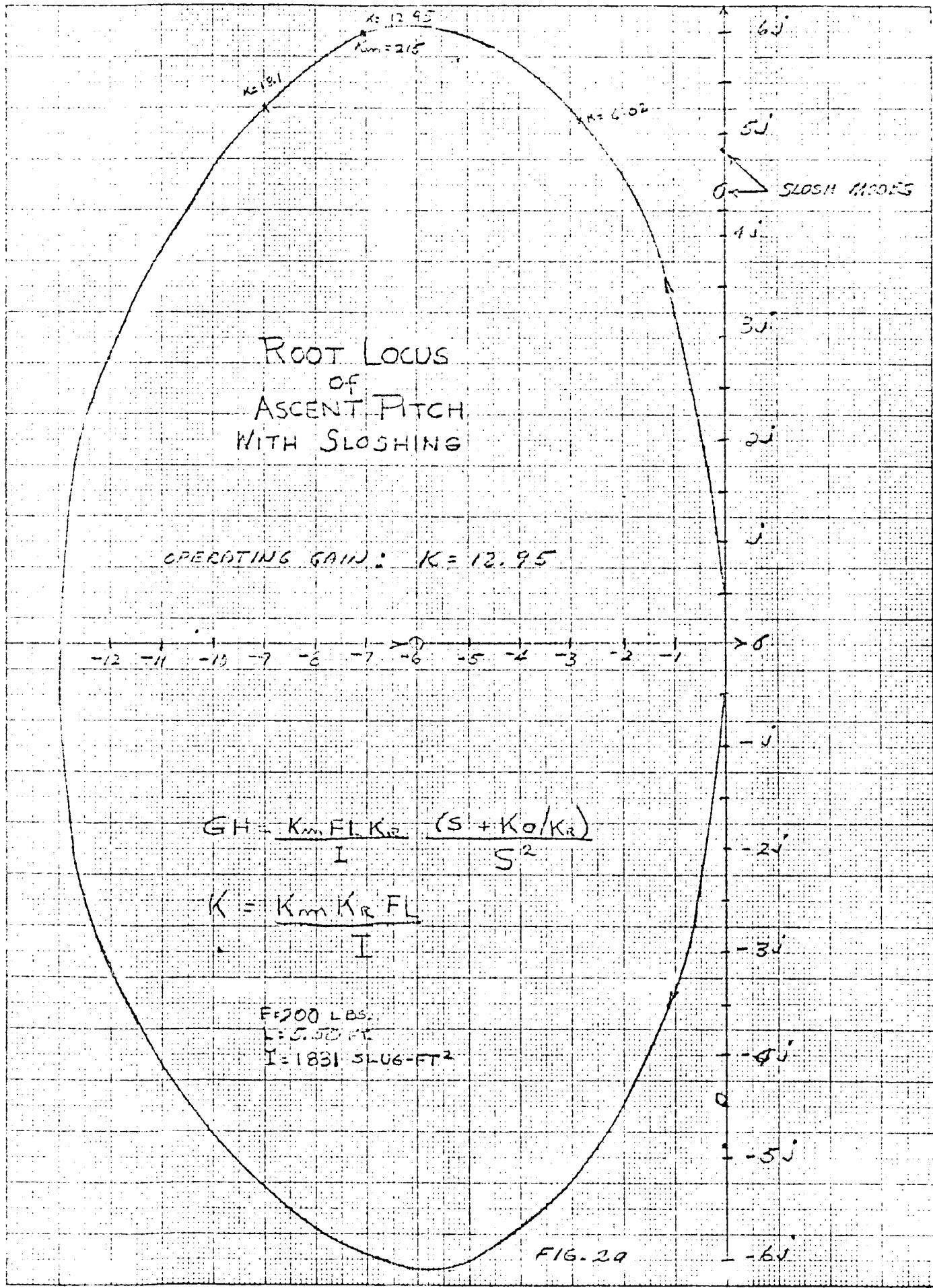
~~CONFIDENTIAL~~



LINEARIZED REACTION CONTROL SYSTEM DURING ASCENT
OPERATING GAIN: $K=11.8$

FIG. 1

~~CONFIDENTIAL~~



REF 10X10 TO THE CM. 359T-14G
 KEUFEL & FISHER CO. MADE IN U.S.A.
 ALBANY, N.Y.

~~CONFIDENTIAL~~

~~CONFIDENTIAL~~

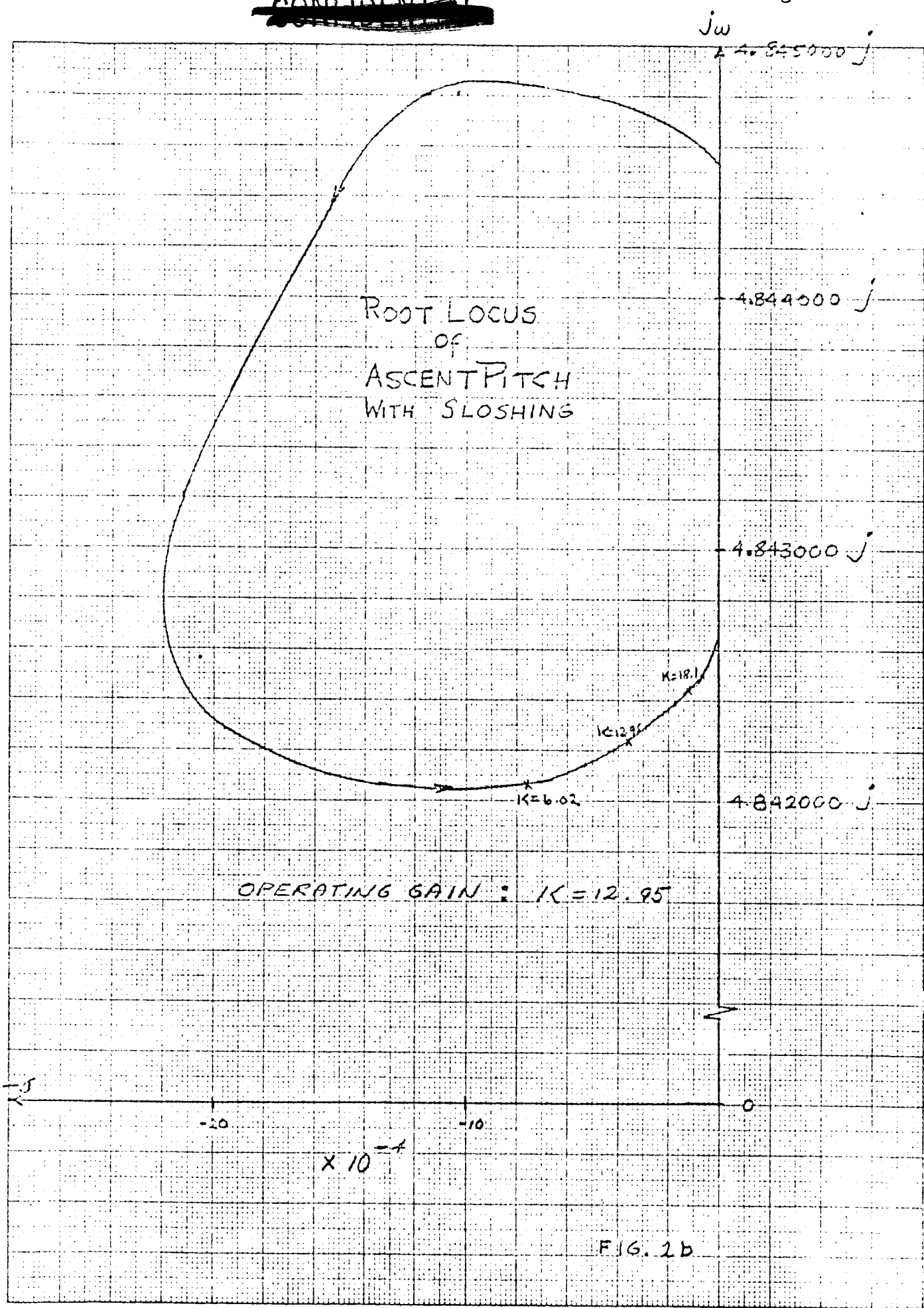


FIG. 2b

~~CONFIDENTIAL~~

REF: 10X10 TO THE CM. 3501-146
K. G. KEUFEL & SONS CO. WILMINGTON
ALABAMA

~~CONFIDENTIAL~~

REF ID: A66100
10 X 10 TO THE CM. 359T-14G
KEUFFEL & ESSER CO. MADE IN U.S.A.
ALBANY, N.Y.

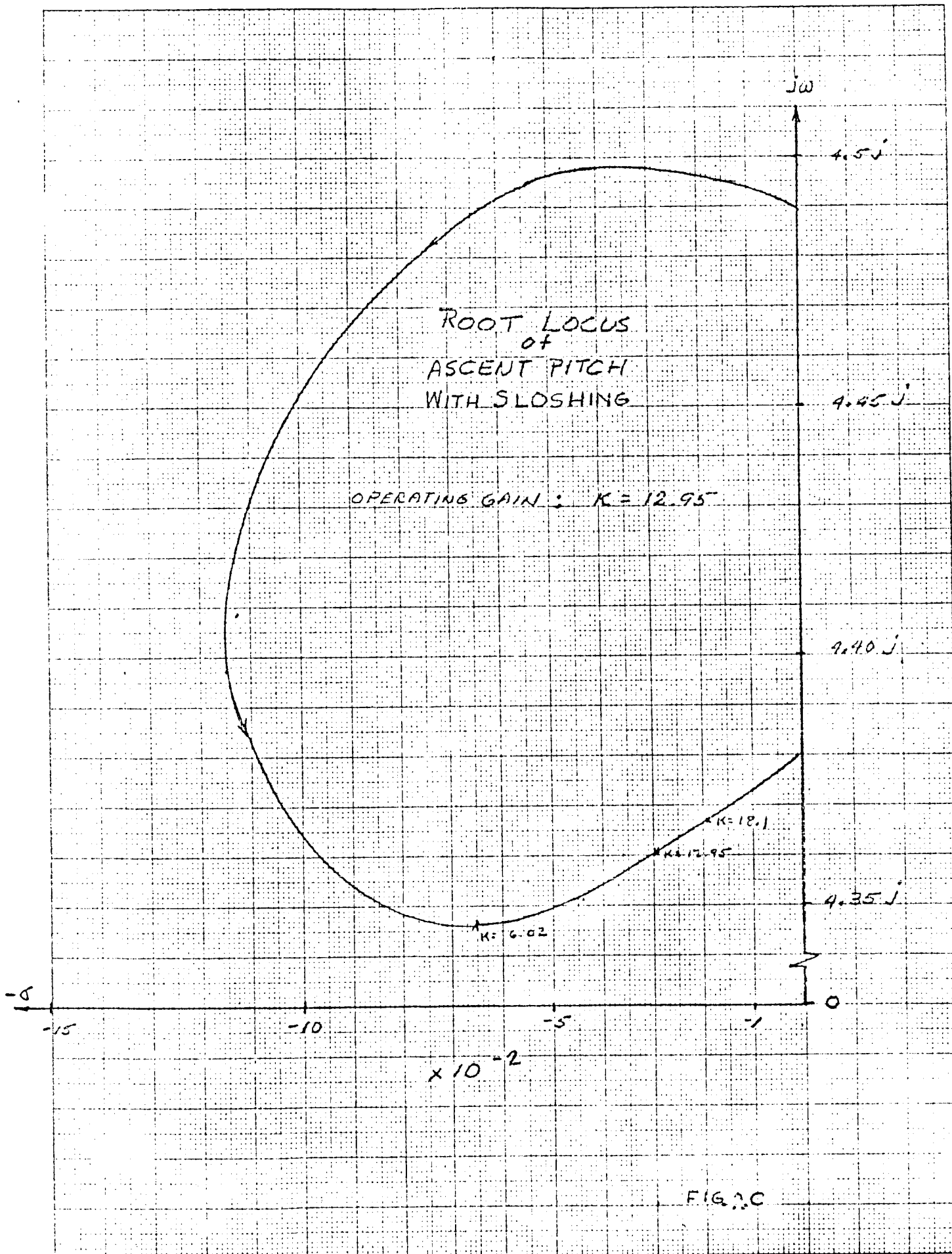
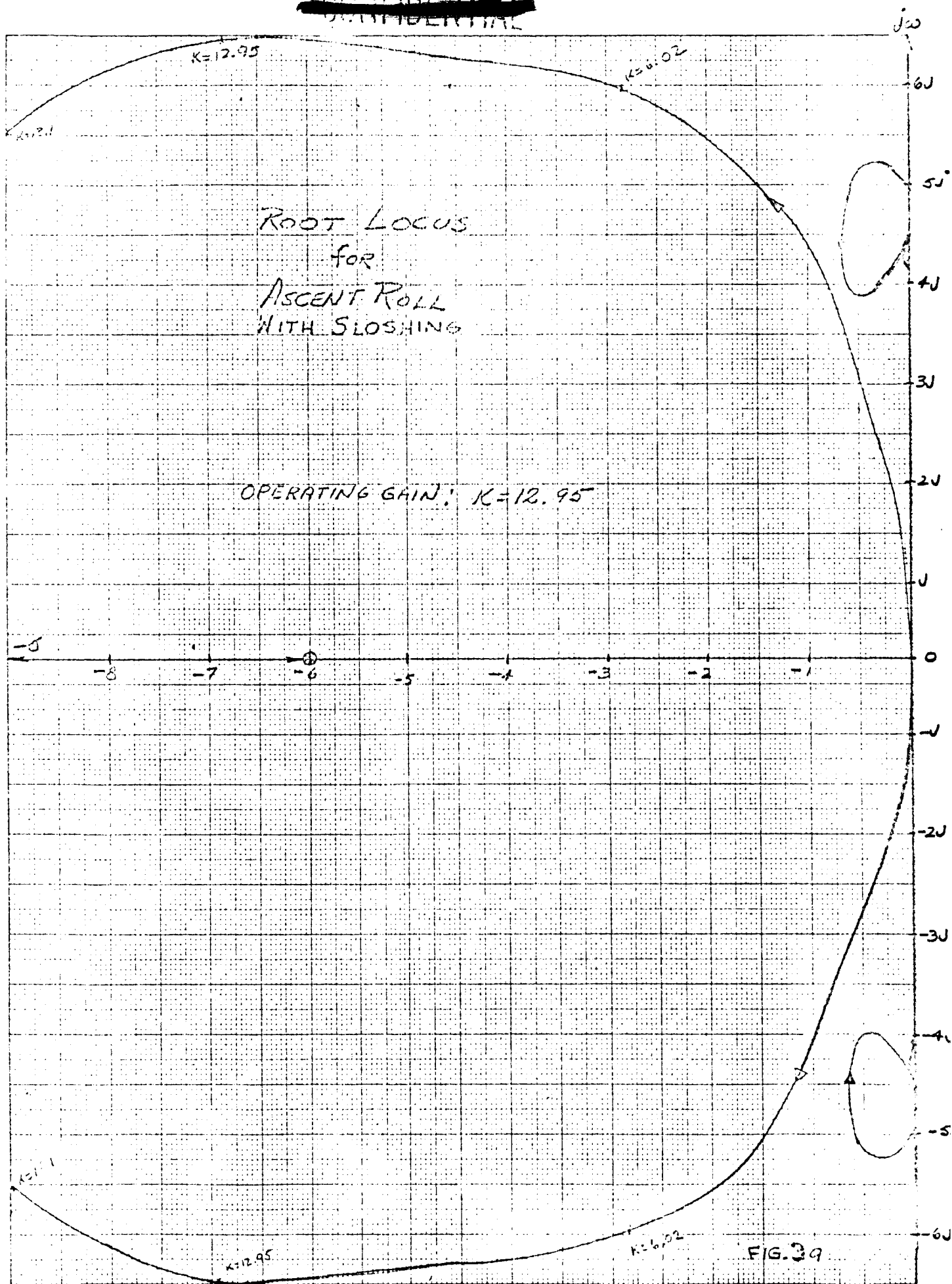


FIG. 2C

~~CONFIDENTIAL~~

~~CONFIDENTIAL~~



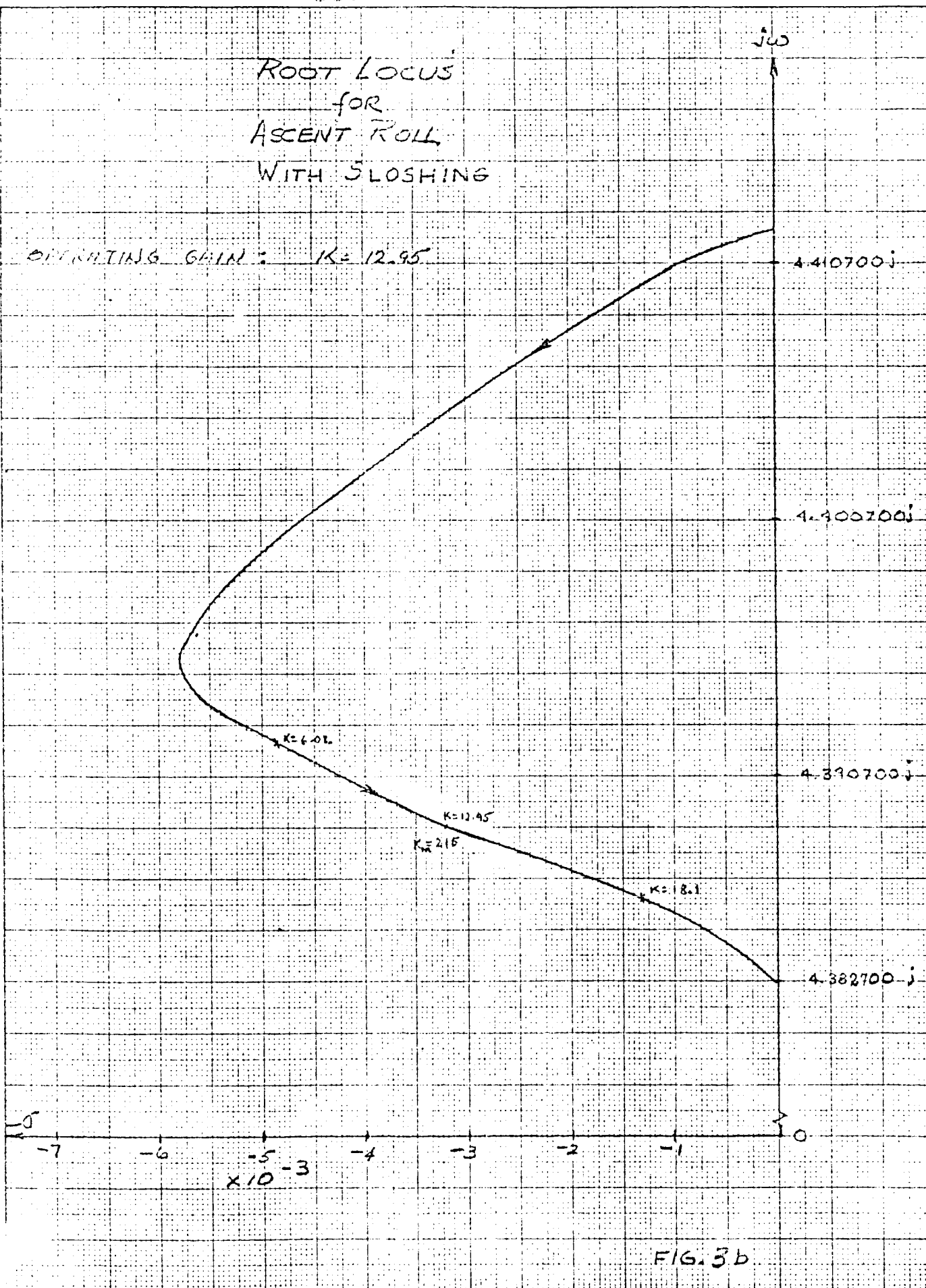
K-22 10 X 10 TO THE CM. 350T-14G
K-22 KEUFEL & DESIGN CO. WILMINGTON, DE.
ALBANY, NY

~~CONFIDENTIAL~~

~~CONFIDENTIAL~~

Root Locus for Ascent Roll With SLOSHING

OPENING GAIN: $K = 12.95$

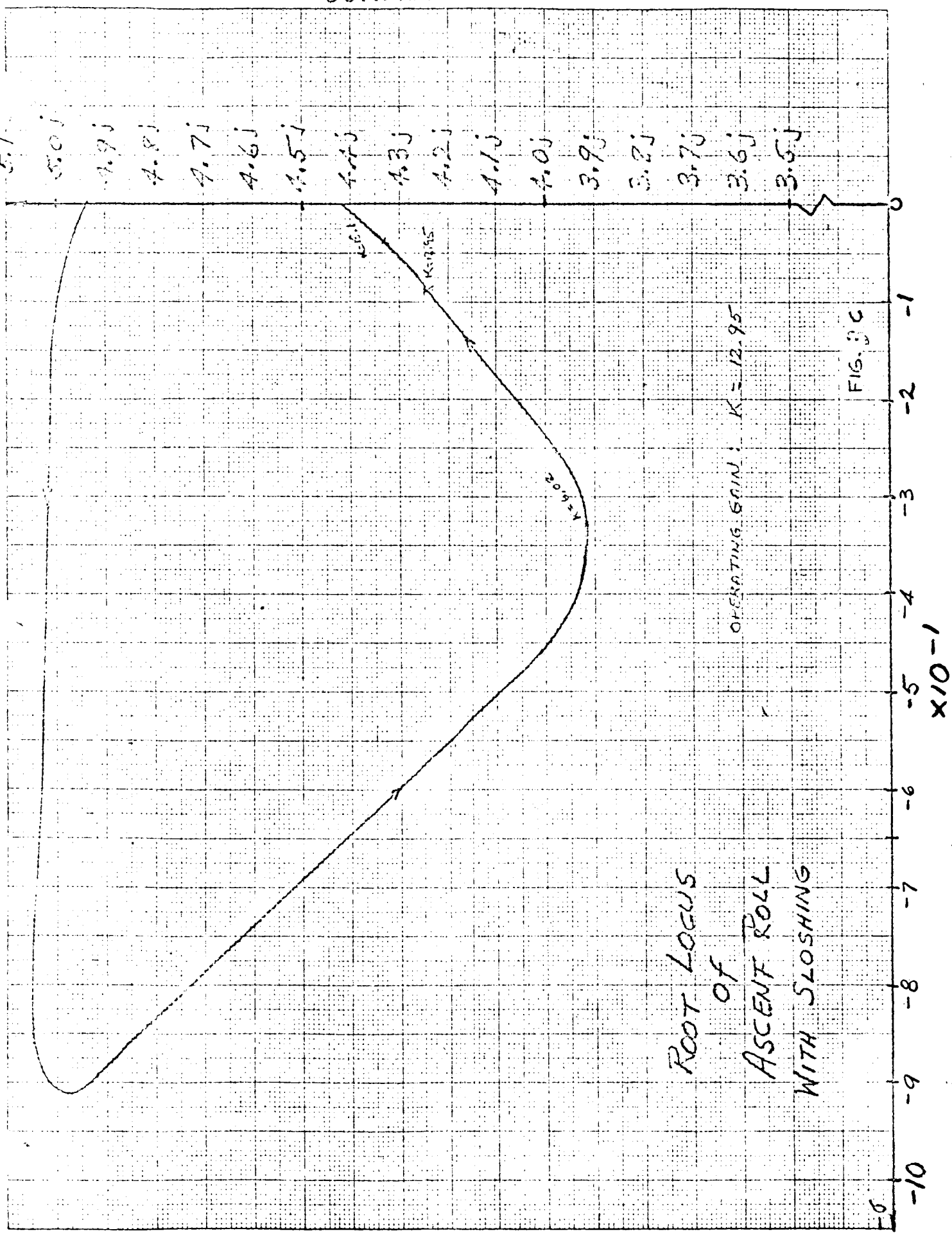


~~CONFIDENTIAL~~

10X10 TO THE CM. 359T-14G
 KEUFFEL & ESSER CO. MADE IN U.S.A.
 ALBANY, N.Y.

~~CONFIDENTIAL~~

5.1
5.0j
4.9j
4.8j
4.7j
4.6j
4.5j
4.4j
4.3j
4.2j
4.1j
4.0j
3.9j
3.8j
3.7j
3.6j
3.5j



K-10 X 10 TO THE CM. 359T-14G
KEUFFEL & ESSER CO.
ALBANY, N.Y.

~~CONFIDENTIAL~~